2018

Identification of QTL Modifying the Activity of the Tcb1-s Locus and Characterization and Sequencing of Two Plutonium-Beryllium Induced Reduced Gametophyte Transmission Mutants in Maize

Merritt Bryer Burch
South Dakota State University

IDENTIFICATION OF QTL MODIFYING THE ACTIVITY OF THE *TCB1-S* LOCUS

AND

CHARACTERIZATION AND SEQUENCING OF TWO PLUTONIUM-BERYLLIUM INDUCED REDUCED GAMETOPHYTE TRANSMISSION MUTANTS IN MAIZE

BY

MERRITT BURCH

A thesis submitted in partial fulfillment of the requirements for the

Master of Science

Major in Biological Sciences

Specialization in Biology

South Dakota State University

2018

IDENTIFICATION OF QTL MODIFYING THE ACTIVITY OF THE *TCB1-S* LOCUS

AND

CHARACTERIZATION AND SEQUENCING OF TWO PLUTONIUM-BERYLLIUM INDUCED REDUCED GAMETOPHYTE TRANSMISSION MUTANTS IN MAIZE

This thesis is approved as a creditable and independent investigation by a candidate for the Master of Science degree in Biological Sciences and is acceptable for meeting the thesis requirements for this degree. Acceptance of this thesis does not imply that the conclusions reached by the candidate are necessarily the conclusions of the major department.

Donald Auger, PhD
Thesis Advisor Date

Volker Brozel, PhD
Head, Biology and Microbiology Date

Dean, Graduate School Date

ACKNOLDGEMENTS

I would like to say thank you to my loving parents who have supported me throughout my entire academic journey with their helpful advice, Hawaiian care packages, pep-talks, and love. Without them I would have never made it as far as I am today.

I would also like to extend my thanks to Dr. Donald Auger who has allowed me to work on such interesting projects during my time here at South Dakota State University. With his knowledgeable advice, insights, criticism, support, and guidance I have come to appreciate the vast field of maize genetics and hope that someday I can become half of the advisor Don has been to me.

I am also incredibly grateful for Jerry Kermicle who first described the *Teosinte crossing barrier 1* locus in maize and kindly suggested this project to our laboratory.

TABLE OF CONTENTS

ABBREVIATIONS

B73	Inbred line Iowa 73
Bp	Base pairs
CI	Cross Incompatibility
cM	Centimorgans
Ga1	*Gametophyte factor 1*
Ga1-m	*Gametophyte factor 1* (male allele)
Ga1-s	*Gametophyte factor 1* (strong female allele)
IBM	Intermated B73 Mo17 recombinant inbred lines
Kb	Kilobases
L	Long arm of a chromosome
LOD	Logarithm of odds
Mb	Megabases
Mo17	Inbred line Missouri 17
PME/PMEI	Pectin methyesterase/Pectin methylesterase inhibitor
PB	Plutonium-beryllium (PuBe)
RIL	Recombinant inbred lines
S	Short arm of a chromosome
Tcb1	*Teosinte crossing barrier 1*
Tcb1-m	*Teosinte crossing barrier 1* (male allele)
Tcb1-s	*Teosinte crossing barrier 1* (strong, female allele)
UTR	Untranslated region
VCF	Variant call file
W22	Inbred line Wisconsin 22
QTL	Quantitative trait loci

LIST OF FIGURES

LIST OF TABLES

ABSRACT

IDENTIFICATION OF QTL MODIFYING THE ACTIVITY OF THE TCB1-S LOCUS AND CHARACTERIZATION AND SEQUENCING OF TWO PLUTONIUM-BERYLLIUM INDUCED REDUCED GAMETOPHYTE TRANSMISSION MUTANTS IN MAIZE

MERRITT BURCH

2018

This thesis is split into two independent projects both involving the male gametophyte generation of maize. The first project looks at how pollen interacts with the female gametophyte to reduce its transmission in cross-incompatible reactions controlled by the unilateral cross-incompatibility system, *teosinte crossing barrier 1*. The second project explores two plutonium-beryllium induced male gametophyte mutants and attempts to uncover their genetic basis.

Identification of QTL Modifying the Activity of the *Tcb1-s* Locus

Teosinte crossing barrier 1 (*Tcb1*) is a unilateral cross-incompatibility system present in maize that provides a pre-zygotic pistil barrier to plants carrying *Tcb1-s* (strong allele) from pollen not carrying that allele (*tcb1*), the reciprocal cross however, is unencumbered. Due to this pollen specificity, *Tcb1-s* can be useful to organic, sweet corn, or maize landrace farmers to prevent cross-contamination from occurring between fields. Kermicle (personal communication) observed that the *Tcb1-s* allele requires the

action of modifiers to confer a stronger pistil barrier. Such modifiers are present in the F1s of the maize inbred lines B73 and Mo17 who are polymorphic in *Tcb1-s* activity. In this study factors modifying the *Tcb1-s* locus were tracked using the F1s of the intermated B73 Mo17 recombinant inbred lines with W22 *Tcb1-s*/*Tcb1-s*. The ability of the *Tcb1-s* pistils to reject *tcb1* pollen containing *R1 C1* color markers and accept its own self-type pollen was measured. Eight QTLs were detected on chromosome arms 2S, 2L, 3S, 4S, 7S, 7L, 8L, and 10L explaining a total of 34.8% of the overall phenotypic variability. Knowledge of the QTL interacting with *Tcb1-s* could assist in the introgression of both *Tcb1-s* and positive acting modifiers so that *Tcb1-s* activity is maximized.

Characterization and Sequencing of Two Plutonium-Beryllium Induced Reduced Gametophyte Transmission Mutants in Maize

Two mutants generated by exposure to a plutonium-beryllium source had reduced transmission of the male gametophyte and not the female gametophyte. Both mutations are linked to the *R1* color marker. We sequenced and compared both deletion haplotypes to the B73 reference genome. We detected a 4.5 Mb region linked to the *R1* locus that may contain the mutation causing the reduced transmission phenotype. In the PB2 mutant we found 25 candidate genes impacted by deletions, one of which is a calcium-dependent protein kinase potentially involved in pollen tube tip growth. Candidate genes for PB1 remain elusive. These results could shed light on the short-lived male gametophyte generation of maize and could be applied to plant breeding to create male sterile lines.

Chapter 1: General Introduction and Literature Review

1.1 Maize Significance and Genome Structure

Frequently used as a model organism for numerous genetic and developmental biology studies, an animal feed, a source for biofuels, plastics, alcohols, along with its importance as a food source for many American Indian and Mesoamerican cultures, maize significantly influences our everyday lives. Maize is one of the most widely grown cereal crops grown in the world, covering an estimated 226 million hectares, and harvesting one billion tons a year (FAOSTAT 2016). The United States leads the world production of maize, harvesting around 385 million tons a year, followed by China producing 230 million tons a year (FAOSTAT 2016). Maize is a monecious monocot in the large grass (Poaceae) family. All *Zea* species have a monoploid complement of ten chromosomes, apart from *Zea perennis*, which has a haploid complement of 20 chromosomes. The frequently used inbred maize line, B73, has a genome size of 2.4 GB with forty thousand predicted protein-coding genes. The average maize transcript is 7638 bp long with four exons, each an average of 156 bp long (JIAO *et al.* 2017).

1.2 Maize Evolution: Many Ears in the Making

The current varieties of maize present today do not look anything like the weedy grass it originated from six to ten thousand years ago. Maize evolution was a highly-debated field of research from the early 1920's to the early 2000's. Four leading hypotheses emerged during this time, the Tripsacum-diploperennis hypothesis, Tripartite hypothesis, the Weatherwax hypothesis, and the Teosinte hypothesis.

The Tripsacum-diploperennis hypothesis suggested a cross between *Tripsacum dactyloides* and Zea diploperennis produced maize (EUBANKS 1995; EUBANKS 1997; EUBANKS 2001). Many issues arose from this hypothesis, namely that modern maize contains no evidence of an ancestral cross between *Tripsacum* and *Zea diploperennis* within the maize genome. Additionally, the hybrids reported between *Tripsacum* and *Zea diploperennis* to create maize-like offspring by Eubanks may have actually been maize-Zea *diploperennis* hybrids (BENNETZEN *et al.* 2001). *Tripsacum* and *Zea diploperennis* hybrids reported by Eubanks (EUBANKS 1995) had a reduced chromosome number of 2n = 20, a reduction more likely explained by a hybrid between *Zea diploperennis* and maize. No evidence for hybrids between *Tripsacum* and *Zea diploperennis* has been shown to have 2n = 20 without the need for numerous backcrosses into maize (MANGELSDORF AND REEVES 1939; DEWET *et al.* 1972; DEWET AND HARLAN 1974). Although hybrids between *Tripsacum* and *Zea diploperennis* can be created, there is no substantial evidence that this hypothesis explains the origin of maize.

The Tripartite hypothesis suggested that an undiscovered form of maize, somewhat resembling pod-corn, gave rise to modern maize. Maize plants then crossed with *Tripsacum* to form teosinte (MANGELSDORF AND REEVES 1938; MANGELSDORF AND REEVES 1939). This hypothesis was favored for many years because it helped explain why the teosintes were very wild and weedy in appearance but could still hybridize with maize. The lack of solid genetic evidence throughout time made the Tripartite hypothesis unlikely. The pod-corn mutation causing glumes to completely envelop kernels is caused by a rearrangement of the MADS box gene *Zmm19* at the *Tunicate1* locus. A subsequent

duplication event caused the complete pod-corn (tunicate) phenotype after the domestication of maize from teosinte (HAN *et al.* 2012).

A hypothesis suggested by Weatherwax and colleagues was short lived and eventually not accepted. It suggested that maize evolved independently from an undiscovered, perennial common ancestor. This common ancestor was also hypothesized to give rise to the genus *Tripsacum*, some of the plants in the tribe *Andropogoneae*, and the teosintes by divergent evolution (WEATHERWAX 1918; WEATHERWAX 1935; WEATHERWAX AND RANDOLPH 1955). Although Weatherwax acknowledged that maize and teosinte lived in close proximity and could produce hybrids, there was no link that suggested that teosinte was the progenitor to maize (WEATHERWAX AND RANDOLPH 1955). The lack of any fossilized, genetic, or anthropological evidence for this common ancestor in Weatherwax's hypotheses made this scenario unlikely.

The most widely accepted hypothesis to maize evolution explains how maize evolved from teosinte, specifically *Zea mays parviglumis*, in a single domestication event 6,000-10,000 years ago in the Balsas River Valley in southwestern Mexico. George Beadle was a strong supporter of this hypothesis from early on (BEADLE 1939). Based off prior research published by MANGELSDORF AND REEVES (1938) describing that hybrids between maize and *Euchlaena* (now teosinte) differ only by four segments of chromatin bearing *Tripsacum* effects, Beadle suggested that these four segregating loci and one additional locus that could not be tracked in the backcrosses performed by Mangelsdorf and Reeves, are what differentiated maize and teosinte.

With a five major factor model explaining the evolution of maize from teosinte, Beadle argued that people in Central America found uses for the weedy, seemingly

inedible teosinte plant. By "popping" teosinte endosperm under the same conditions as modern-day popcorn, Beadle reported that the flavor is fundamentally similar to popcorn and provides the initial incentive for farmers to cultivate teosinte into modern day maize (BEADLE 1939).

The support for the teosinte hypothesis after Beadle's initial observations are strong. Numerous studies over the years using microsatellite data (MATSUOKA *et al.* 2002), isozyme variation (DOEBLEY *et al.* 1984; DOEBLEY *et al.* 1987), population genetics (EYRE-WALKER *et al.* 1998; HUFFORD *et al.* 2012), phylogenetics of the internal transcribed spacer (ITS) (BUCKLER AND HOLTSFORD 1996), systematics (KELLOGG AND BIRCHLER 1993), and quantitative genetics (DOEBLEY *et al.* 1990) all show that *Zea mays parviglumis* gave rise to maize. Also, maize and *Zea mays parviglumis* are readily hybridized to produce fertile offspring and do so spontaneously when in close proximity (ELLSTRAND *et al.* 2007).

1.3 Maize Gametogenesis and Fertilization

Maize, like all other angiosperms goes through an alteration of generations spending most of its life cycle in the diploid sporophytic stage and a very short period in the haploid gametophytic stage. This gametophytic stage is the reproductive phase of a plant's life cycle where the male haploid pollen grain meets the pistil tissues, grows a pollen tube directed towards the female gametophyte and fertilizes the haploid egg cell to create a diploid embryo and a triploid endosperm which develops into the one seeded maize fruit, the kernel. Although the gametophyte generation is short-lived, it plays a crucial role in the transmission of genetic information from one generation to the next. If mutations deleterious to the gametophytic generation of plants arise that slow or prevent

allelic transmission, genetic information could be lost in the next generation. Because mutants that affect the gametophyte generation of plants are difficult to recover from nature, much of the discovery of genes involved in male or female gamete transmission have been performed by mutant analysis.

1.3.1 Development of the Female Inflorescence and Egg

The female inflorescence, also known as the ear, houses the female gametes. Each node produces an auxiliary branch bud and only one or two of the uppermost nodes produce an ear, often producing one nine inches in length (KIESSELBACH 1949). Like the developing tassel primordia, the ear is initially smooth, but lobes soon start to form in rows from the base of the ear to the tip. Each lobe then divides and becomes two-lobed, forming a spikelet with two flowers. Only one spikelet survives and forms a single kernel. Elongated styles called silks emerge from each embryo, and work to catch, hydrate, and guide pollen grains down the transmission tract towards the embryo sac.

The embryo within an ear develops from archesporium cells that divide and produce megaspore mother cells. Two rounds of meiosis produce a two-cell and four-cell stage like developing pollen grains. At the four-cell stage, the three outermost spores degenerate while the innermost spore functions as the embryo sac. The single egg cell enlarges and divides to produce a cluster of antipodal cells that constantly proliferate, two vacuoles that surround a central cell with two polar nuclei, and two synergid cells that surround the embryo sac. The primary endosperm of this egg is diploid (2N) and the embryo sac is haploid (1N). After double fertilization, a triploid endosperm (3N) and a diploid embryo (2N) are produced, following a polygonum-type fertilization (TAIZ AND ZEIGER 2002).

1.3.2 Development of the Male Inflorescence and Pollen

The male inflorescence, commonly known as the tassel develops within two to three weeks after seedling emergence from the shoot apical meristem. Initially, there is no defined central axis or tassel branches, the tassel primordia appear smooth before two lobes appear which give rise to a spikelet and two flowers. After several divisions, the glumes, the upper and lower flowers, lemma, three stamens, and two lodicules begin to form. Just before the pollen sheds, the lodicules swell, the lemma and palet break free and expose the anthers who form pores to release the pollen grains. Pollen begins to shed from the anthers located on the central tip of the axis before progressing upwards and downwards. Tassel branches begin to shed pollen after the central axis (KIESSELBACH 1949). Each tassel on a maize plant can produce about eighteen million pollen grains, very few of which ever come close to fertilizing an embryo (STURTEVANT 1881).

Within the anthers of a developing male inflorescence a cluster of sporogenous tissue is surrounded by dividing rows of archesporial cells and epidermis. As this structure continues to divide, the innermost layer containing numerous sporogenous cells who give rise to the microsporocytes, is now surrounded by a nutrient-rich tapetum which fuels subsequent cell divisions.

These microspore mother cells, or microsporocytes, undergo meiosis twice. The first round of meiosis produces two spore cells, while the second round of meiosis produces four spores, each containing an immature haploid pollen grain. This four-spore tetrad is housed within a microspore mother cell which quickly degrades before pollen is shed. Each of these four spores, shortly before the shedding of pollen from the tassel, breaks away from the four-spore tetrad and undergoes mitotic division. This process

yields a vegetative cell and a generative cell containing two sperm cells which assist in double fertilization (KIESSELBACH 1949).

At the molecular level, before the pollen is released from the four-cell tetrad, the tapetum cells play a critical role in a pollen grain's success upon reaching the pistils. Each pollen grain consists of an outer coat called an exine and an inner wall called an intine. The intine is made up of polysaccharides (TIAN *et al.* 2017) and various proteins like pectin esterases (ALBANI *et al.* 1991), pectin lyase (WING *et al.* 1990), and hydrolases (DOBRITSA *et al.* 2011) synthesized by the pollen itself or the surrounding microspore mother cell. The exine coating would be the first interaction a pollen grain would have with the pistil, so the associated surface proteins are important in the breakdown and movement of the pollen grain into the transmission tract of the style. The exine surrounding the intine is not covalently bound and contains two major proteins that were synthesized by the tapetum cells and transported into the exine: a beta-glucanase and exoxylanase (BIH *et al.* 1999; WU *et al.* 2002).

The beta-glucanase hydrolyzes and frees the four-spore tetrad bound together by callose bound in the microspore mother cell (FRANKEL *et al.* 1969). Later beta-glucanase appears within the exine, working with the exoxylanase to potentially to help penetrate the pollen tube into the transmission tract of the style (WU *et al.* 2002; SUEN *et al.* 2003; SUEN AND HUANG 2007). Additional proteins found within the exine like expansins, allergens, extensins, and cation binding proteins may be used to help grow the pollen tube towards the embryo sac and potentially loosen the cell walls within the pistil for continued pollen tube penetrance (SUEN *et al.* 2003; DOBRITSA *et al.* 2011).

1.3.3 Pollen Tube Growth, Guidance, and Recognition

Once the gametes within the inflorescences are fully developed fertilization can occur. Pollen sheds near the tip of the central axis on the tassel and moves down to additional tassel branches. The pollen sheds for several days until the elongated stigma (or silks) on the ear capture a pollen grain and successfully fertilize an egg.

Five distinct phases have been described for the flowering plant fertilization process in both monocots and dicots (JOHNSON AND PREUSS 2002; SWANSON *et al.* 2004; DRESSELHAUS AND FRANKLIN-TONG 2013). Phase I begins when a desiccated haploid pollen grain lands on a receptive trichome attached to the stigma of the female inflorescence (HESLOP-HARRISON *et al.* 1985). The pollen grain then hydrates and germinates by interacting with specialized stigma papillae cells that are rich in lipids who assist in pollen tube growth (ELLEMAN *et al.* 1992; WOLTERS-ARTS *et al.* 1998). The uptake of water allows for the activation of metabolism in each pollen grain. Hydration also allows the surface coat proteins surrounding the exine walls to interact with the sigmatic cells, one of the first steps in the recognition of self or foreign pollen grains.

During Phase II the pollen grain germinates, and the pollen tube grows through the papilla cells in the trichomes of the stigma and into the transmitting tract of the style. Because some trichomes are set at a perpendicular angle, pollen tubes are directed into the transmitting tract towards the ovule due to mechanical constraints and potentially chemical or proteomic cues (HESLOP-HARRISON *et al.* 1985). During Phase II the beta-glucanase and exoxylanase within the exine are the most active in assisting the pollen tube in invading the female tissues. Pollen tubes gain nutrients from the surrounding female tissues in cross compatible pollinations. In incompatible crosses, the pollen must

use their own endogenous resources which only allow for the pollen tube to grow two centimeters in length (HESLOP-HARRISON 1982). The growing pollen tube interacts with signals from the stigma that can enhance or repress further growth towards the style. In maize, one such species-specific signal conferring a micropylar pollen tube guidance is excreted by the synergids and embryo sac called *Egg Apparatus 1* (*ZmEA1*). Downregulation of *ZmEA1* transcripts shows partial female sterility due to the lack of guidance to the micropyle (MARTON *et al.* 2005; MARTON *et al.* 2012).

During Phase III the pollen tube passes completely through the stigma and grows through the extracellular matrix of the transmitting tract. The growing pollen tube relies heavily on the activity of actin and calcium in its directional tube growth towards the egg cell. Steep calcium gradients near the tip of the pollen tube, present in short bursting oscillations, propel the pollen tube tip forward (PIERSON *et al.* 1996). Oscillations of actin microfilament (F-actin) and exocytosis of Golgi vesicles containing new cell wall materials follow shortly thereafter, stretching and growing the tip in short pulses further down the transmitting tract towards the egg cell (MESSERLI AND ROBINSON 1997; MESSERLI *et al.* 2000; PARTON *et al.* 2001; STEINHORST AND KUDLA 2013). This tip growth is mediated by clathrin-dependent endocytosis in the subapical regions of the pollen tube tip to gain proteins, plasma membrane, and cell wall materials to assist in long distance pollen tube growth (PICTON AND STEER 1983; DHONUKSHE *et al.* 2007; MOSCATELLI *et al.* 2007).

At Phase IV of the plant fertilization process, the pollen tubes leave the nutrient-rich transmitting track within the style and go through ovarial cavity growth (LAUSSER AND DRESSELHAUS 2010; LAUSSER *et al.* 2010). This phase differs between monocots and

dicots. In dicots, the pollen tube exits the transmitting tract and continues its growth on the surface of the funiculus, a bridge of tissues that connects the developing egg to the surrounding maternal tissues (SWANSON *et al.* 2004). In monocots, pollen tubes also leave the transmitting tract but instead grow on the surface of the integument towards the nucellar cone of the micropyle, a small opening near the base of the egg cell (HESLOP-HARRISON *et al.* 1985).

During the final stage of pollen tube growth, Phase V, the pollen tube reaches the micropyle and the surrounding synergid cells and releases the two sperm cells into the egg cell. In maize, the rapid burst of the pollen tube tip is caused by defensin-like protein *ZmES4* (embryo sac), a cystine-rich protein excreted by the synergid cells (AMIEN *et al.* 2010). The two synergid cells then rapidly degrade and the two sperm cells fertilize the embryo sac to produce the diploid embryo and the central cell to produce the triploid endosperm.

The phases of the plant fertilization process have been a detailed field of study in prior years. In maize, the key genes describing pollen tube attraction and burst help to explain how the guidance of male gametes occurs in normal, cross-compatible pollinations. Little is known, however, about the molecular recognition and subsequent rejection that occurs between pollen of incompatible crosses and the female reproductive tissues. The recognition of compatible and incompatible pollen is the basis of cross-incompatibility research.

1.4 Cross Incompatibility in Maize

With its increasing importance to the global economy, maize has been genetically engineered to confer resistance to chemical pesticides, insect attacks, and drought resistance (JAMES 2015). In 2015, the global production of genetically engineered maize covered 60 million hectares while conventional maize spanned twice as much land, at 125 million hectares. With the growing prevalence of biotech crops, many organic farmers and consumers are concerned about the contamination of their fields by non-organic sources. In addition, specialty farmers growing sweet corn, stocks high in amylose, or colored varieties used in cooking can be affected by cross-contamination (NELSON 1994). It has previously been shown that cross contamination between maize fields is maize pollen can occur at low rates up to 600-700 meters away (HALSEY *et al.* 2005; BANNERT AND STAMP 2007). Although most cross-contamination drops off after 60-125 meters, farmers with fields surrounding unwanted pollen sources could be directly affected (HALSEY *et al.* 2005). Currently, to avoid cross contamination, farmers separate their fields, displace planting times, or place barrier crops (MA *et al.* 2004; HALSEY *et al.* 2005). These methods are laborious and sometimes difficult to achieve, which opens the possibility for the use of naturally occurring genetic cross-incompatibility systems to prevent unwanted cross-contamination.

Cross-incompatibility is a pre-zygotic fertilization barrier that prevents pollen from a foreign pollen parent from successfully fertilizing an egg. Pollination is only successful when a recognized, or self-type pollen grain is received. Maize has nine known cross-incompatibility systems located throughout the genome, *gametophyte factor*

1 (*ga1*, 4S), *ga2* (5L), *ga3* (7), *ga4* (1), *ga6* (1), *ga7* (3L), *ga8* (9S), *ga10* (5S), and *teosinte crossing barrier 1* (*tcb1*, 4S) (NELSON 1994; NEUFFER *et al.* 1997)

The two best documented cross-incompatibility systems in maize are *ga1* and *tcb1*. In both cases the cross-incompatibility systems act in a similar fashion (Figure 0.1). When the recessive allele (i.e., *ga1, tcb1*) is present in the pistil it can accept pollen containing any other allele. When a 'strong' dominant allele (i.e., *Ga1-s, Tcb1-s*) is present in the pistil, pollen containing the recessive allele are rejected while pollen possessing the strong allele or the 'male-type' allele (i.e., *Ga1-m, Tcb1-m*) are accepted. The male-type alleles (i.e., *Ga1-m, Tcb1-m*) in the pollen grain are compatible with the strong-type allele (i.e., *Ga1-s, Tcb1-s*) but plants with the male-type alleles can be fertilized by any other pollen alleles types (NELSON 1994). Both *Ga1-s* and *Tcb1-s* have been patented (HOEGEMEYER 2005; KERMICLE *et al.* 2006).

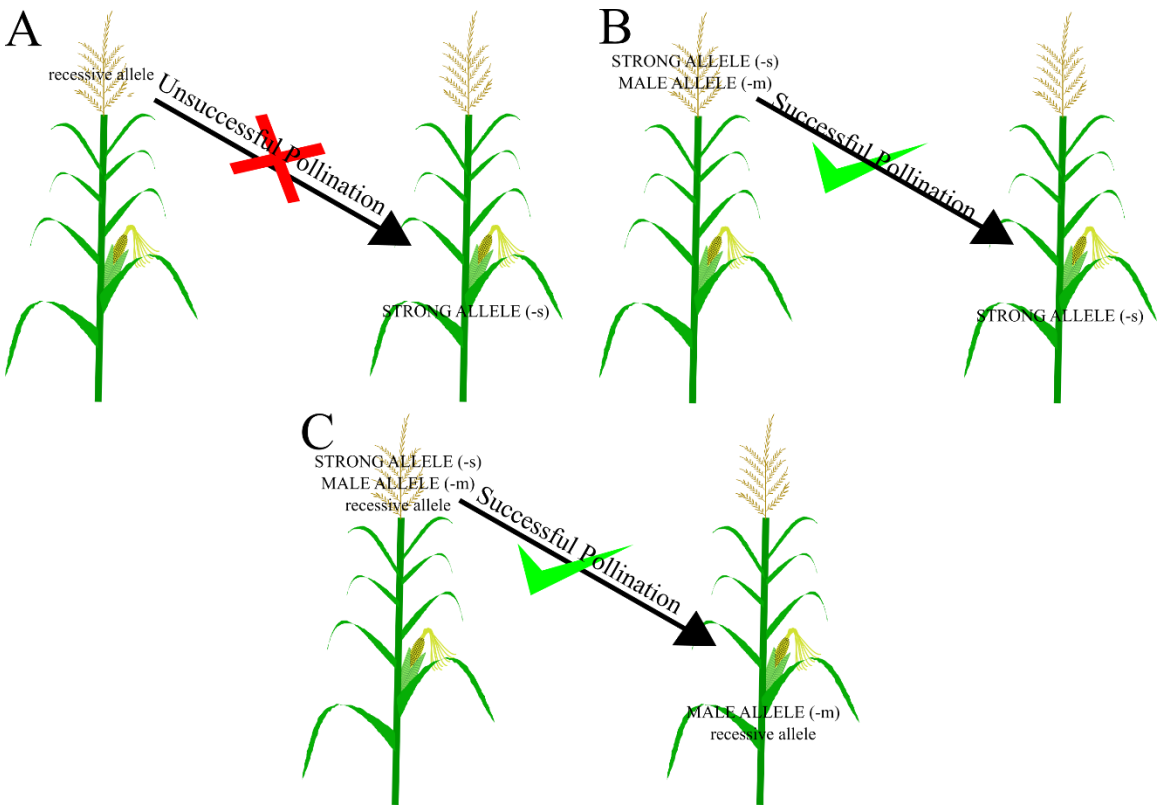

Figure 0.1. Generalized schematic to the maize cross-incompatibility systems.
The *ga1*, *ga2*, and *tcb1* cross-incompatibility mechanisms all work in a similar fashion. A) Pollen containing the recessive allele cannot pollinate pistils containing the strong allele (-s) B) Pollen containing either the strong allele (-s) or the male allele (-m) can pollinate pistil containing the strong allele successfully C) Pollen containing the strong allele (-s), male allele (-m), or recessive allele can successfully pollinate pistils containing either the male allele (-m) or the recessive allele.

1.4.1 Gametophyte factor 1

Gametophyte factor 1 (*Ga1*) cross-incompatibility was observed as early as 1902 by Correns when a Rice Popcorn strain was crossed with a *sugary1* sweet corn. An aberrant F2 ratio when crossing onto the Rice Popcorn arose where sixteen percent *su1*/*su1* kernels were found when twenty-five percent were expected. This deviation from Mendelian segregation was studied again in 1925 and 1926 by Emerson and Mangelsdorf, respectively. Emerson suggested that a gametophyte acting gene linked to

sugary1 caused this unusual segregation (EMERSON 1934). Further investigations by MANGELSDORF AND JONES (1926) showed that this gametophyte acting gene, now named *gametophyte factor 1* (*Ga1*) by Emerson (1925), 35 cM away from *sugary1*, was a dominant acting gene that conferred a competitive advantage of *Ga1* pollen over *ga1* when added to *ga1*/*Ga1* or *Ga1/Ga1* pistils. No competitive advantage was seen for *Ga1* pollen onto *ga1*/*ga1* pistils when competing with *ga1* pollen (SCHWARTZ 1950).

It was later discovered by SCHWARTZ (1950) there were three alleles at the *ga1* locus. The *Ga1* that had been studied previously, provided the 'strong' reaction in rejecting *ga1* pollen and was aptly renamed $Ga1^s$ (now *Ga1-s*). An additional *Ga1* (now *Ga1-m*) allele had a competitive advantage over *ga1* pollen when applied to *Ga1-s* pistils but could be fertilized by any other allele type with no specificity. *Ga1-m* in the pollen could overcome the strong female barrier. The ability of the *Ga1* pollen to fertilize plants containing *ga1*, but *ga1* pollen not able to fertilize *Ga1* plants was the first documented case of non-reciprocal cross sterility in maize.

Ga1-s is not common. The strong allele is found in some Central and South American maize lines along with some popcorn varieties. The recessive allele, *ga1*, is found in all North American dent corn (NELSON 1960). The abundance of the *ga1* allele in most dent corn makes the *Ga1-s* system an interesting method to prevent cross-contamination between populations. However, it was recently shown that many of the US Nested Association Mapping parental lines carry the *Ga1-m* allele, making the use of these systems a little tricky (JONES AND GOODMAN 2018).

Continued research over the years has led to fine mapping and RNA expression studies of the *Ga1-s* locus. Fine mapping narrowed the location of *Ga1-s* to a 100 Kb

region on chromosome 4 housed within a 1.5 cM area (ZHANG *et al.* 2012; LIU *et al.* 2014). An RNA expression study of unpollinated W22 pistils carrying the *ga1* allele and pistils carrying the *Ga1-s* allele was performed by MORAN LAUTER *et al.* (2017). Numerous genes were differentially expressed between the two pistil alleles, but a putative pectinesterase (PME) named *ZmPme3*, on the short arm of chromosome 4, mapped to the same 2.6 Mb genomic position as the *Ga1-s* (BLOOM AND HOLLAND (2012) and was only expressed in *Ga1-s* tissues. The two annotated genes that fell within the 100 Kb mapped region as described by LIU *et al.* (2014) were not differentially expressed between the *ga1* and *Ga1-s* pistils. More interestingly, the region surrounding the *Ga1-s* locus contains fifty-eight partial to full-length PME-like sequence repeats within a 1.1 Mb region. Of these fifty-eight PME-like sequences, the only transcript that was differentially expressed in the *Ga1-s* pistils had a full-length open reading frame.

To determine the identity that the *Ga1-m* allele had within this locus of nested PME repeats, hybrids NC390/NC394 who were homozygous for *Ga1-m/Ga1-m* were sequenced. A two-base pair insertion caused a frameshift mutation to inactivate *ZmPme3* in the *Ga1-m* allele. The lack of a functional PME sequence and corresponding gene expression within the *ga1* and *Ga1-m*, which is only seen within *Ga1-s* pistils agrees with the notion that the *Ga1-s* locus provides the female function that blocks foreign pollen that the *ga1* and *Ga1-m* alleles do not have. Additional analysis of the *ga1* locus is necessary to determine if *ZmPme3* truly bears the function of the *Ga1-s* allele.

1.4.2 Teosinte crossing barrier 1

Teosinte crossing barrier 1 was first described by KERMICLE AND ALLEN (1990) when six accessions from *Zea mays spp. mexicana* and *huehuetenangensis* from Central

Mexico were found to have cross-incompatibility traits. Promising accessions from Chalco and Central Mexico were backcrossed for six to eight generations to W22. The Teosinte Incompatibility Complex Chalco (TIC-Chalco) from Chalco, Mexico was able to block *ga1* pollen but could accept pollen from plants with *Ga1-s, Ga1-m,* TIC-Central Plateau, and self-type pollen suggesting that the accessions from Chalco contained *Ga1-s*. The TIC from the Central Plateau (TIC-CP, now *teosinte crossing barrier 1, tcb1*) was able to reject *ga1, Ga1-s, Ga1-m, TIC-Chalco,* and surprisingly did not accept its own pollen very well. Three separate alleles were found at the TIC-CP locus named TIC-CP1, acting similarly to *Ga1-m* who can pollinate *ga1*/*ga1* and *Ga1-s/Ga1-s* pistils. A second allele named TIC-CP2 can pollinate pistils carrying the third TIC-CP allele conferring the female function but cannot fertilize *Ga1-s/Ga1-s* pistils. The TIC-CP allele requires another, unknown linked factor to function properly (KERMICLE AND ALLEN 1990).

In functionally diploid pollen where *Tcb1-s* or *Ga1-s* were translocated onto accessory B chromosomes (TB-4Sa) in stocks normally homozygous *tcb1* or *ga1*, KERMICLE AND EVANS (2005) demonstrated that there is no active rejection of the recessive *tcb1* or *ga1* pollen on *Tcb1-s* or *Ga1-s* pistils. Even in the presence of the *tcb1* or *ga1* alleles, *Tcb1-s* or *Ga1-s* pistils required their matching allele, either *-s* or *-m*, to be present to fertilize the egg cell. When *Ga1-m* and *Tcb1-s* are present in the same pollen grain, their activity is independent and is not inhibited or promoted by the presence of the other allele. A congruity model was proposed in that *Tcb1-s* and *Ga1-s* pistils require the matching allele present in the pollen and silk tissues to ‘fit’ together to overcome the crossing barrier and successfully carry out fertilization.

Mapping of *tcb1* showed a close linkage with *sugary 1* (*su1*) and *tassel-seed 5* (*ts5*). A full genetic map of the chromosomal location of *tcb1* is shown in Figure 0.2 modified from EVANS AND KERMICLE (2001) and LU *et al.* (2014). Located on the short arm of chromosome 4 near the centromere, *tcb1* is 44 cM away from *ga1* and nested between *virescent 17* (*v17*) and *brown-midrib 3 (bm3)* and only 6 cM away from *sugary 1*. *Tcb1-s* and *Tcb1-m* can be separated in rare recombination events and are 0.02 cM away from each other, with *Tcb1-m* distal to *Tcb1-s.*

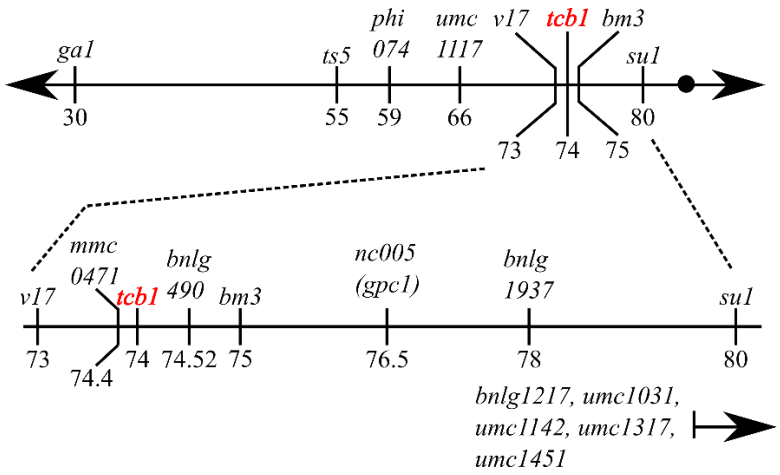

Figure 0.2. Genetic map of tcb1.

Located on the short arm of chromosome 4 near the centromere, *tcb1* is 44 cM away from *ga1* and nested between *virescent 17* (*v17*) and *brown-midrib 3 (bm3)*. *Tcb1-m* and *Tcb1-s* can be separated at the *tcb1* locus, with *Tcb1-m* being 0.02 cM distal to *Tcb1-s.*

There is evidence that *Tcb1-s* does not act alone. In addition to a separable *Tcb1-m* allele, additional modifiers influence *Tcb1-s* activity. A full strength *Tcb1-s* containing positive modifiers can block *Ga1-s* and *ga1* pollen with only a 3% receptivity rate. An attenuated version of *Tcb1-s* lacking modifiers accepts more *Ga1-s* and *ga1* pollen with a 10% receptivity rate (EVANS AND KERMICLE 2001). When backcrossed into W22 for ten

generations, *Tcb1-s* activity decreased over time (LU *et al.* 2014). The progressive loss of *Tcb1-s* activity was suggested to be caused by epigenetic silencing of the *-s* allele and/or potentially the segregation of modifying loci. Evidence for the presence of modifying loci of *Tcb1-s* between the inbred lines B73 and Mo17 has been observed and have yet to be identified (Kermicle, personal communication).

1.4.3 Pollen Tube Growth in Incompatible Pistils

When pollen from the recessive alleles of *tcb1* or *ga1* is added to pistils containing the respective female barrier (*Tcb1-s* or *Ga1-s*) the pollen tube morphology provides insights on the behavior of these unilateral cross-incompatibility systems. In cross compatible crosses of *tcb1* or *ga1* pollen to *tcb1* or *ga1* pistils, pollen tubes grew straight down the transmitting tract and reached the egg cell or came within 1-1.5 cm within 24 hours (LU *et al.* 2014). Visualizing *ga1* pollen on *Ga1-s* pistils showed kinked and erratic pollen tubes that entered and exited the transmitting tract. Regions of intense callose staining at more unpredictable intervals than compatible crosses were also observed. Pollen tubes started to slow their growth five hours after pollination and stopped completely twenty-four hours after pollination (LAUSSER *et al.* 2010; ZHANG *et al.* 2012; LU *et al.* 2014; MORAN LAUTER *et al.* 2017).

Although no model exists for *ga1* behavior in *Ga1-s* pistils it can be hypothesized that after the recognition of *ga1* pollen as non-self-type pollen, *ZmPme3*, expressed only in *Ga1-s* pistils, creates hardened cell walls through the deesterification of homogalacturanan that slow *ga1* pollen tubes. As these pollen tubes go through Ca^{2+} induced bursts of oscillating growth, they are forced to travel down the path of the least hardened cell wall resistance, sometimes taking them outside of the transmitting tract.

Pollen tubes eventually stop twenty-four hours after pollination due to the lack of nutrition provided from the female or finding a region of cell wall within the transmitting tract that was too hard to overcome. Because no pollen specific inhibition activity has been described for the de-activation of ZmPME3 in *Ga1-s* or *Ga1-m* pollen compared to *ga1* pollen it is difficult to determine if this model is true.

When *tcb1* pollen is added to *Tcb1-s* pistils, pollen tube growth begins to slow six hours after pollination (Lu *et al.* 2014). Unlike *Ga1-s*, *tcb1* pollen within *Tcb1-s* pistils does not show erratic and kinked pollen tube growth. Pollen tubes grow straight and do not exit the transmitting tract. Instead, pollen tube growth seems to slow starting at six hours after pollination until it eventually stops twenty-four hours after pollination. In *Tcb1-s* ears where *tcb1* pollen was successfully able to fertilize an egg cell, more fertilization events took place near the tip of the ear rather than the base, suggesting that it is the restriction of pollen tube growth during Phase III, or the continued growth through the transmitting tract that slows incompatible pollen tubes.

To date, no RNA expression studies of *tcb1* and *Tcb1-s* pistils have been performed. Due to the differences in pollen tube growth between *ga1* and *Ga1-s* and *tcb1* and *Tcb1-s* pistils, it might not be the activity of similar pectin methylesterase protein acting within *Tcb1-s.* Another similarly acting gene may be slowing down *tcb1* pollen that does not require erratic, or kinked growth through the transmitting tract.

The *Tcb1* and *Ga1* cross-incompatibility systems involve much more than their pistil-based pollen rejection abilities. The network of complex interactions occurring between the growing pollen tube of the male gametophyte and both the sporophytic pistil tissues and gametophytic embryo sac tissues make this system very intricate. Information

how a pollen grain carrying foreign allele is recognized, why heteroallelic pollen carrying both the *Tcb1-s* and *tcb1* alleles provides a recognizable congruity and can fertilize *Tcb1-s/Tcb1-s* plants, why *Tcb1-s* activity is lost over many generations, and the defense-like response in the pistil halting pollen tube growth has yet to be uncovered. Additionally, the underlying population genetics of how these unilateral cross-incompatibility systems persist, how they arose, and what their role was in the reproductive isolation of teosinte from maize has yet to be deduced.

1.5 Male Gametophyte Mutants in Maize

While *Gametophyte factor 1* and *Teosinte crossing barrier 1* are two methods of reducing the transmission of the recessive *ga1* or *tcb1* pollen through a pistil-acting barrier, many male gametophyte mutants exist whose activity is independent of a female-based barrier. Mutations that affect the male gametophyte generation reduce the transmission of the male gametes independent of the pistil genotype. These mutations can occur in many places along the developmental pathway of a pollen grain. Before the pollen grain ever reaches a receptive pistil, mutations that influence the tapetum cells surrounding the four-spore tetrad have been involved in cytoplasmic male sterility which completely removes the functionality of the pollen (SCHNABLE AND WISE 1998). Pollen grains may also have deleterious mutations that inhibit their ability to move throughout the five phases of the plant fertilization process where the pollen must first 1) land on a receptive stigma and hydrate the desiccated pollen grain, 2) Germinate the pollen tube, 3) sustain directed pollen tube growth towards the micropyle, 4) leave the transmitting tract and travel through the ovarial cavity, and 5) reach the micropyle and release the two sperm cells (JOHNSON AND PREUSS 2002; SWANSON *et al.* 2004; DRESSELHAUS AND

FRANKLIN-TONG 2013). Additionally, mutants influencing meiosis within the microspore mother cells have been implicated in many male gametophyte mutants.

1.5.1 Cytoplasmic Male Sterility

Cytoplasmic male sterility (CMS) is a maternally inherited trait caused by chimeric repeats in open reading frames of mitochondrial genomes. CMS plants are unable to produce viable pollen but produce fertile female embryos making their use in the hybrid seed industry intriguing. Plants carrying this cytoplasm would not need to be emasculated to prevent self-fertilization. The CMS phenotype has been associated with the premature degradation of the tapetum cell layer surrounding the microspore mother cells in the developing anthers (SCHNABLE AND WISE 1998). Male fertility can be recovered with fertility restorer genes who contain pentatricopeptide repeats that repress cytoplasmic activity (BENTOLILA *et al.* 2002). Three different CMS cytoplasm types have been reported, the -S, -C, and -T. The -S and -C cytoplasm require one dominant restorer, *Rf3* and *Rf4*, respectively, to return fertility. The -T cytoplasm requires *Rf1* and *Rf2* to return fertility (DEWEY *et al.* 1987; LIU *et al.* 2001). The *Rf2* restorer genes encode aldehyde dehydrogenases hypothesized to detoxify acetaldehyde produced during pollen development by ethanolic fermentation, assist in energy metabolism, or directly interact with the proteins causing CMS (CUI *et al.* 1996).

1.5.2 Non-Cytoplasmic Maize Gametophyte Mutants

Numerous male sterile mutants have been described in maize, however, most mutants have only been mapped to chromosomal arms or visualized for distinctive cytological features. These male sterile mutants span across all ten maize chromosomes and include features such as thickened or thinned microspore walls, altered spindle

function, lipid body accumulation in tapetum cells, or arrested nuclear development of microspores (NEUFFER *et al.* 1997). For some of these mutants it is unknown if the male sterility is caused by the cytoplasmic genome or the nuclear genome acting in sporophytic or gametophytic tissues.

The Maize Genetics and Genomics Database records mutants based on their phenotypes, male sterility (https://www.maizegdb.org/data_center/phenotype?id=24992) includes many genes like some *desynaptic1* (*des1*) mutants who have difficulty making the bouquet structure attached to the nuclear envelope during early meiotic prophase (BASS *et al.* 2003). *Multiple archesporial cells1* (*mac1*) over-proliferates archesporial cells before the tapetum cell layer is formed while normally functioning *MAC1* is required for regulated cell proliferation in locule development within the anthers (WANG *et al.* 2012). *Polymitotic1* (*po1,* 6S) mutants showed additional meiotic divisions proceeding meiosis II without additional DNA synthesis steps, leading to complete male sterility and only partial female sterility (WOLFE AND LIU 1999). *Lethal pollen 1* (*lp1,* 4) may potentially be related to *tcb1* or *ga1*, where *lp1* pollen 14 cM away from *sugary1,* shows a disadvantage in achieving fertilization to *Lp1* pollen (NELSON 1981).

Another mutant, *r-x1* is linked to the *r1* locus on the long arm of chromosome 10 in maize and can produce monosomic and trisomic progeny of any of the ten chromosomes. When heterozygous *R*/*r-x1* is crossed as a male pollen parent, *r-x1* does not transmit but the normal *R* transmits normally. Within the female gametophyte, *r-x1* causes nondisjunction at the second megagametophyte division causing monosomic and trisomic megaspores. For the male gametophyte, *r-x1* causes nondisjunction during the

first microspore division and not the second microspore division, resulting in pollen with irregular chromosome numbers who are lethal (ZHAO AND WEBER 1988).

Although some of these genes might not be gametophyte mutations in the sense that their transmission defects are encoded solely by their haploid genomes. Many gametophyte mutations arise from mistakes during the cell division and regulation of diploid sporophytic tissues that give rise to the gametes. These mutants are nevertheless, still valuable to observe and determine how they influence male gametophyte transmission in maize.

1.6 References

Albani, D., I. Altosaar, P. G. Arnison and S. F. Fabijanski, 1991 A gene showing sequence similarity to pectin esterase is specifically expressed in developing pollen of Brassica napus. Sequences in its 5' flanking region are conserved in other pollen-specific promoters. Plant Molecular Biology 16**:** 501-513.

Amien, S., I. Kliwer, M. L. Marton, T. Debener, D. Geiger *et al.*, 2010 Defensin-like ZmES4 mediates pollen tube burst in maize via opening of the potassium channel KZM1. PLoS Biol 8**:** e1000388.

Bannert, M., and P. Stamp, 2007 Cross-pollination of maize at long distance. European Journal of Agronomy 27**:** 44-51.

Bass, H. W., S. J. Bordoli and E. M. Foss, 2003 The desynaptic (dy) and desynaptic1 (dsy1) mutations in maize (Zea mays L.) cause distinct telomere-misplacement phenotypes during meiotic prophase. Journal of Experimental Botany 54**:** 39-46.

Beadle, G. W., 1939 Teosinte and the Origin of Maize. Journal of Heredity 30**:** 245-247.

Bennetzen, J., E. Buckler, V. Chandler, J. Doebley, J. Dorweiler *et al.*, 2001 Genetic Evidence and the Origin of Maize. Society for American Archaeology 12**:** 84-86.

Bentolila, S., A. A. Alfonso and M. R. Hanson, 2002 A pentatricopeptide repeat-containing gene restores fertility to cytoplasmic male-sterile plants. Proc Natl Acad Sci U S A 99**:** 10887-10892.

Bih, F. Y., S. S. H. Wu, C. Ratnayake, L. L. Walling, E. A. Nothnagel *et al.*, 1999 The Predominant Protein on the Surface of Maize Pollen Is an Endoxylanase

Synthesized by a Tapetum mRNA with a Long 5′ Leader. Journal of Biological Chemistry 274**:** 22884-22894.

Bloom, J. C., and J. B. Holland, 2012 Genomic localization of the maize cross-incompatibility gene, Gametophyte factor 1 (ga1) Maydica 56**:** 379-387.

Buckler, E. S., and T. P. Holtsford, 1996 Zea systematics: ribosomal ITS evidence. Mol Biol Evol 13**:** 612-622.

Cui, X., R. P. Wise and P. S. Schnable, 1996 The rf2 nuclear restorer gene of male-sterile T-cytoplasm maize. Science 272**:** 1334-1336.

deWet, J. M. J., L. Engle, C. Grant and S. Tanaka, 1972 Cytology of Maize-Tripsacum Introgression. American Journal of Botany 59**:** 1026-1029.

deWet, J. M. J., and J. R. Harlan, 1974 Tripsacum-maize interaction: a novel cytogenetic system. Genetics 78**:** 493-502.

Dewey, R. E., D. H. Timothy and C. S. Levings, 3rd, 1987 A mitochondrial protein associated with cytoplasmic male sterility in the T cytoplasm of maize. Proceedings of the National Academy of Sciences 84**:** 5374-5378.

Dhonukshe, P., F. Aniento, I. Hwang, D. G. Robinson, J. Mravec *et al.*, 2007 Clathrin-mediated constitutive endocytosis of PIN auxin efflux carriers in Arabidopsis. Current Biology 17**:** 520-527.

Dobritsa, A. A., A. Geanconteri, J. Shrestha, A. Carlson, N. Kooyers *et al.*, 2011 A large-scale genetic screen in Arabidopsis to identify genes involved in pollen exine production. Plant Physiology 157**:** 947-970.

Doebley, J., A. Stec, J. Wendel and M. Edwards, 1990 Genetic and morphological analysis of a maize-teosinte F2 population: implications for the origin of maize. Proceedings of the National Academy of Sciences of the United States of America 87**:** 9888-9892.

Doebley, J. F., M. M. Goodman and C. W. Stuber, 1984 Isoenzymatic Variation in Zea (Gramineae). Systematic Botany 9**:** 203.

Doebley, J. F., M. M. Goodman and C. W. Stuber, 1987 Patterns of isozyme variation between maize and Mexican annual teosinte. Economic Botany 41**:** 234-246.

Dresselhaus, T., and N. Franklin-Tong, 2013 Male-female crosstalk during pollen germination, tube growth and guidance, and double fertilization. Molecular Plant 6**:** 1018-1036.

Elleman, C. J., V. Franklin-Tong and H. G. Dickinson, 1992 Pollination in species with dry stigmas: the nature of the early stigmatic response and the pathway taken by pollen tubes. New Phytologist 121**:** 413-424.

Ellstrand, N. C., L. C. Garner, S. Hegde, R. Guadagnuolo and L. Blancas, 2007 Spontaneous hybridization between maize and teosinte. Journal of Heredity 98**:** 183-187.

Emerson, R. A., 1934 RELATION OF THE DIFFERENTIAL FERTILIZATION GENES, Ga ga, TO CERTAIN OTHER GENES OF THE Su-Tu LINKAGE GROUP OF MAIZE. Genetics 19**:** 137-156.

Eubanks, M. W., 1995 A Cross between Two Maize Relatives: Tripsacum dactyloides and Zea diploperennis (Poaceae). New York Botanical Garden Press 49.

Eubanks, M. W., 1997 Molecular analysis of crosses between Tripsacum dactyloides and Zea diploperennis (Poaceae). Theoretical and Applied Genetics 94**:** 707-712.

Eubanks, M. W., 2001 The Mysterious Origin of Maize. Economic Botany 55**:** 492-514.

Evans, M. M. S., and J. L. Kermicle, 2001 Teosinte crossing barrier1 , a locus governing hybridization of teosinte with maize. Theoretical and Applied Genetics 103**:** 259-265.

Eyre-Walker, A., R. L. Gaut, H. Hilton, D. L. Feldman and B. S. Gaut, 1998 Investigation of the bottleneck leading to the domestication of maize. Proceedings of the National Academy of Sciences 95**:** 4441-4446.

FAOSTAT, 2016 Countries by Commodity, pp. Food and Agriculture Organization of the United Nations.

Frankel, R., S. Izhar and J. Nitsan, 1969 Timing of callase activity and cytoplasmic male sterility in Petunia. Biochemical Genetics 3**:** 451-455.

Halsey, M. E., K. M. Remund, C. A. Davis, M. Qualls, P. J. Eppard *et al.*, 2005 Isolation of maize from pollen-mediated gene flow by time and distance. Crop Science 45**:** 2172-2185.

Han, J. J., D. Jackson and R. Martienssen, 2012 Pod corn is caused by rearrangement at the Tunicate1 locus. Plant Cell 24**:** 2733-2744.

Heslop-Harrison, J., 1982 Pollen-stigma interaction and cross-incompatibility in the grasses. Science 215**:** 1358-1364.

Heslop-Harrison, Y., J. Heslop-Harrison and B. J. Reger, 1985 The Pollen-Stigma Interaction in the Grasses. 7. Pollen-Tube Guidance and the Regulation of Tube Number in Zea Mays L. Acta Botanica Neerlandica 34**:** 193-211.

Hoegemeyer, T. C., 2005 Method of Producing Field Corn Seed and Plants, pp., edited by U. S. Patent. Cerrado Natural Systems Group Inc.,, United States of America.

Hufford, M. B., X. Xu, J. van Heerwaarden, T. Pyhajarvi, J. M. Chia *et al.*, 2012 Comparative population genomics of maize domestication and improvement. Nature Genetics 44**:** 808-811.

James, C., 2015 20th Anniversary of the Global Commercialization of Biotech Crops (1996 to 2015) and Biotech Crop Highlights in 2015, pp.

Jiao, Y., P. Peluso, J. Shi, T. Liang, M. C. Stitzer *et al.*, 2017 Improved maize reference genome with single-molecule technologies. Nature 546**:** 524-527.

Johnson, M. A., and D. Preuss, 2002 Plotting a Course. Developmental Cell 2**:** 273-281.

Jones, Z. G., and M. M. Goodman, 2018 Identification of -Type Gametophyte Factors in Maize Genetic Resources. Crop Science 58.

Kellogg, E. A., and J. A. Birchler, 1993 Linking Phylogeny and Genetics: Zea mays as a Tool for Phylogenetic Studies. Systematic Biology 42**:** 415-439.

Kermicle, J. L., and J. P. Allen, 1990 Cross-incompatibility between maize and teosinte. Maydica 35**:** 399-408.

Kermicle, J. L., and M. M. S. Evans, 2005 Pollen–pistil barriers to crossing in maize and teosinte result from incongruity rather than active rejection. Sexual Plant Reproduction 18**:** 187-194.

Kermicle, J. L., M. M. S. Evans and S. R. Gerrish, 2006 CROSS-INCOMPATIBILITY TRAITS FROM TEOSINTE AND THEIR USE IN CORN, pp. Wisconsin Alumni Research Foundation (Madison, WI, US) United States of America.

Kiesselbach, T. A., 1949 *The Structure and Reproduction of Corn*. University of Nebraska, Lincoln.

Lausser, A., and T. Dresselhaus, 2010 Sporophytic control of pollen tube growth and guidance in grasses. Biochemical Society Transactions 38**:** 631-634.

Lausser, A., I. Kliwer, K. o. Srilunchang and T. Dresselhaus, 2010 Sporophytic control of pollen tube growth and guidance in maize. Journal of Experimental Botany 61**:** 673-682.

Liu, F., X. Cui, H. T. Horner, H. Weiner and P. S. Schnable, 2001 Mitochondrial Aldehyde Dehydrogenase Activity Is Required for Male Fertility in Maize. The Plant Cell 13**:** 1063-1078.

Liu, X., H. Sun, P. Wu, Y. Tian, D. Cui *et al.*, 2014 Fine Mapping of the Maize Cross-Incompatibility Locus Gametophytic factor 1 (ga1) Using a Homogeneous Population. Crop Science 54**:** 873.

Lu, Y., J. L. Kermicle and M. M. Evans, 2014 Genetic and cellular analysis of cross-incompatibility in Zea mays. Plant Reproduction 27**:** 19-29.

Ma, B. L., K. D. Subedi and L. M. Reid, 2004 Extent of cross-fertilization in maize by pollen from neighboring transgenic hybrids. Crop Science 44**:** 1273-1282.

Mangelsdorf, P. C., and D. F. Jones, 1926 THE EXPRESSION OF MENDELIAN FACTORS IN THE GAMETOPHYTE OF MAIZE. Genetics 11**:** 423-455.

Mangelsdorf, P. C., and R. G. Reeves, 1938 The Origin of Maize. Proceedings of the National Academy of Sciences 24**:** 303-312.

Mangelsdorf, P. C., and R. G. Reeves, 1939 *The origin of Indian corn and its relatives*. Texas Agricultural Experiment Station.

Marton, M. L., S. Cordts, J. Broadhvest and T. Dresselhaus, 2005 Micropylar pollen tube guidance by egg apparatus 1 of maize. Science 307**:** 573-576.

Marton, M. L., A. Fastner, S. Uebler and T. Dresselhaus, 2012 Overcoming hybridization barriers by the secretion of the maize pollen tube attractant ZmEA1 from Arabidopsis ovules. Current Biology 22**:** 1194-1198.

Matsuoka, Y., Y. Vigouroux, M. M. Goodman, G. J. Sanchez, E. Buckler *et al.*, 2002 A single domestication for maize shown by multilocus microsatellite genotyping. Proceedings of the National Academy of Sciences 99**:** 6080-6084.

Messerli, M. A., R. Creton, L. F. Jaffe and K. R. Robinson, 2000 Periodic increases in elongation rate precede increases in cytosolic Ca2+ during pollen tube growth. Developmental Biology 222**:** 84-98.

Messerli, M. A., and K. R. Robinson, 1997 Tip localized Ca2+ pulses are coincident with peak pulsatile growth rates in pollen tubes of Lilium longiflorum. Journal of Cell Science 110 (Pt 11)**:** 1269-1278.

Moran Lauter, A. N., M. G. Muszynski, R. D. Huffman and M. P. Scott, 2017 A Pectin Methylesterase ZmPme3 Is Expressed in Gametophyte factor1-s (Ga1-s) Silks and Maps to that Locus in Maize (Zea mays L.). Frontiers in Plant Science 8**:** 1-11.

Moscatelli, A., F. Ciampolini, S. Rodighiero, E. Onelli, M. Cresti *et al.*, 2007 Distinct endocytic pathways identified in tobacco pollen tubes using charged nanogold. Journal of Cell Science 120**:** 3804-3819.

Nelson, O. E., 1994 *The Gametophyte Factors of Maize*. Springer-Verlag, New York.

Nelson, O. E., Jr., 1960 The Fourth Chromosome Factor in Some Central and South American Races. Maize Genetics Cooperation News Letter 34**:** 114-116.

Nelson, O. E., Jr., 1981 A reexamination of the Aberrant Ratio phenomenon Maize Genetics Cooperation Newsletter 55**:** 68-73.

Neuffer, M. G., E. H. Coe and S. R. Wessler, 1997 *Mutants of Maize*. Cold Spring Harbor Laboratory Press, New York.

Parton, R. M., S. Fischer-Parton, M. K. Watahiki and A. J. Trewavas, 2001 Dynamics of the apical vesicle accumulation and the rate of growth are related in individual pollen tubes. Journal of Cell Science 114**:** 2685-2695.

Picton, J. M., and M. W. Steer, 1983 Membrane recycling and the control of secretory activity in pollen tubes. Journal of Cell Science 63**:** 303-310.

Pierson, E. S., D. D. Miller, D. A. Callaham, J. van Aken, G. Hackett *et al.*, 1996 Tip-localized calcium entry fluctuates during pollen tube growth. Developmental Biology 174**:** 160-173.

Schnable, P., and R. P. Wise, 1998 The molecular basis of cytoplasmic male sterility and fertility restoration. Trends in Plant Science 3**:** 175-180.

Schwartz, D., 1950 The analysis of a case of cross-sterility in maize. Proceedings of the National Academy of Sciences 36**:** 719-724.

Steinhorst, L., and J. Kudla, 2013 Calcium - a central regulator of pollen germination and tube growth. Biochimica et Biophysica Acta 1833**:** 1573-1581.

Sturtevant, E. L., 1881 The superabundace of pollen in Indian corn. American Naturalist 15**:** 1000.

Suen, D. F., and A. H. Huang, 2007 Maize pollen coat xylanase facilitates pollen tube penetration into silk during sexual reproduction. Journal of Biological Chemistry 282**:** 625-636.

Suen, D. F., S. S. Wu, H. C. Chang, K. S. Dhugga and A. H. Huang, 2003 Cell wall reactive proteins in the coat and wall of maize pollen: potential role in pollen tube growth on the stigma and through the style. Journal of Biological Chemistry 278**:** 43672-43681.

Swanson, R., A. F. Edlund and D. Preuss, 2004 Species specificity in pollen-pistil interactions. Annual Review of Genetics 38**:** 793-818.

Taiz, L., and E. Zeiger, 2002 *Plant Physiology*. Sinauer Associates.

Tian, Y., S. Xiao, J. Liu, Y. Somaratne, H. Zhang *et al.*, 2017 MALE STERILE6021 (MS6021) is required for the development of anther cuticle and pollen exine in maize. Scientific Reports 7**:** 16736.

Wang, C. J., G. L. Nan, T. Kelliher, L. Timofejeva, V. Vernoud *et al.*, 2012 Maize multiple archesporial cells 1 (mac1), an ortholog of rice TDL1A, modulates cell proliferation and identity in early anther development. Development 139**:** 2594-2603.

Weatherwax, P., 1918 The Evolution of Maize. Bulletin of the Torrey Botanical Club 45**:** 309-342.

Weatherwax, P., 1935 The Phylogeny of Zea Mays. American Midland Naturalist 16**:** 1.

Weatherwax, P., and L. F. Randolph, 1955 *History and Origin of Corn*. Academic Press Inc., New York.

Wing, R. A., J. Yamaguchi, S. K. Larabell, V. M. Ursin and S. McCormick, 1990 Molecular and genetic characterization of two pollen-expressed genes that have sequence similarity to pectate lyases of the plant pathogen Erwinia. Plant Molecular Biology 14**:** 17-28.

Wolfe, K. W., and Q. Liu, 1999 The maize mutant polymitotic affects cell cycle events during microspore development. Planta 210**:** 27-33.

Wolters-Arts, M., W. M. Lush and C. Mariani, 1998 Lipids are required for directional pollen-tube growth. Nature 392**:** 818-821.

Wu, S. S., D. F. Suen, H. C. Chang and A. H. Huang, 2002 Maize tapetum xylanase is synthesized as a precursor, processed and activated by a serine protease, and deposited on the pollen. Journal of Biological Chemistry 277**:** 49055-49064.

Zhang, H., X. Liu, Y. Zhang, C. Jiang, D. Cui *et al.*, 2012 Genetic analysis and fine mapping of the Ga1-S gene region conferring cross-incompatibility in maize. Theoritical Applied Genetics 124**:** 459-465.

Zhao, Z. Y., and D. F. Weber, 1988 Analysis of Nondisjunction Induced by the R-X1 Deficiency during Microsporogenesis in Zea Mays L. 119 4.

Chapter 2: Identification of QTLs Modifying the Activity of the *Tcb1-s* Locus

2.1 Abstract

Teosinte crossing barrier 1 (*Tcb1*) is a unilateral cross-incompatibility system present in maize that provides a pre-zygotic pistil barrier to plants carrying *Tcb1-s* (strong allele) from pollen not carrying that allele (*tcb1*), the reciprocal cross however, is successful. Due to this pollen specificity, *Tcb1-s* can be useful to organic, sweet corn, or maize landrace farmers wanting to prevent cross-contamination from occurring between fields. It was observed that the *Tcb1-s* locus does not work alone and requires the action of modifiers to confer a stronger pistil barrier. Such modifiers are present in the F1s of the maize inbred lines B73 and Mo17 who are polymorphic in *Tcb1-s* activity. In this study QTL modifying the *Tcb1-s* locus were tracked using the F1s of the intermated B73 Mo17 recombinant inbred lines with W22 *Tcb1-s*/*Tcb1-s*. The ability of the *Tcb1-s* pistils to reject *tcb1* pollen containing a *R1 C1* color marker on day one and accept its own self-type pollen on day two was measured using a standardized scale. A total of eight QTLs were detected on chromosomes 2S, 2L, 3S, 4S, 7S, 7L, 8L, and 10L explaining a total of 34.8% of the overall phenotypic variability. Knowledge of the QTL interacting with *Tcb1-s* could assist in the introgression of both *Tcb1-s* and positive acting modifiers so that *Tcb1-s* activity is maintained.

2.2 Introduction

Maize is one of the most widely grown cereal crops grown in the world, covering an estimated 226 million hectares and harvesting one billion tons a year (FAOSTAT 2016). Of this land, almost one-fourth (60 million hectares) were used to grow maize that

has been genetically engineered to confer resistance to insect attacks, herbicides, or drought resistance (ISAAA 2016). With the growing prevalence of genetically modified crops, many organic farmers as well as farmers of maize high in amylose, sweet corn, or colored varieties used in cooking can be affected by unwanted cross-contamination between fields (NELSON 1994). It has previously been shown that cross-contamination between maize fields can occur at low rates up to 600-700 meters away (HALSEY *et al.* 2005; BANNERT AND STAMP 2007). Although most cross-contamination drops off after 60-125 meters, farmers with fields surrounding unwanted pollen sources could be directly affected (HALSEY *et al.* 2005). Currently to avoid cross-contamination farmers separate their fields, displace planting times, or place barrier crops (MA *et al.* 2004; HALSEY *et al.* 2005). These methods are laborious and sometimes difficult to achieve, which opens the possibility for the use of naturally occurring genetic cross-incompatibility systems to prevent cross-contamination.

Cross-incompatibility (CI) is a pre-zygotic fertilization barrier that prevents pollen from a foreign pollen source from successfully fertilizing an egg, however, the outcross is fertile. Hybridization is only successful when a recognized, or self-type pollen is received. The *Gametophyte factor 1* (*ga1*) and *Teosinte crossing barrier 1* (*tcb1*) are two maize CI systems that work in a manner similar to each other. A ‘strong’ dominant allele (-*s*), when present in the pistil, can reject pollen containing the recessive allele and only accepts its own ‘-s’ allele pollen or the male-allele pollen (-*m*). The male allele (-*m*) works in the pollen grain to overcome the female barrier in the pistil but can be fertilized by any other pollen alleles types (NELSON 1994). The recessive allele (i.e., *ga1*, *tcb1*) accepts any other pollen allele type. When both the strong allele and recessive allele are

present in functionally diploid heteroallelic pollen and applied to homozygous *Tcb1-s* or *Ga1-s* silks fertilization takes place, suggesting that the matching allele is required within the pistils and that active rejection of incompatible alleles is not taking place (KERMICLE AND EVANS 2005).

Ga1 was initially discovered when a Rice Popcorn strain was crossed with *sugary1*. Aberrant F2 ratios when backcrossing onto the Rice Popcorn arose and was later attributed to a dominant, gametophyte acting gene 35 cM away from *sugary1* on the short arm of chromosome 4 that conferred a competitive advantage of *Ga1-s* pollen over *ga1* when added to *ga1*/*Ga1-s* or *Ga1-s/Ga1-s* pistils (MANGELSDORF AND JONES 1926; EMERSON 1934; SCHWARTZ 1950). Since *Ga1-s* and *Tcb1-s* pollen is commonly found in Central and Southern American maize and not among midwestern dents, these CI systems can be employed to prevent cross-contamination between populations (NELSON 1960).

Transcriptomic studies of the *Ga1-s* locus have revealed *ZmPme3,* a gene for pectinesterase (PME), upregulated in *Ga1-s* but not *ga1* pistils, which maps to the *Ga1-s* locus (BLOOM AND HOLLAND 2012; ZHANG *et al.* 2012; LIU *et al.* 2014; MORAN LAUTER *et al.* 2017). Interestingly, the region surrounding the *Ga1-s* locus contains fifty-eight partial to full-length PME-like sequence repeats within a 1.1 Mb region. Of these fifty-eight PME-like sequences, the only transcript that was differentially expressed in the *Ga1-s* pistils had a full-length open reading frame.

Teosinte crossing barrier 1, 44 cM proximal to *ga1* and 6 cM distal to *sugary1* on the short arm of chromosome 4 (EVANS AND KERMICLE 2001; LU *et al.* 2014) was identified in *Zea mays spp. mexicana* (KERMICLE AND ALLEN 1990). The Teosinte

Incompatibility Complex originating from the Central Plateau (TIC-CP) rejects *ga1, Ga1-s, Ga1-m, TIC-Chalco,* and, surprisingly only accepts its own pollen in a limited regard. The separate incompatibility complexes were found for the TIC-CP locus. The TIC-CP1 complex acts in a fashion similar to *Ga1-m*. The second complex, TIC-CP2 can pollinate pistils conferring the female function but cannot fertilize *Ga1-s/Ga1-s* pistils.

It has been suggested that the *Tcb1-s* locus relies on a modifying factor to function properly and confer a strong resistance to *tcb1* pollen. Repeated backcrossing to W22 for ten generations showed a decline in *Tcb1-s* activity which could be attributed either to the loss of positive modifiers or to epigenetic silencing of the locus (LU *et al.* 2014). Although epigenetics may play a role in the loss of the *Tcb1-s* function, the presence of modifying loci can be observed by comparing the efficacy of *Tcb1-s* in the F1s of W22 *Tcb1-s* with B73 and Mo17 (Kermicle, personal communication). F1s of W22 *Tcb1-s* with B73 have a higher resistance to incompatible pollen (*tcb1*) while F1s of Mo17 with *Tcb1-s* have a weaker resistance (Figure 2.1). The difference that exists between B73 and Mo17 suggests employing intermated B73 and Mo17 (IBM) recombinant inbred lines (RIL) to find quantitative trait loci (QTL) that modify *Tcb1-s* activity. Because *Tcb1-s* is a dominant allele in sporophytic pistillate tissue, heterozygosity at the *tcb1* locus will not be an issue. Identification of modifying QTL may lead to insight on the behavior and molecular mechanisms of the *Tcb1-s* system and provide insight for plant breeders on other loci that need to maintain complete *Tcb1-s* activity.

2.3 Materials and Methods

2.3.1 Plant Materials

IBM RILs were generated by LEE *et al.* (2002). Briefly, the inbred lines B73 and Mo17 were hybridized to form an F1 that was self-pollinated. The F2s were intermated for four generations to create the recombinant inbred lines. Intermating, or the crossing between the B73 and Mo17 individuals increases the number of recombination events occurring between loci, potentially breaking chromosomal regions that previously showed tight linkage. Genetic stocks were obtained from the Maize Genetic Cooperation Stock Center. Of the 94 lines constituting the IBM main set, F1s were successfully made with 77 RILs. The W22 *Tcb1-s/Tcb1-s* line was provided by Jerry Kermicle. This line was made by crossing W22 with *Zea mays* spp. *Mexicana* and backcrossing to W22 for six to eight times. Stocks provided by Kermicle carry two observed modifiers, one that carries the *Ga1-m* like allele at the *Tcb1-s* locus and another modifier of unknown function and location. When the *Ga1-m* like allele is lost from the *Tcb1-s* locus the *Tcb1-s* pistil incompatibility barrier decreases (Kermicle, personal communication).

2.3.2 Field Design

The 77 IBM F1s and the parental B73 and Mo17 F1s derived from the cross of IBM RIL x W22 *Tcb1-s*/*Tcb1-s* were planted in 13 kernel rows in research plots of South Dakota State University, Brookings, SD in May 2017. Pollen parents containing colored *R1 C1 tcb1* and colorless *r1 c1 Tcb1-s* pollen were planted through a series of delays to provide sufficient pollen throughout the experiment. Five F1 plants from each RIL F1 were tested for their *Tcb1-s* strength by pollinating the pistils with *R1 C1 tcb1* pollen a full 24 hours before pollination by *r1 c1 Tcb1-s* pollen (Figure 2.2). Two additional

control pollinations were also generated: one IBM x W22 *Tcb1-s* F1 plant pollinated solely with *R1-C1 tcb1* pollen and another solely with *r1-c1 Tcb1-s* pollen.

2.3.3 Phenotyping

The mean percent contamination for each F1 RIL was calculated by the number of kernels resulting from an *R1 C1 tcb1* pollination over the total number of kernels on the ear. The kernels at the topmost 5 cm of the ear were not counted, as they may have been contaminants from late emerging pistils. For each F1 plant tested, this contamination data was translated into a standardized scale of contamination from 0-5, where 0 = no colored kernels, 1 = up to 4% colored, 2 = up to 8% colored, 3 = up to 16% colored, 4 = up to 32% colored, and 5 = greater than 32% colored. This method of scoring was chosen to indicate fold-changes.

2.3.4 QTL Mapping

We mapped QTL for modifiers of the *Tcb1-s* locus using the existing IBM-302 genetic map obtained from the Maize Genetics and Genomics Database (https://www.maizegdb.org/mapscore_ibm302score) that was previously described and genotyped (COE *et al.* 2002; CONE *et al.* 2002; LEE *et al.* 2002). The RILs contain 2178 markers spread across the ten maize chromosomes. QTLs were mapped using R/qtl (BROMAN *et al.* 2003). A genome-wide significance threshold (LOD) was estimated using 1,000 permutations and an alpha level of $\alpha = 0.05$. Genotype probabilities were calculated using the Kosambi mapping function and QTL scans were performed using the extended Haley-Knott regression for its robustness and ability to handle selective genotyping (BROMAN AND SEN 2009). The presence of single, unlinked QTL, as well as two-dimensional and multiple-QTL analyses were explored to search for the presence of

multiple, linked QTL. For each modifying QTL, the top marker nearest to the QTL peak was selected and its estimated genetic map coordinates were taken from the Maize Genetics and Genomics Database. Genes falling within this candidate interval were translated into B73 RefGen_v4 coordinates and explored in further detail. QTL results are based on LOD scores, marker confidence intervals, and the percentage of variation explained (R^2).

2.4 Results

QTL mapping of *Tcb1-s* modifiers using the binned contamination data in the IBM population found eight QTL explaining 34.8% of the phenotypic variability (Table 2.1, Table 2.2, and Figure 2.4). Two QTL were located on chromosome 2 (2S and 2L, Figure 2.5), one QTL was found on the short arm of chromosome 3 (3S, Figure 2.6), one QTL on the short arm of chromosome 4 (4S, Figure 2.7), two QTLs on chromosome 7 (7S and 7L, Figure 2.8), one QTL on the long arm of chromosome 8 (8L, Figure 2.9), and one QTL on the long arm of chromosome 10 (10L, Figure 2.10). The F1s of the founder B73 and Mo17 both showed high incompatibility responses where B73 showed μ = 0.037% contamination and Mo17 showed μ = 1.35% contamination.

These eight QTLs explained small portions of the total phenotypic variability ranging from 0.86% (q-*Tcb1-s*-5; umc1546) on chromosome 7S to 4.8% (q-*Tcb1-s*-3; umc2263) on chromosome 3S, with a mean of 2.52%, suggesting that no single QTL has a large influence of *Tcb1-s* activity. LOD scores ranged from 1.21 (q*Tcb1-s*-5; umc1546) to 1.43 (q*Tcb1-s*-8; umc2021). A LOD threshold based on 1000 permutations using the Hayley-Knott regression set the genome-wide LOD threshold at 2.97 for α = 0.05, and 2.65 for α = 0.10. No QTLs in this study surpassed these LOD thresholds. A reduced 1-

LOD confidence interval for each QTL roughly began at the short arm of each chromosome and ended at the end of the long arm of each chromosome (Table 2.1).

Of the eight QTL, three showed the expected parental allele contribution where plants homozygous for the B73 allele lead to higher *Tcb1-s* resistance over the Mo17 alleles (q*Tcb1-s*-1, q*Tcb1-s*-4, q*Tcb1-s*-5; Table 2.1). Surprisingly, five loci (q*Tcb1-s*-2, q*Tcb1-s*-3, q*Tcb1-s*-6, q*Tcb1-s*-7, and q*Tcb1-s*-8) showed transgressive effects, where plants homozygous for the Mo17 allele conferred a higher resistance to *tcb1* pollen. Of the twenty-eight possible interactions between these loci, twenty-four show simple additivity when coupled together (data not shown). The four remaining loci pairs, namely *qTcb1-s*-1:q*Tcb1-s*-7, q*Tcb1-s*-2:q*Tcb1-s*-3, q*Tcb1-s*-3:q*Tcb1-s*-8, q*Tcb1-s*-4:q*Tcb1-s*-6 show evidence for possible interactions where either one copy of the B73 or Mo17 allele causes an irregular phenotype (**Error! Reference source not found.**). In the q*Tcb1-s*-2:q*Tcb1-s*-3 (**Error! Reference source not found.**B) and q*Tcb1-s*-3:q*Tcb1-s*-8 (**Error! Reference source not found.**C) interactions, plants with at least one copy of the Mo17 allele confers a higher resistance to *tcb1* pollen relative to plants homozygous for the B73 alleles.

For the interactions between the QTL pairs *qTcb1-s*-1:q*Tcb1-s*-7 and q*Tcb1-s*-4:q*Tcb1-s*-6 (**Error! Reference source not found.**A & D, respectively), plants homozygous for B73, homozygous for Mo17, and heterozygous for B73 at the first peak QTL marker and Mo17 at the second peak QTL marker all show strong resistance phenotypes. The third genotype that is heterozygous for Mo17 at the first peak QTL position and B73 at the second peak QTL position show weak resistance phenotypes, suggesting that allelic interactions between certain pairs of loci make a difference in

Tcb1-s resistance. The estimated genomic locations and the number of predicted genes is summarized in Table 2.3 and Table 2.4. Candidate genes for q*Tcb1-s*-3 were not obtained due to the large genetic interval estimate provided by *umc2263*.

To ensure that there was not an inbred-specific cross-incompatibility mechanism working between B73 and Mo17 in the absence of *Tcb1-s*, the inbred lines were tested separately. Pollen from a B73 *R-scm2* parent and a colorless Mo17 parent were mixed and applied to B73 and Mo17 ears. There was a slight difference in the proportion of resulting kernels suggesting a preference of self-type pollen in each inbred line (Figure 2.12).

2.5 Discussion

It has previously been observed that *Tcb1-s* relies on the activity of positive modifiers to function as a strong incompatibility barrier to foreign *tcb1* pollen (KERMICLE AND ALLEN 1990; LU *et al.* 2014). In this study, modifiers of the *Teosinte crossing barrier 1* locus were mapped using F1 hybrids of *Tcb1-s* with the intermated B73 x Mo17 recombinant inbred lines. A total of eight QTLs were detected explaining a total of 34.8% of the overall phenotypic variability. Of these, q*Tcb1-s*-1 (2S), q*Tcb1-s*-3 (3S), q*Tcb1-s*-7 (8L) explained almost one-third of this variation (12.36%). The numerous QTL influencing *Tcb1-s* behavior is consistent with the model that complex traits in maize are not controlled by single, large effect QTL but are instead controlled by numerous QTL having additive effects (BUCKLER *et al.* 2009).

The QTL on the short arm of chromosome two mapped to a 289 Kb region containing nine protein-coding genes (Table 2.3). Of these candidates, a subtilisin-like

protease which are serine proteases that may be involved in the degradation of foreign pollen. In rice, subtilisin-like proteases are highly expressed in reproductive tissues but their function is unknown (YOSHIDA AND KUBOYAMA 2001). In developing Arabidopsis seeds, a subtilisin-like protease is necessary for triggering the accumulation or activation of cell wall modification enzymes like pectin methylesterase (RAUTENGARTEN *et al.* 2008), however, a similar pistil-based action of these subtilisin-like proteases has not yet been discovered. Other candidate genes near peak QTL positions showed cell wall synthesis enzymes, transcription factors, and numerous uncharacterized gene models.

One QTL mapped to the short arm of chromosome 4 (q*Tcb1-s*-4) in the estimated location of the *tcb1* locus mapped previously (EVANS AND KERMICLE 2001; LU *et al.* 2014). The marker at this locus, *umc2061* maps to a 9.5 Mb region containing 514 genes. Unfortunately, only 147 genes remained after the conversion from B73 RefGen_v3 to B73 RefGen_v4 for gene annotation purposes. Of these 147 genes, a *pectinesterase inhibitor 28* (*PMEI-28*, Zm00001d049722) was found. This pectinesterase inhibitor may be the result of the *Ga1-m* like allele whose activity was thought to be crucial for strengthening the *Tcb1-s* pistil barrier (Kermicle, personal communication). In the *Gametophyte factor 1* cross-incompatibility system, a *pectin methylesterase 38* transcript upregulated in *Ga1-s* and not *ga1* pistils was associated with the rejection of foreign pollen in *Ga1-s* pistils (MORAN LAUTER *et al.* 2017). *PMEI-28* transcripts are upregulated in B73 pistil tissues without the presence of *Tcb1-s* (WALLEY *et al.* 2016). This suggests that there may be another allele of *PMEI-28* acting from the *Tcb1-s* locus specific to *Tcb1-s* pistil behavior or it is the action of another uncharacterized or lost gene model from the conversion of B73 RefGen_v3 to RefGen_v4 conferring *Tcb1-s* activity. A

functional gene within the B73 reference may not even be present at the *Tcb1-s* locus because the locus was introduced via backcrossing from *Zea mays mexicana* (KERMICLE AND ALLEN 1990).

Although numerous QTLs were found that may modify *Tcb1-s* activity they all had relatively low LOD scores that did not pass the genome-wide significance threshold. Although a broad range of phenotypes was observed (Figure 2.3), the results may be attributed to the small population size that was tested. The complete IBM population contains 302 individuals of which only 77 were tested in this study. Although the results presented here provide a good survey of the behavior surrounding *Tcb1-s*, additional analysis is necessary of the larger IBM population.

A similar study looking for modifiers of the *Ga1-s* locus in the NAM B73 x M162w RILs found two QTL peaks on 5L and 10L (SHRESTHA 2016). The QTL on 10L in the B73 x M162w lines maps to the same general region as the QTL shown to modify *Tcb1-s* activity also on 10L. The 10L B73 x M162w explained a total of 12% of the phenotypic variability and mapped to PZA02390.1 while the 10L IBM QTL explained 2.91% of the phenotypic variability and mapped *umc2021.* It is currently unknown if the underlying genes are similar and both work to enhance cross-incompatibility responses in *Ga1-s* and *Tcb1-s*.

In this study, eight QTLs that may modify the pistil based *Tcb1-s* cross-incompatibility system were mapped to chromosomes 2S, 2L, 3S, 4S, 7S, 7L, 8L, and 10L in the IBM population. Cumulatively these QTL explained 34.8% of the phenotypic variability. Further investigation is needed to test how the parental B73 and Mo17 alleles contribute to the performance of these eight individual QTL and determine their

molecular interactions with *Tcb1-s* that provide a stronger or weaker incompatibility response. Knowledge of interactions between modifying QTL and *Tcb1-s* could help inform plant breeding programs to ensure that the positive modifiers are maintained during the introgression of the *Tcb1* cross-incompatibility system into other maize varieties so that its activity is maintained (LU *et al.* 2014).

2.6 References

Bannert, M., and P. Stamp, 2007 Cross-pollination of maize at long distance. European Journal of Agronomy 27**:** 44-51.

Bloom, J. C., and J. B. Holland, 2012 Genomic localization of the maize cross-incompatibility gene, Gametophyte factor 1 (ga1) Maydica 56**:** 379-387.

Broman, K. W., and S. Sen, 2009 *A Guide to QTL Mapping with R/qtl*. Springer, New York.

Broman, K. W., H. Wu, S. Sen and G. A. Churchill, 2003 R/qtl: QTL mapping in experimental crosses. Bioinformatics 19**:** 889-890.

Buckler, E. S., J. B. Holland, P. J. Bradbury, C. B. Acharya, P. J. Brown *et al.*, 2009 The genetic architecture of maize flowering time. Science 325**:** 714-718.

Coe, E., K. Cone, M. McMullen, S. S. Chen, G. Davis *et al.*, 2002 Access to the Maize Genome: An Integrated Physical and Genetic Map. Plant Physiology 128**:** 9-12.

Cone, K. C., M. D. McMullen, I. V. Bi, G. L. Davis, Y. S. Yim *et al.*, 2002 Genetic, physical, and informatics resources for maize. On the road to an integrated map. Plant Physiology 130**:** 1598-1605.

Emerson, R. A., 1934 RELATION OF THE DIFFERENTIAL FERTILIZATION GENES, Ga ga, TO CERTAIN OTHER GENES OF THE Su-Tu LINKAGE GROUP OF MAIZE. Genetics 19**:** 137-156.

Evans, M. M. S., and J. L. Kermicle, 2001 Teosinte crossing barrier1 , a locus governing hybridization of teosinte with maize. Theoretical and Applied Genetics 103**:** 259-265.

FAOSTAT, 2016 Countries by Commodity, pp. Food and Agriculture Organization of the United Nations.

Halsey, M. E., K. M. Remund, C. A. Davis, M. Qualls, P. J. Eppard *et al.*, 2005 Isolation of maize from pollen-mediated gene flow by time and distance. Crop Science 45**:** 2172-2185.

ISAAA, 2016 *Global Status of Commercialized Biotech/GM Crops: 2016. ISAAA Brief No. 52*. The International Service for the Acquisition of Agri-biotech Applications (ISAAA), Ithaca, New York.

Kermicle, J. L., and J. P. Allen, 1990 Cross-incompatibility between maize and teosinte. Maydica 35**:** 399-408.

Kermicle, J. L., and M. M. S. Evans, 2005 Pollen–pistil barriers to crossing in maize and teosinte result from incongruity rather than active rejection. Sexual Plant Reproduction 18**:** 187-194.

Lee, M., N. Sharopova, W. D. Beavis, D. Grant, M. Katt *et al.*, 2002 Expanding the genetic map of maize with the intermated B73 × Mo17 (IBM) population. Plant Molecular Biology 48**:** 453-461.

Liu, X., H. Sun, P. Wu, Y. Tian, D. Cui *et al.*, 2014 Fine Mapping of the Maize Cross-Incompatibility Locus Gametophytic factor 1 (ga1) Using a Homogeneous Population. Crop Science 54**:** 873.

Lu, Y., J. L. Kermicle and M. M. Evans, 2014 Genetic and cellular analysis of cross-incompatibility in Zea mays. Plant Reproduction 27**:** 19-29.

Ma, B. L., K. D. Subedi and L. M. Reid, 2004 Extent of cross-fertilization in maize by pollen from neighboring transgenic hybrids. Crop Science 44**:** 1273-1282.

Mangelsdorf, P. C., and D. F. Jones, 1926 THE EXPRESSION OF MENDELIAN FACTORS IN THE GAMETOPHYTE OF MAIZE. Genetics 11**:** 423-455.

Moran Lauter, A. N., M. G. Muszynski, R. D. Huffman and M. P. Scott, 2017 A Pectin Methylesterase ZmPme3 Is Expressed in Gametophyte factor1-s (Ga1-s) Silks and Maps to that Locus in Maize (Zea mays L.). Frontiers in Plant Science 8**:** 1-11.

Nelson, O. E., 1994 *The Gametophyte Factors of Maize*. Springer-Verlag, New York.

Nelson, O. E., Jr., 1960 The Fourth Chromosome Factor in Some Central and South American Races. Maize Genetics Cooperation News Letter 34**:** 114-116.

Rautengarten, C., B. Usadel, L. Neumetzler, J. Hartmann, D. Bussis *et al.*, 2008 A subtilisin-like serine protease essential for mucilage release from Arabidopsis seed coats. Plant Journal 54**:** 466-480.

Schwartz, D., 1950 The analysis of a case of cross-sterility in maize. Proceedings of the National Academy of Sciences 36**:** 719-724.

Shrestha, V., 2016 The search for modifiers of the maize gametophyte factor Ga1-s and Quantitative trait polymorphisms emerging from doubled-haploid maize lines, pp. 1-78 in *Biology and Microbiology*. South Dakota State University, Brookings, SD.

Walley, J. W., R. C. Sartor, Z. Shen, R. J. Schmitz, K. J. Wu *et al.*, 2016 Integration of omic networks in a developmental atlas of maize. Science 353**:** 814-818.

Yoshida, K. T., and T. Kuboyama, 2001 A subtilisin-like serine protease specifically expressed in reproductive organs in rice. Sexual Plant Reproduction 13**:** 193-199.

Zhang, H., X. Liu, Y. Zhang, C. Jiang, D. Cui *et al.*, 2012 Genetic analysis and fine mapping of the Ga1-S gene region conferring cross-incompatibility in maize. Theoritical Applied Genetics 124**:** 459-465.

2.7 Figures – *Tcb1-s* Project

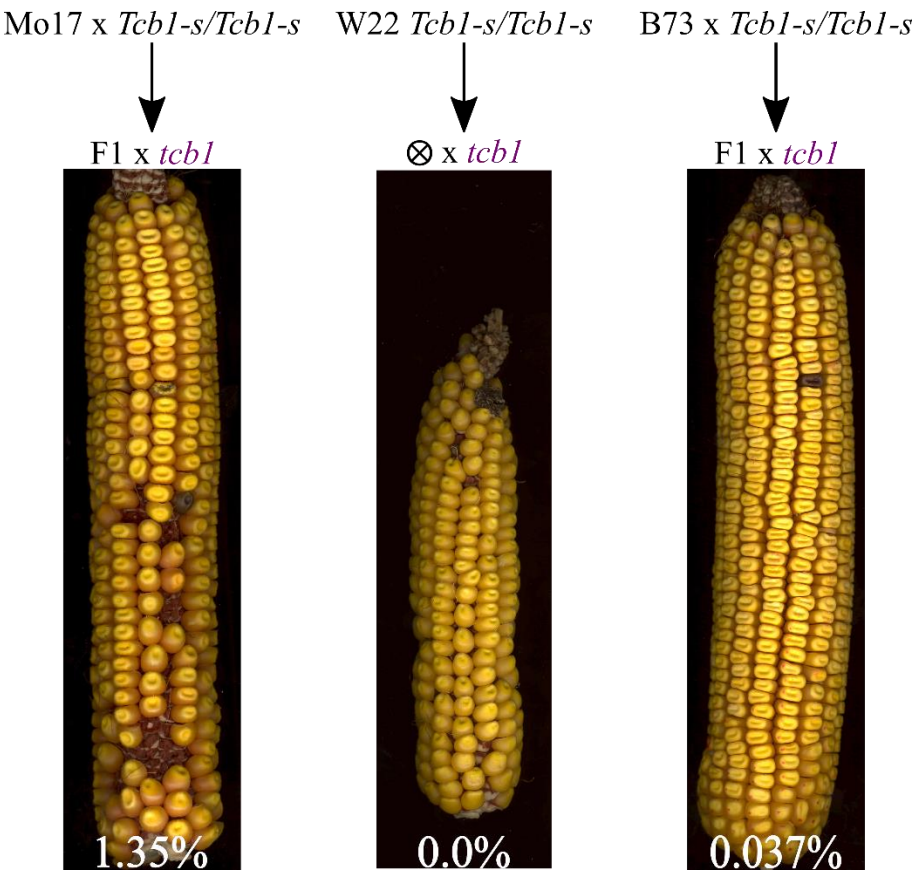

Figure 2.1. Responses of W22 Tcb1-s, B73 F1s, and Mo17 F1s with Tcb1-s.

B73 and Mo17 F1s with *Tcb1-s* show a small, yet noticeable difference in their *tcb1* incompatibility response, making the Intermated B73-Mo17 population a good candidate for *Tcb1-s* modifying QTL detection.

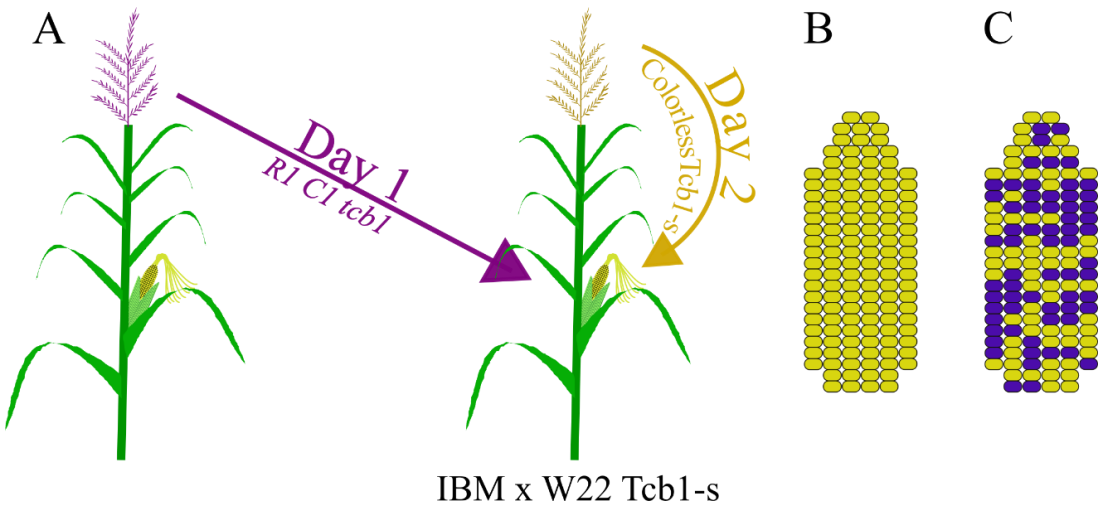

Figure 2.2. Experimental design to test for modifiers of the Tcb1-s locus.

A) Experimental crossing design where on day 1, IBM x *Tcb1-s* would be tested with *R1 C1 tcb1* pollen and on day 2 the plants would be selfed with colorless *Tcb1-s* pollen. B) An example ear with a strong incompatibility to the *R1 C1 tcb1* pollen. C) An example ear with a weak incompatibility to the *R1 C1* tcb1 pollen.

Figure 2.3. Standardized scale for binning IBM x Tcb1-s F1 tested ears.

From left to right: 0 = no colored kernels, 1 = up to 4% colored, 2 = up to 8% colored, 3 = up to 16% colored, 4 = up to 32% colored, and 5 = greater than 32% colored.

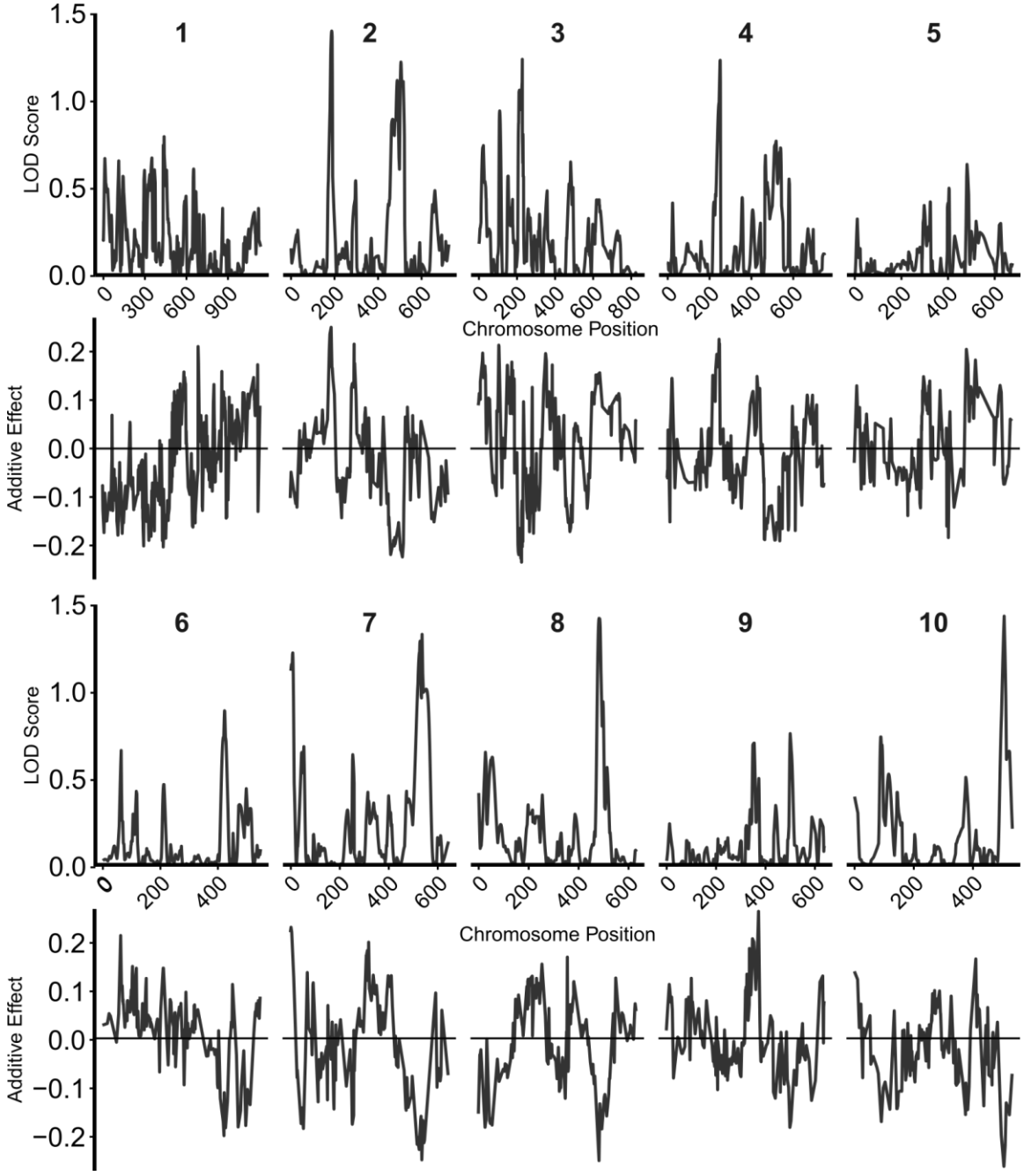

Figure 2.4. QTL map for modifiers of the Tcb1-s locus.

Facets indicate separate chromosomes. The recombination fraction for each marker position is shown along the x-axis. Eight QTL peaks on chromosomes 2S, 3S, 4S, 7S, 7L, 8L, and 10L explained 38.4% of the phenotypic variability.

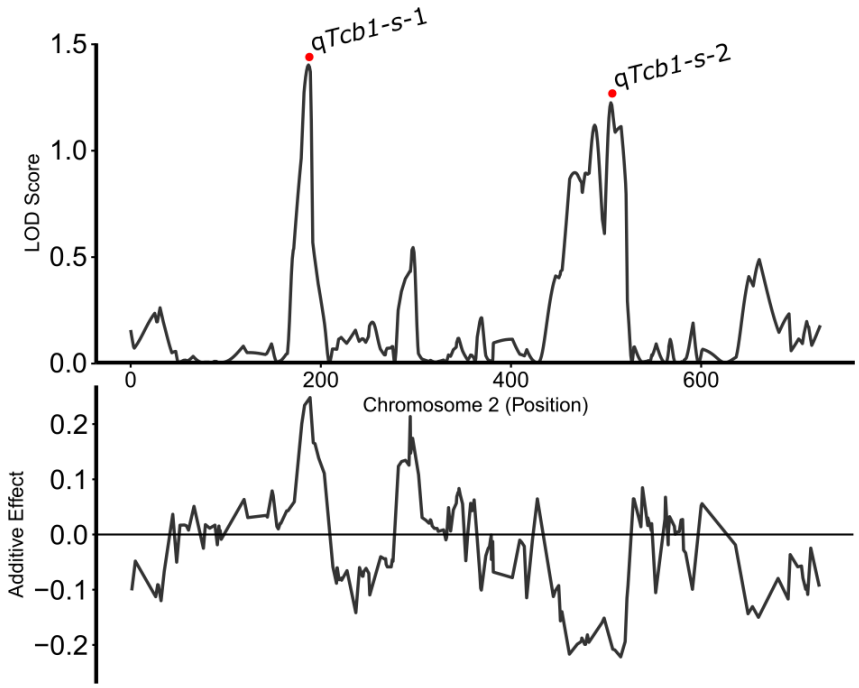

Figure 2.5. QTL map for modifiers of the Tcb1-s locus on chromosome 2S and 2L.

QTL plot is shown above with the estimated QTL effects below. Two QTLs, *qTcb1-s-1* (2S) and *qTcb1-s-2* (2L) cumulatively explained 5.46% of the phenotypic variability.

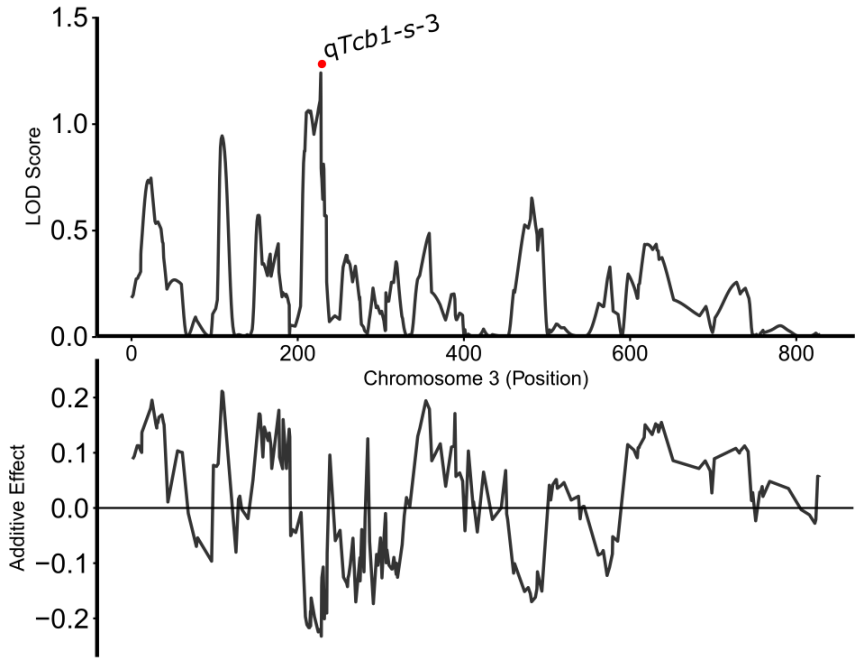

Figure 2.6. QTL map for modifiers of the Tcb1-s locus on chromosome 3S.

QTL plot is shown above with the estimated QTL effects below. One QTL1, q*Tcb1-s*-3 (3S) explained 4.8% of the phenotypic variability.

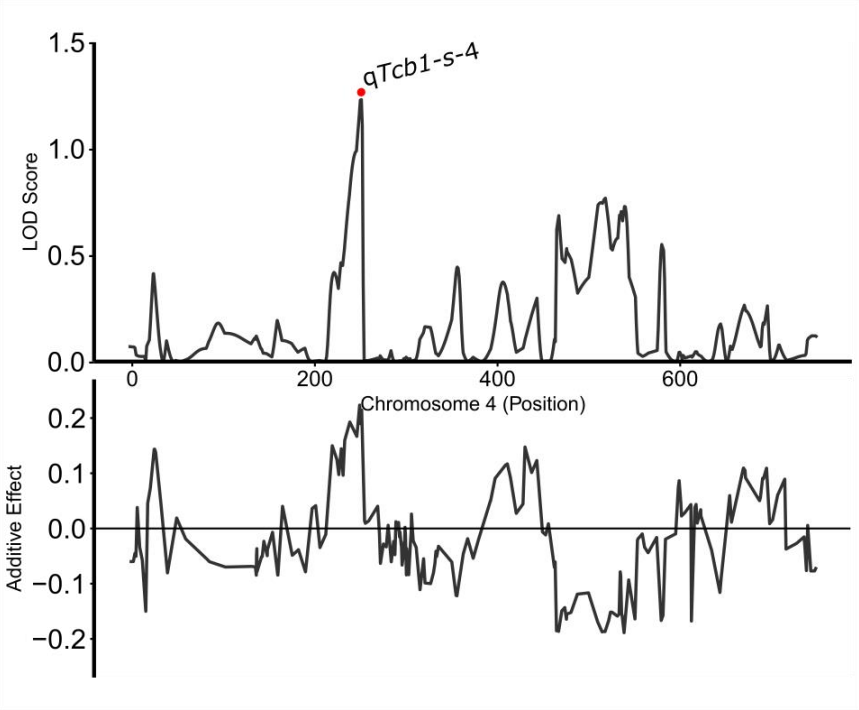

Figure 2.7. QTL map for modifiers of the Tcb1-s locus on chromosome 4S.

QTL plot is shown above with the estimated QTL effects below. One QTL, q*Tcb1-s*-4 (4S) explained 0.86% of the phenotypic variability.

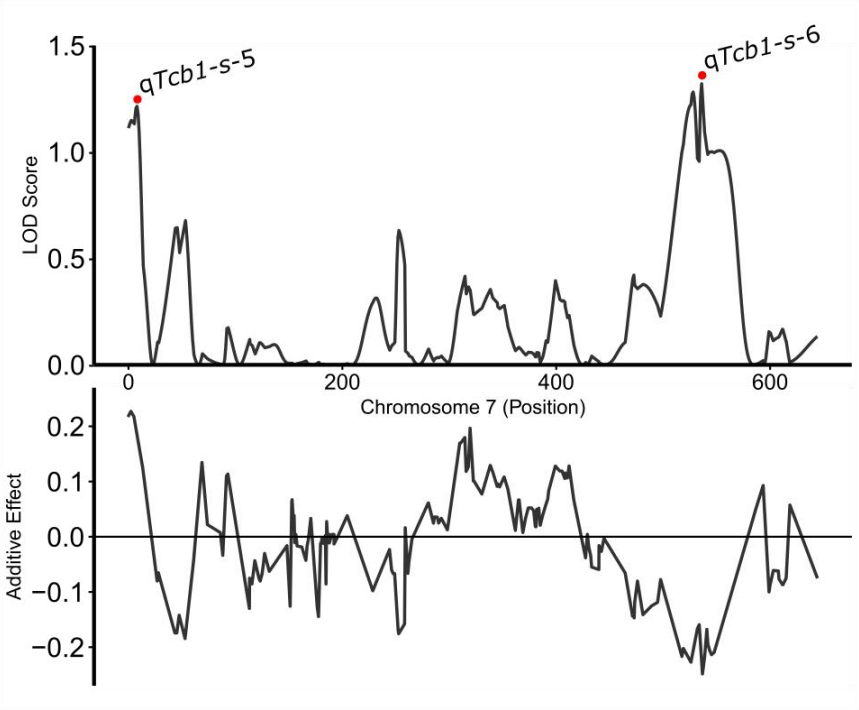

Figure 2.8. QTL map for modifiers of the Tcb1-s locus on chromosome 7S and 7L.

QTL plot is shown above with the estimated QTL effects below. Two QTLs, q*Tcb1-s*-5 (7S) and q*Tcb1-s*-6 (7L) cumulatively explained 2.14% of the phenotypic variability.

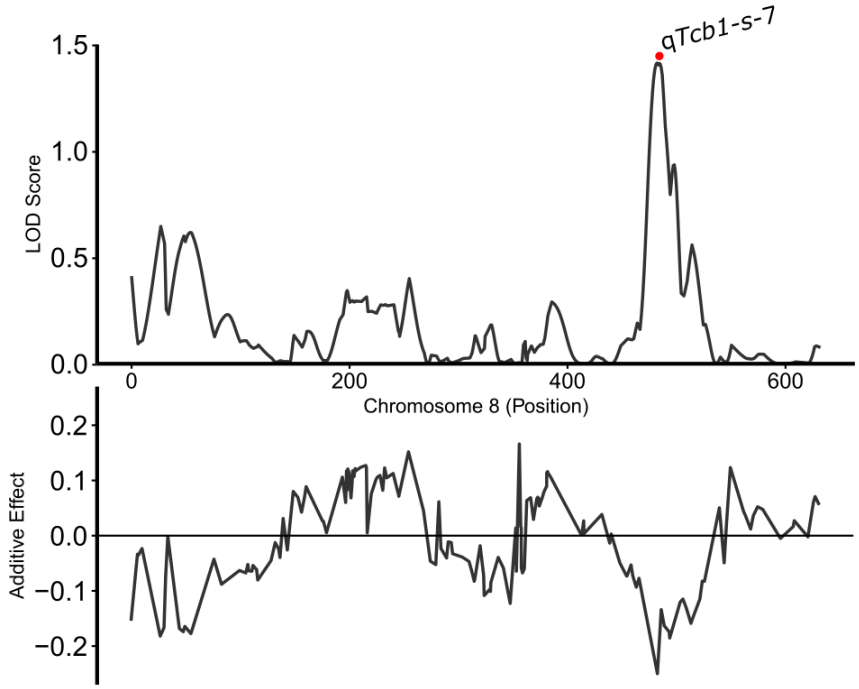

Figure 2.9. QTL map for modifiers of the Tcb1-s locus on chromosome 8L.

QTL plot is shown above with the estimated QTL effects below. One QTL, q*Tcb1-s*-7 (8L) explained 4.0% of the phenotypic variability.

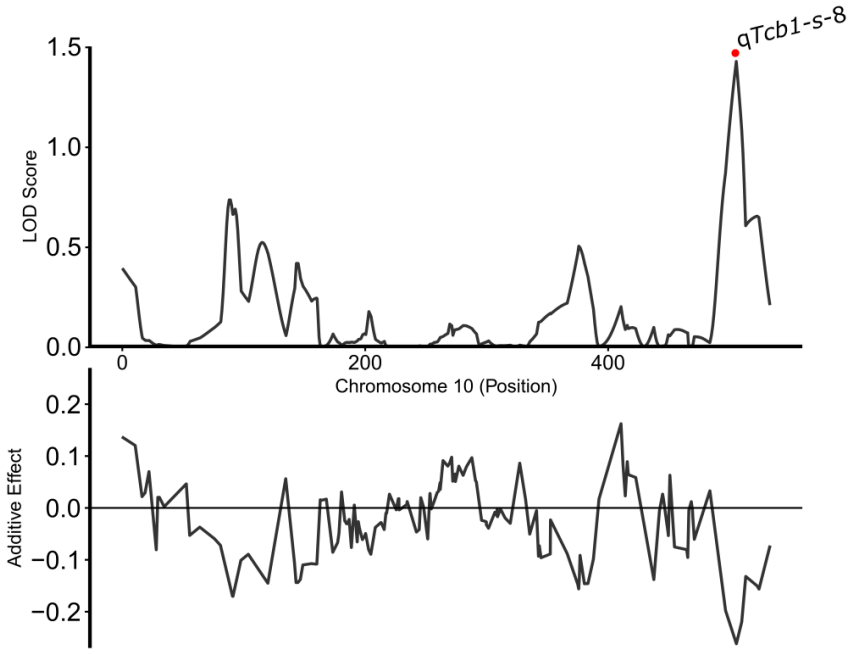

Figure 2.10. QTL map for modifiers of the Tcb1-s locus on chromosome 10L.

QTL plot is shown above with the estimated QTL effects below. One QTL, q*Tcb1-s*-8 (10L) explained 2.91% of the phenotypic variability.

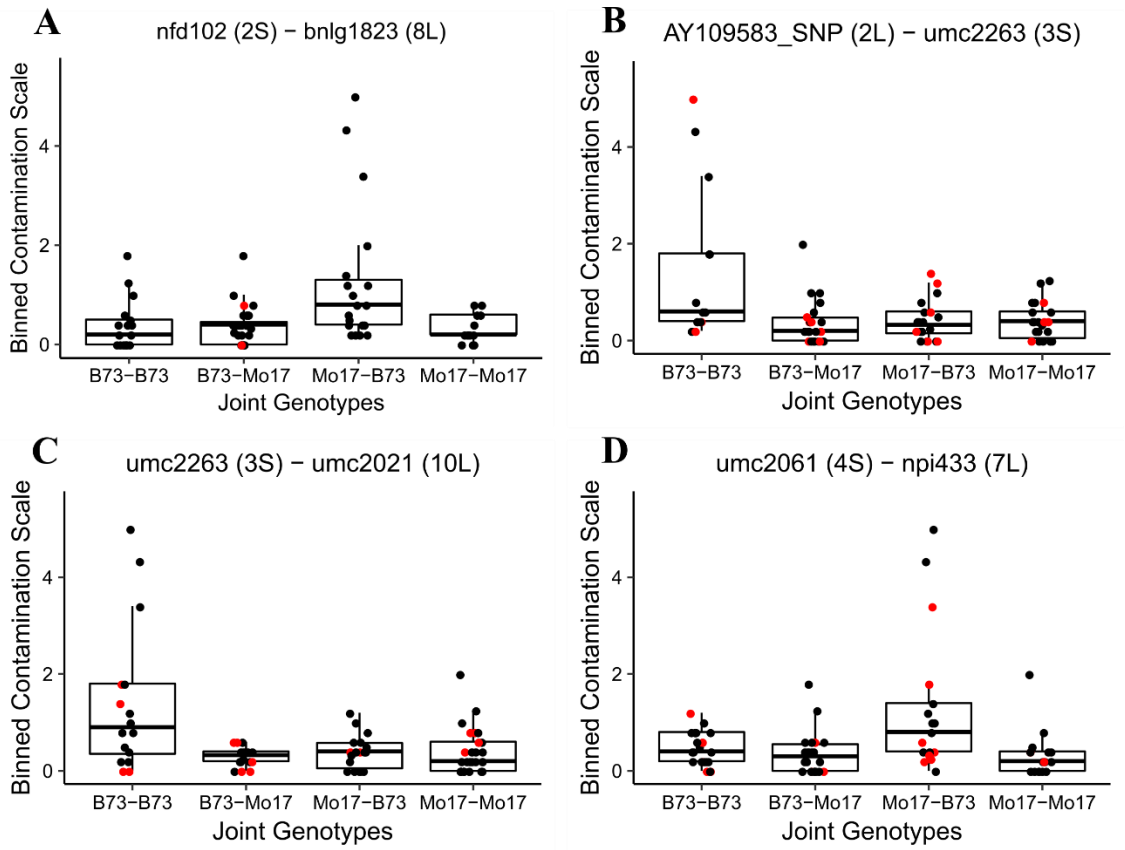

Figure 2.11. Interactions between the eight modifying Tcb1-s QTL pairs.

A) Interaction between *qTcb1-s*-1(2S):q*Tcb1-s*-7(8L) **B)** Interaction between q*Tcb1-s*-2(2L):q*Tcb1-s*-3(3S), **C)** Interaction between q*Tcb1-s*-3(3S):q*Tcb1-s*-8(10L), **D)** Interaction between q*Tcb1-s*-4(4S):q*Tcb1-s*-6(7L). Boxplots show the joint effect each marker (shown across top of plots) provides in a mixed allelic background. B73-B73 is homozygous for the both listed markers; B73-Mo17 is homozygous B73 for the first marker and homozygous Mo17 at the second marker; Mo17-B73 is homozygous Mo17 for the first marker and homozygous B73 at the second marker; Mo17-Mo17 is homozygous for both the listed markers. Black dots show actual phenotypes, red dots are imputed phenotype values.

Figure 2.12. B73 and Mo17 inbred specific cross incompatibility test.

B73 and Mo17 ears (without *Tcb1-s*) resulting from pollination by a mixture of B73 *R-scm2* and colorless Mo17 pollen parents. The proportion of resulting kernels is slightly biased between inbred lines, suggesting that there is a slight pollen preference to self-type inbred pollen for B73 and Mo17. A) B73 ears tested B) Mo17 ears tested.

2.8 Tables – *Tcb1-s* Project

Table 2.1. Summary of the eight modifying QTL found for Tcb1-s.

The analyzed binned data showing the QTL name, chromosome, peak QTL position, closest locus marker, logarithm of the odds (LOD) score, 1-LOD confidence intervals, additive effect with standard error, the parental allele that conferred the higher resistance, and the percent variation explained (r2).

QTL	Chr	Peak Pos.	Locus	LOD Score	1-LOD CI	Additive Effect (s.e.)	Allele	PVE (%)
qTcb1-s-1	2S	187	*nfd102*	1.40	0.0-725	0.185±0.096	B73	3.56
qTcb1-s-2	2L	505	*AY109583*	1.22	0.0-725	-0.137±0.098	Mo17	1.90
qTcb1-s-3	3S	228	*umc2263*	1.24	0.0-829	-0.209±0.094	Mo17	4.80
qTcb1-s-4	4S	251	*umc2061*	1.23	-4.1-750	0.091±0.096	B73	0.87
qTcb1-s-5	7S	8.0	*hsp3*	1.21	0.0-644	0.103±0.109	B73	0.86
qTcb1-s-6	7L	536	*npi433*	1.32	0.0-644	-0.111±0.096	Mo17	1.28
qTcb1-s-7	8L	482	*bnlg1823*	1.41	0.0-632	-0.188±0.093	Mo17	4.00
qTcb1-s-8	10L	506	*umc2021*	1.43	0.0-533	-0.166±0.096	Mo17	2.91

Table 2.2. Candidate loci of Tcb1-s modifying QTL.

Candidate QTLs for modifiers of the *Tcb1-s* locus, their location, the peak QTL position and marker, the starting position to the left of the QTL peak, the ending position to the right of the QTL peak, the size of the candidate region for the main QTL peak, number of predicted genes within the main QTL interval from B73 RefGen_v3, and the number of predicted genes within the main QTL interval translated into B73 RefGen_v4 coordinates. The umc2263 marker was excluded from this analysis because its estimated genetic map position encompassed most of chromosome 3. Genes were converted from V3 to V4 to assist in high throughput gene annotation efforts.

QTL	Chr	Peak Pos	Peak Mar.	Left Border	Right Border	Len	V3 Genes	V4 Genes
qTcb1-s-1	2S	187	*nfd102*	164	208	289 Kb	33	9
qTcb1-s-2	2L	505	*AY109583*	430	526	249 Kb	24	13
qTcb1-s-3	3S	228	*umc2263*	201	238	143 Mb	-	-
qTcb1-s-4	4S	251	*umc2061*	212	254	9.5 Mb	514	147
qTcb1-s-5	7S	8.0	*hsp3*	0	25	273 Kb	28	14
qTcb1-s-6	7L	536	*npi433*	451	589	791 Kb	85	23
qTcb1-s-7	8L	482	*bnlg1823*	446	539	277 Kb	44	14
qTcb1-s-8	10L	506	*umc2021*	483	533	501 Kb	55	27

Table 2.3. Candidate genes for modifying Tcb1-s QTLs explaining more than three-percent of the phenotypic variability.

Candidate genes were taken from genetic map interval estimates of the peak QTL position for *Tcb1-s* modifiers. Only QTLs that explained more than three-percent of the overall phenotypic variability are shown here. All genes shown are protein coding according to B73 RefGen_v4.

QTL	Gene ID	Description
q-Tcb1-s-1	Zm00001d002687	putative cytochrome P450 superfamily protein
q-Tcb1-s-1	Zm00001d002688	mitogen-activated protein kinase kinase kinase YODA
q-Tcb1-s-1	Zm00001d002690	transmembrane protein
q-Tcb1-s-1	Zm00001d002693	NA
q-Tcb1-s-1	Zm00001d002694	branched-chain-amino-acid aminotransferase
q-Tcb1-s-1	Zm00001d002695	Phosphatidylinositol N-acety-glucosaminlytransferase subunit P-related
q-Tcb1-s-1	Zm00001d002696	Rop guanine nucleotide exchange factor 2
q-Tcb1-s-1	Zm00001d002698	subtilisin-like protease SBT1.7
q-Tcb1-s-1	Zm00001d002700	uncharacterized LOC100277587
q-Tcb1-s-7	Zm00001d012321	uncharacterized LOC100382754
q-Tcb1-s-7	Zm00001d012322	putative cytochrome P450 superfamily protein
q-Tcb1-s-7	Zm00001d012325	uncharacterized LOC100275415
q-Tcb1-s-7	Zm00001d012326	putative cytochrome P450 superfamily protein
q-Tcb1-s-7	Zm00001d012329	NA
q-Tcb1-s-7	Zm00001d012330	WUSCHEL-related homeobox 9
q-Tcb1-s-7	Zm00001d012332	uncharacterized LOC100274887
q-Tcb1-s-7	Zm00001d012333	HXXXD-type acyl-transferase family protein
q-Tcb1-s-7	Zm00001d012335	cis-zeatin O-glucosyltransferase 2
q-Tcb1-s-7	Zm00001d012336	Ras association and pleckstrin y domain 1
q-Tcb1-s-7	Zm00001d012337	MYB-type transcription factor
q-Tcb1-s-7	Zm00001d012338	uncharacterized LOC100382859
q-Tcb1-s-7	Zm00001d012339	uncharacterized LOC100501085
q-Tcb1-s-7	Zm00001d012340	pentatricopeptide repeat-containing protein At3g09060

Table 2.4.Candidate genes for modifying Tcb1-s QTLs explaining less than three-percent of the phenotypic variability.

Candidate genes were taken from genetic map interval estimates of the peak QTL position for *Tcb1-s* modifiers. Only QTLs that explained less than three-percent of the overall phenotypic variability are shown here. All genes shown are protein coding according to B73 RefGen_v4.

QTL	Gene ID	Description
q-*Tcb1-s*-2	Zm00001d006780	RPD3 histone deacetylase homolog
q-*Tcb1-s*-2	Zm00001d006786	NA
q-*Tcb1-s*-2	Zm00001d006787	Agenet domain-containing protein
q-*Tcb1-s*-2	Zm00001d006788	NA
q-*Tcb1-s*-2	Zm00001d006789	uncharacterized LOC100216933
q-*Tcb1-s*-2	Zm00001d006790	mitogen-activated protein kinase 14
q-*Tcb1-s*-2	Zm00001d006791	transcription factor KUA1
q-*Tcb1-s*-2	Zm00001d006793	uncharacterized LOC100381909
q-*Tcb1-s*-2	Zm00001d006794	uncharacterized LOC100285504
q-*Tcb1-s*-2	Zm00001d006795	NA
q-*Tcb1-s*-2	Zm00001d006796	NA
q-*Tcb1-s*-2	Zm00001d006797	GUP1
q-*Tcb1-s*-2	Zm00001d006798	probable ATP-dependent DNA helicase CHR12
q-*Tcb1-s*-5	Zm00001d018628	NA
q-*Tcb1-s*-5	Zm00001d018630	NA
q-*Tcb1-s*-5	Zm00001d018631	Dirigent protein 11
q-*Tcb1-s*-5	Zm00001d018632	NA
q-*Tcb1-s*-5	Zm00001d018634	hypothetical protein
q-*Tcb1-s*-5	Zm00001d018635	phytosulfokine receptor 2
q-*Tcb1-s*-5	Zm00001d018636	hypothetical protein
q-*Tcb1-s*-5	Zm00001d018637	uncharacterized LOC100277954
q-*Tcb1-s*-5	Zm00001d018638	putative MATE efflux family protein
q-*Tcb1-s*-5	Zm00001d018639	NA
q-*Tcb1-s*-5	Zm00001d018642	uncharacterized LOC100280358
q-*Tcb1-s*-5	Zm00001d018645	NA
q-*Tcb1-s*-5	Zm00001d018647	NA
q-*Tcb1-s*-5	Zm00001d018648	FAD/NAD(P)-binding oxidoreductase family protein
q-*Tcb1-s*-6	Zm00001d022263	NA
q-*Tcb1-s*-6	Zm00001d022264	NA
q-*Tcb1-s*-6	Zm00001d022265	uncharacterized LOC107521957
q-*Tcb1-s*-6	Zm00001d022266	uncharacterized LOC100273696
q-*Tcb1-s*-6	Zm00001d022267	chromatin remodeling factor18
q-*Tcb1-s*-6	Zm00001d022271	NA

Continued from above

QTL	Gene ID	Description
q-*Tcb1-s*-6	Zm00001d022272	uncharacterized LOC100273851
q-*Tcb1-s*-6	Zm00001d022274	NA
q-*Tcb1-s*-6	Zm00001d022275	novel plant SNARE 11
q-*Tcb1-s*-6	Zm00001d022276	kinesin-like protein KIN-12E
q-*Tcb1-s*-6	Zm00001d022277	tolB protein-related
q-*Tcb1-s*-6	Zm00001d022278	NA
q-*Tcb1-s*-6	Zm00001d022286	DExH-box ATP-dependent RNA helicase DExH12
q-*Tcb1-s*-6	Zm00001d022290	peroxidase 2-like
q-*Tcb1-s*-6	Zm00001d022294	NA
q-*Tcb1-s*-6	Zm00001d022300	NA
q-*Tcb1-s*-6	Zm00001d022302	pyrrolidone carboxyl peptidase
q-*Tcb1-s*-6	Zm00001d022303	corticosteroid 11-beta-dehydrogenase isozyme 1
q-*Tcb1-s*-6	Zm00001d022305	putative protein kinase superfamily protein
q-*Tcb1-s*-6	Zm00001d022306	uncharacterized LOC100284298
q-*Tcb1-s*-6	Zm00001d022307	chaperonin
q-*Tcb1-s*-6	Zm00001d022308	hypothetical protein
q-*Tcb1-s*-6	Zm00001d022310	NA
q-*Tcb1-s*-8	Zm00001d026580	Exostosin family protein
q-*Tcb1-s*-8	Zm00001d026581	NA
q-*Tcb1-s*-8	Zm00001d026582	Plant UBX domain-containing protein 7
q-*Tcb1-s*-8	Zm00001d026584	uncharacterized LOC100283341
q-*Tcb1-s*-8	Zm00001d026585	Trypsin family protein
q-*Tcb1-s*-8	Zm00001d026586	uncharacterized LOC100384522
q-*Tcb1-s*-8	Zm00001d026587	zinc finger C-x8-C-x5-C-x3-H type family protein
q-*Tcb1-s*-8	Zm00001d026588	hypothetical protein
q-*Tcb1-s*-8	Zm00001d026590	uncharacterized LOC100382863
q-*Tcb1-s*-8	Zm00001d026592	pentatricopeptide repeat-containing protein At3g50420
q-*Tcb1-s*-8	Zm00001d026593	Putative homeodomain-like transcription factor superfamily protein
q-*Tcb1-s*-8	Zm00001d026594	cytokinin response regulator 2
q-*Tcb1-s*-8	Zm00001d026595	Early nodulin-like protein 1
q-*Tcb1-s*-8	Zm00001d026597	hypothetical protein
q-*Tcb1-s*-8	Zm00001d026598	ubiquinone biosynthesis protein COQ4
q-*Tcb1-s*-8	Zm00001d026599	light harvesting chlorophyll a/b binding protein 6
q-*Tcb1-s*-8	Zm00001d026600	protein S-acyltransferase 11-like
q-*Tcb1-s*-8	Zm00001d026603	uncharacterized LOC100382191
q-*Tcb1-s*-8	Zm00001d026604	probable metal-nicotianamine transporter YSL10
q-*Tcb1-s*-8	Zm00001d026605	endoglucanase 13
q-*Tcb1-s*-8	Zm00001d026606	dnaJ domain containing protein
q-*Tcb1-s*-8	Zm00001d026607	oligosaccharyl transferase STT3 subunit

Continued from above

QTL	Gene ID	QTL
q-*Tcb1-s*-8	Zm00001d026608	thioredoxin X
q-*Tcb1-s*-8	Zm00001d026609	hypothetical protein
q-*Tcb1-s*-8	Zm00001d026610	dihydroorotate dehydrogenase
q-*Tcb1-s*-8	Zm00001d026611	uncharacterized LOC100275470
q-*Tcb1-s*-8	Zm00001d026612	Protection of telomeres protein 1b

Table 2.5. Results from the inbred-specific incompatibility test lacking Tcb1-s.

B73 and Mo17 ears (without *Tcb1-s*) resulting from pollination by a mixture of B73 *R-scm2* and colorless Mo17 (*r1/r1*) pollen parents. The proportion of *R-scm2* to the total number of kernels is slightly biased between inbred lines, suggesting that there is an inbred specific preference for self-type pollen between B73 and Mo17. Primarily, however, it is the activity of *Tcb1-s* and the associated modifiers that show the large range of phenotypes in the main experiment.

Genotype	B73 *R-scm2*	Mo17 *r1/r1*	Proportion
B73-1	97	271	0.27
B73-2	80	248	0.24
Mo17-1	32	149	0.17
Mo17-2	23	87	0.21

Chapter 3: Conclusions and Future Directions – *Tcb1* Project

Although eight modifiers were found to interact with the *Tcb1-s* locus in this study, more work must be done to fully understand how this cross-incompatibility system functions and could be used as a naturally occurring barrier to prevent unwanted cross contamination. A series of experiments are outlined below to help further understand *Tcb1-s* behavior.

One of the downsides of the experiment conducted is the limited sample size that was tested. The intermated B73 x Mo17 recombinant inbred line population consists of 302 individuals of which only 77 were tested. The low LOD scores obtained by the modifying *Tcb1-s* QTL may have been a result of the low diversity of the population that was surveyed. Also, it has previously been shown that the IBM lines are biased at some loci for either B73 or Mo17 due to the lack of recombination events between chromosomal arms making calls for differences between the two parents more difficult (LEE *et al.* 2002; FU *et al.* 2006). Testing more of the RILs provides the opportunity to sample a larger pool of individual alleles and allelic combinations that may interact with *Tcb1-s.* In the summer of 2018 we will be doing the initial cross of the W22 *Tcb1-s/Tcb1-s* with the remaining 208 IBM lines to test the ability of the F1 pistils to reject *tcb1* pollen in the summer of 2019.

QTL mapping of traits in any species can only provide an overview of the loci that may be involved with the phenotype in question. Because so little is known about the genes at the *Tcb1-s* locus, sequencing may be an interesting option to understand this system in further detail. Recently the RNA expression profiles of pistils containing *Ga1-s* and *ga1* found *ZmPme3,* a pectin methylesterase (PME) transcript, to be upregulated only

in *Ga1-s* pistils (MORAN LAUTER *et al.* 2017). The *Ga1* locus is 44 cM away from the *Tcb1* locus on the short arm of chromosome 4. It is possible that one locus may be a duplication of the other and a similar *ZmPme3* gene is functioning in *Tcb1*. Some evidence for this exists in that the *Tcb1* locus contains a *Ga1-m* like allele that can overcome the *Ga1-s* barrier, but the *Ga1-s* locus does not have such a reciprocal allele and cannot pollinate *Tcb1-s* pistils. This *Ga1-m* like allele at the *Tcb1* locus may have resulted in a duplication event and subsequent neofunctionalization to permit some cross-fertilization between plants containing *Tcb1* with *Ga1*. As for a functional duplication of the *ZmPme3* gene at the *Tcb1-s* locus, fifty-eight partial to full repeats of PME exist within a 1.1 Mb region at the *Ga1-s* locus. If *Tcb1* shared a duplication event with *Ga1* in the past, fine mapping and cloning of the functional candidate gene may be difficult. DNA sequencing of the *Tcb1-s* and *tcb1* locus in a similar W22 background may be the best method to determine the genetic structure of the locus.

To understand the expression profiles of the *Tcb1* locus performing a similar RNA expression study as *Ga1-s* where pistils containing *Tcb1-s* and *tcb1* were sequenced (MORAN LAUTER *et al.* 2017). Pistil tissue could be collected from silks of the same ear in a split pollination design where half of the silks were treated with *tcb1* and the other half treated with *Tcb1-s* pollen. To add another layer of complexity, the reciprocal cross should also be sequenced where *tcb1* pollen is added to *Tcb1-s* pistils and *Tcb1-s* pollen is added to *tcb1* pistils. It would be interesting to see if changes in signaling patterns occur when *tcb1* pollen interacts with *Tcb1-s* pistils to eventually halt pollen tube growth. Additionally, the model put forth by KERMICLE AND EVANS (2005) that heteroallelic pollen containing both the *Tcb1-s* allele and the *tcb1* allele, when added onto *Tcb1-*

s/Tcb1-s pistils can successfully carry out fertilization could be tested. Their results suggested a congruity model where the matching allele is required for fertilization rather than active rejection for the foreign (*tcb1*) allele in *Tcb1-s* pistils. Ordering these TB4-Sa *Tcb1-s tcb1* stocks from the Maize Genetics Stock Center, performing the reciprocal crosses onto *Tcb1-s* and *tcb1* pistils and observing their RNA expression profiles to see if *tcb1* heteroallelic pollen is even recognized within *Tcb1-s* pistils would be interesting.

Carrying out an RNA sequencing experiment may find the major genes acting within *Tcb1-s* pistils, but it may also shed light on the presence of *Tcb1-s* modifiers. Although it is possible to fine map and clone modifiers found from the IBM QTL studies, DNA or RNA sequencing may be an expedited method of obtaining these modifying loci. If such modifiers cannot be found in expression studies between W22 lines carrying *Tcb1-s* and *tcb1*, sequencing of IBM RIL lines with highly contrasting *Tcb1-s* phenotypes may be productive. A similar experiment could be performed with *Ga1-s* modifiers to determine their interactions with the *Ga1-s* locus.

Modifiers of the *Ga1-s* locus have been previously reported in F1s of *Ga1-s* with the nested association mapping populations of B73 x Ky21 and B73 x M162w (SHRESTHA 2016). Because *Ga1-s* has been sequenced and primers amplifying the functional *ZmPme3* have been published, one could perform a quantitative real-time PCR experiment examining the expression profiles between RILs having high and low incompatibility responses to *ga1* pollen. Two F1 RILs with highly contrasting phenotypes to *ga1* pollen may express *ZmPme3* at varying levels or may even express *ZmPme3* at the same level but interactions between other *Ga1-s* modifiers may impact the *Ga1-s* pistil barrier.

Modifying loci are important to *Tcb1-s* behavior as they are with *Ga1-s* (EVANS AND KERMICLE 2001). Within ten generations of backcrossing the *Tcb1-s* locus into W22, the ability of the pistils to reject *tcb1* pollen decreased substantially over every generation (LU *et al.* 2014). It was suggested that the weakened pistil barrier could be the result of the loss of *Tcb1-s* modifiers but potentially the epigenetic silencing of the locus. It would be interesting to see if it is truly the loss of these positive modifiers that leads to the weakened pistil barrier by finding markers to these modifiers and attempting to amplify them in numerous backcrosses to see if they are retained and necessary for *Tcb1-s* activity. If the markers are still present, yet *Tcb1-s* activity diminishes over time, bisulfite sequencing to study methylation patterns of the locus could help explain this phenomenon.

Studying the modifiers and the major genes underlying the *Tcb1-s* and *Ga1-s* locus are useful if plant breeders introgressed these systems into organic or specialty maize varieties to prevent unwanted cross contamination (NELSON 1952; NELSON 1960; NELSON 1994). Stepping away from the applied genetics aspect of this system and looking at the overall population genetics of how and where these cross-incompatibility systems arose during the evolutionary history of maize has many unanswered questions. When did the *Ga1* system arise and why is it prevalent in popcorn strains where it was first discovered (MANGELSDORF AND JONES 1926; EMERSON 1934)? Why does *Tcb1-s* have a functional *Ga1-m* like domain at the *Tcb1* locus? Why do some *Tcb1* loci confer a bidirectional cross-incompatibility system where the *Tcb1-s* pistils can reject *tcb1* pollen but *Tcb1-s* pollen is at a competitive disadvantage on *tcb1* pistils (KERMICLE 2006)?

Sampling and sequencing a broad range of *Tcb1* systems from Central and South America may be the only way to answer some of these questions.

3.1 References

Emerson, R. A., 1934 RELATION OF THE DIFFERENTIAL FERTILIZATION GENES, Ga ga, TO CERTAIN OTHER GENES OF THE Su-Tu LINKAGE GROUP OF MAIZE. Genetics 19**:** 137-156.

Evans, M. M. S., and J. L. Kermicle, 2001 Teosinte crossing barrier1 , a locus governing hybridization of teosinte with maize. Theoretical and Applied Genetics 103**:** 259-265.

Fu, Y., T. J. Wen, Y. I. Ronin, H. D. Chen, L. Guo *et al.*, 2006 Genetic dissection of intermated recombinant inbred lines using a new genetic map of maize. Genetics 174**:** 1671-1683.

Kermicle, J. L., 2006 A selfish gene governing pollen-pistil compatibility confers reproductive isolation between maize relatives. Genetics 172**:** 499-506.

Kermicle, J. L., and M. M. S. Evans, 2005 Pollen–pistil barriers to crossing in maize and teosinte result from incongruity rather than active rejection. Sexual Plant Reproduction 18**:** 187-194.

Lee, M., N. Sharopova, W. D. Beavis, D. Grant, M. Katt *et al.*, 2002 Expanding the genetic map of maize with the intermated B73 × Mo17 (IBM) population. Plant Molecular Biology 48**:** 453-461.

Lu, Y., J. L. Kermicle and M. M. Evans, 2014 Genetic and cellular analysis of cross-incompatibility in Zea mays. Plant Reproduction 27**:** 19-29.

Mangelsdorf, P. C., and D. F. Jones, 1926 THE EXPRESSION OF MENDELIAN FACTORS IN THE GAMETOPHYTE OF MAIZE. Genetics 11**:** 423-455.

Moran Lauter, A. N., M. G. Muszynski, R. D. Huffman and M. P. Scott, 2017 A Pectin Methylesterase ZmPme3 Is Expressed in Gametophyte factor1-s (Ga1-s) Silks and Maps to that Locus in Maize (Zea mays L.). Frontiers in Plant Science 8**:** 1-11.

Nelson, O. E., 1994 *The Gametophyte Factors of Maize*. Springer-Verlag, New York.

Nelson, O. E., Jr., 1952 Non-Reciprocal Cross-Sterility in Maize. Genetics Research 37**:** 101-124.

Nelson, O. E., Jr., 1960 The Fourth Chromosome Factor in Some Central and South American Races. Maize Genetics Cooperation News Letter 34**:** 114-116.

Shrestha, V., 2016 The search for modifiers of the maize gametophyte factor Ga1-s and Quantitative trait polymorphisms emerging from doubled-haploid maize lines, pp. 1-78 in *Biology and Microbiology*. South Dakota State University, Brookings, SD.

Chapter 4: Characterization and Sequencing of Two Plutonium-Beryllium Induced Male Gametophyte Mutants in Maize

4.1 Abstract

Maize goes through an alteration of generations spending most of its life cycle in the diploid sporophytic stage and a very short period in the haploid, reproductive gametophytic stage. In this study, two mutants were generated using plutonium-beryllium exposure whose phenotypes impact genes affecting transmission of the male gametophyte and not the female gametophyte, linked to the *R1* color marker. To uncover the genetic basis of these two male gametophyte mutants, we sequenced and compared their deletion haplotypes to the B73 reference genome. We uncovered a 4.5 Mb region linked to the *R1* locus that may contain the putative deletion causing our reduced transmission phenotype. In the PB2 mutant we found 25 candidate genes impacted by deletions, one of which is a calcium-dependent protein kinase potentially involved in pollen tube tip growth. Candidate genes for PB1 remain elusive until further data is obtained. These results could shed light on the short-lived male gametophyte generation of maize and could be applied to plant breeding to create male sterile lines.

4.2 Introduction

Maize goes through an alteration of generations spending most of its life cycle in the diploid sporophytic stage and a very short period in the haploid, reproductive gametophytic stage. It is in this gametophytic generation where the male pollen grain meets the pistil tissues and fertilizes the female egg cell to create a diploid embryo and a triploid endosperm that both develop into the maize kernel. Though this haploid generation is short-lived, mutations that arise that reduce the transmission and subsequent

fertilization events of this genetic information would be eliminated rapidly and are thus hard to discover.

Within the anthers of a developing male inflorescence (or tassel), a cluster of sporogenous tissue is surrounded by dividing rows of archesporial cells and epidermis cells. After continued divisions, the innermost layer contains sporogenous cells, who later form the microspores and are surrounded by a nutrient-rich layer of tapetum cells. These microspore mother cells, or microsporocytes, undergo meiosis twice. The first round of meiosis produces two spore cells, while the second round of meiosis produces four spores, each containing an immature haploid pollen grain. This four-spore tetrad is housed within a microspore mother cell who quickly degrade by beta-glucanase activity (FRANKEL *et al.* 1969). Shortly before pollen shed, the freed pollen grains undergo mitotic division to produce a vegetative cell and a generative cell containing two sperm cells which assist in double fertilization (KIESSELBACH 1949).

To carry out a successful fertilization event, each pollen grain must pass through the five described phases in the plant fertilization process (JOHNSON AND PREUSS 2002; SWANSON *et al.* 2004; DRESSELHAUS AND FRANKLIN-TONG 2013). The pollen must first 1) land on a receptive stigma and hydrate the desiccated pollen grain, 2) Germinate the pollen tube, 3) sustain directed pollen tube growth towards the micropyle, 4) leave the transmitting tract and travel through the ovarial cavity, and 5) reach the micropyle and release the two sperm cells.

In this study, two mutations reducing male gametophyte transmission linked to the *R1* locus on the long arm of chromosome 10 were generated by plutonium-beryllium induced mutagenesis. Plutonium-beryllium radiation emits a mixture of fast-neutrons and

gamma-rays and have been shown to produce interstitial deletions in plant genomes (URLAUB *et al.* 1986; LI *et al.* 2001). To determine the genes impacted by these deletions, the two mutants were sequenced on an Illumina HiSeq X and deletions potentially affecting calcium protein kinase genes among others involved in male gametophyte transmission were explored.

4.3 Materials and Methods

4.3.1 Plant Materials

Zea mays seeds heterozygous for *R1/r1 and c1/C1* B73 color factors, were exposed to a plutonium-beryllium source emitting a combination of fast neutrons and gamma rays in the South Dakota State University Department of Physics in 2015. Kernels were subject to plutonium-beryllium bombardment for three or six months (PB1 and PB2, respectively). M_1 plants were grown at South Dakota State University's experiment plots in Brookings, SD. Reduced male gametophyte transmission was tested in reciprocal crosses with *r1 C1* B73 and *R1 c1* B73 testers in the M_1 - M_4 generations. Seeds derived from six months of plutonium-beryllium (hereafter named PB2) exposure were backcrossed into B73 for two generations. Seeds derived from three months of plutonium-beryllium exposure (hereafter named PB1) were backcrossed into B73 for three generations. Seedlings of both PB1 and PB2 were grown in a darkened 30°C incubator for 5-7 days before flash-freezing in liquid nitrogen for DNA extraction.

4.3.2 DNA Isolation

PB1 and PB2 genomic DNA from etiolated seedlings were extracted using a modified protocol from Mayjonade *et al*. (2016). Briefly, flash-frozen tissue was ground into a fine powder before treatment with preheated lysis buffer and RNase A (100 mg/mL

Qiagen, Germantown, MD, USA). The samples were incubated at 65°C for one hour, inverting the tubes every ten minutes. Potassium acetate (5M) at was added to the samples before incubation on ice for ten minutes. After incubation, the samples were centrifuged at 5000 g for ten minutes at 4°C before transferring the supernatant into a new tube. One volume of binding buffer and 1:18 (v:v) of Sera-Mag SpeedBeads (5% solids, GE Healthcare, Pittsburg, PA, USA) at room temperature were homogenized gently into the supernatant for ten minutes. The DNA and Sera-Mag beads were collected using a 3D printed magnetic tube rack (https://www.thingiverse.com/thing:79424) with neodymium block magnets (B842, K&J Magnetics, Pipersville, PA, USA). The samples were then washed 3-4 times on the magnetic rack with 70% ethanol before they were air-dried for one minute. A total volume of 100 µL of 50°C Buffer EB (Qiagen, Germantown, MD, USA). Samples were left on the magnetic rack overnight to increase the DNA resuspension efficiency. An additional purification step was performed, adding one volume of Sera-Mag beads to the DNA solution, incubating with light agitation for ten minutes, and washing with 70% ethanol 8 to 10 times on the magnetic tube rack before elution in 100 µL of 50°C Buffer EB.

4.3.3 Quality Control

To ensure that high molecular weight DNA has been isolated, samples were visualized on a Bio-Rad Chef-DR III pulsed electrophoresis system (Hercules, CA, USA). Samples were loaded in a 1% Bullseye agarose gel (MidSci, Valley Park, MO, USA) in 0.5X TAE buffer for twenty-four hours with the following parameters: Initial Switch time: 1.0 seconds, Final Switch Time: 40.0, Volts/cm: 6.0, Included Angle: 120°, Buffer Temperature: 12°C, Pump Speed: 1.0 liters/minute (60-70% pump speed). A

ProMega-Markers Lambda Ladder (Promega, Madison, WI, USA) were loaded alongside the samples for DNA size determination. The gel was post-stained in an orbital shaker with 200 µL of ethidium bromide suspended in molecular grade water for thirty minutes and destained for fifteen minutes.

Once the samples were deemed of good quality, the DNA was prepared for sequencing by size selection on a Pippin Prep (Sage Science, Beverly, MA, USA). A total of 5 µg of high molecular weight DNA was loaded into a BluePippin BUF7510 pre-cast 0.75% agarose gel cassette (Sage Science). The manufacturer's instructions were followed. A high pass filter of 30 – 80 Kb (target 50 Kb) was selected before running the Pippin Prep for 15 hours. Samples were recovered and cleaned by adding one volume of Sera-Mag beads to the DNA solution, incubating with light agitation for ten minutes, and washing with 70% ethanol 8-10 times on the magnetic tube rack before elution in 100 µL of 50°C Buffer EB. DNA quality was measured on a Nanodrop 2000 (ThermoFisher Scientific, Waltham, MA, USA) and DNA quantity was measured on a Qubit 4 Fluorometer (ThermoFisher Scientific) using a Qubit dsDNA BR Assay Kit (ThermoFisher Scientific).

4.3.4 DNA Sequencing and Analysis

PB2 was sent to the Genomic Services Laboratory at HudsonAlpha for sequencing with a Chromium Genome Library Kit (10X Genomics, Pleasanton, CA, USA) in a single lane of Illumina HiSeq X generating 150 bp paired-end reads. Reads were demultiplexed by the Genomic Services Laboratory before analysis on the 10X Genomics Long Ranger software. The Long Ranger Whole Genome Mode was used to clean and sort fastq files, perform genome alignments to the B73 RefGen_v4 reference

genome (Jiao *et al*., 2017), call variants, and phase haplotypes. Long Ranger calls structural variants by discordantly mapped read pairs and changes in read depth. The data were visualized using Loupe (10X Genomics, Pleasanton, CA, USA) and R version 3.5.0 (R CORE TEAM 2018).

PB1 was sent for sequencing at Macrogen using an Illumina TruSeq PCR Free Library Kit (Illumina, San Diego, CA, USA) on the Illumina HiSeq X for 150 bp paired-end reads. Sequencing reads were trimmed for quality using FASTQC (ANDREWS 2010) and aligned to the B73 RefGen_v4 genome using BWA-MEM (LI 2013). Structural variants were called using LUMPY that flags variants based on discordantly mapped read pairs and split reads as well as changes in read depth (LAYER *et al.* 2014).

Due to the nature of plutonium-beryllium mutagenesis, the final Variant Call Files (VCF) files generated for each mutant were subsetted to only include deletions. VCFtools was used to subset out candidate deletions and summarize the total number of mutations falling between set intervals (DANECEK *et al.* 2011). These VCF files were then analyzed by Ensembl Plant's Variant Effect Predictor to provide gene annotation and categorize the deletions into: upstream gene variants (max of 5 Kb from the 5'UTR), downstream gene variants (max of 5 Kb from the 3'UTR), exon variants, intron variants, intergenic, or 5' or 3' UTR variants.

Deletions that were shared between both PB1 and PB2 within a ten base pair interval were flagged as originating from the recurrent B73 parent. Although it is possible PB1 and PB2 are caused by a deletion in the same gene, the likelihood that they share the same exact deletion is small. To further narrow down the list of candidate genes, Gene IDs were compared against prior RNA expression and proteomic analyses generated by

the John Fowler laboratory at Oregon State University detailing RNA expression levels of the candidate genes over key reproductive and developmental stages in maize. These stages included B73 seedlings, embryo sacs, ovules without embryo sacs, tassel primordia, microspores, mature pollen, and sperm cells. Proteomic data for mature non-germinated pollen and germinated pollen was also explored.

4.4 Results

4.4.1 Reduced Male Gametophyte Transmission of PB1 and PB2

Plutonium-beryllium mutagenesis is thought to cause interstitial deletions throughout plant genomes. To test the impact these deletions would have on gametophyte development in maize, kernels heterozygous for *R1*/*r1 C1*/*c1* were exposed to a plutonium-beryllium source for three to six months. These mutant plants were backcrossed into B73 and tested in 2015, 2016, and 2017 by reciprocal crosses with *r1 C1* and *R1 c1* testers. PB2, which was treated with plutonium-beryllium for six months, had the lowest male transmission of the *R1* marker, 1.48% ± 0.443% (mean ± se, n = 5) where 50% male transmission is expected (Figure 4.1, Table 4.1). Male transmission of the *C1* marker in PB2 onto *R1 c1* testers yielded 51.8% ± 1.11% allele frequency (n = 5). PB2 appears to be closely linked to *R1* and its phenotype of reduced male transmission is highly penetrant.

PB1, which emerged from a plant exposed to plutonium-beryllium for three months, had a slightly higher male *R1* marker transmission in the *r1 C1* testers 23.6% ± 0.61% (n = 3) (Figure 4.1, Table 4.1). Two other PB1 siblings, PB1-1 and PB1-5 were tested but not used for further analyses because they appeared to undergo recombination events. Male transmission of the *C1* color marker in PB1 to the *R1 c1* testers yielded the

expected 50.7% ± 1.49% allele frequency (n = 3). Due to the low rates of *R1* transmission through the male gametophyte, these stocks were always propagated through the female. To test whether male transmission of the *R1* marker in PB1 was due to recombination or incomplete penetrance, full colored kernels were taken from the *r1 C1* tested ears and crossed onto *r1 c1* stocks. In five of the fourteen lines tested transmission of the *R1* marker was significantly less than 50% and ranged from 23.6% ± 0.61% to 11.3% ± 0.87% (Table 4.2). This indicates that marker transmission in PB1 is due both to recombination and incomplete penetrance.

The mechanism for the reduction in male gametophyte transmission when transmitted through the male rather than the female is currently unknown. It is possible that epigenetic silencing of the locus on 10L or independent segregation of other loci involved in male gametophyte transmission may be involved.

4.4.2 Sequencing and Identification of Candidate Genes for PB2

Sequencing of PB2 yielded a total of 882,624,072 paired-end reads at 54.1X with 98% of the reads mapping back to the B73 RefGen_v4 (Table 4.3). PB2 was phased into N50 phase blocks of at least 34,981 bp (Table 4.4). Long Ranger makes mid-scale deletion calls from 50 bp – 30 Kb and large-scale calls 30 Kb and greater. Only mid-scale events were explored in these analyses because they match previous reports on plutonium-beryllium induced mutagenesis. Long Ranger detected a total 2,834 deletions within PB2.

Transmission data to *r1 C1* testers suggested that the PB2 mutation is tightly linked to the *R1* locus. The low rate of *R1* transmission (1.48% ± 0.443%) indicates that there is little recombination between the PB2 mutation and *R1*, so it was hypothesized

that the linkage drag introduced by the foreign *R1* locus could be a sequence-based marker when compared to the wild-type *r1* B73 that was previously sequenced. In addition, three generations of backcrossing the PB2 mutant into an *r1* B73 background would lead to a finer linkage drag 'signature' for the probable location of the mutation. To search for this, VCF files generated by Long Ranger were explored using custom Bash and R scripts to search for the number of new deletion mutations occurring within a sliding 500 Kb window. Figure 4.2 shows the number of new deletions occurring 7 Mb proximal and distal to *R1*. A 4.5 Mb 'curve' proximal to *R1* shows the linkage drag brought the *R1* locus and the surrounding regions. Within this 4.5 Mb 'curve' are 224 deletion sites affecting 114 predicted genes unique to PB2 (Table 4.5).

Of the 224 deletion sites discovered for PB2, the functional consequences of the 114 predicted genes unique to PB2 were explored using the Variant Effect Predictor on Ensembl Plants. Most of the mutations that occurred either upstream or downstream of the gene and could potentially influence gene expression. Deletions causing intron variants and feature truncations were the next most prevalent category followed by intergenic variants which may influence distant promoters or may contain genes that current genome annotation methods may not have discovered. Additional functional consequences such as transcript ablation, feature truncations, and 3' and 5' UTR variants were also explored (Figure 4.5).

To narrow the list of potential PB2 candidates as well as classify their functions, B73_v4 gene IDs generated by Ensembl Plants were translated into B73_v3 gene IDs. Due to differences in gene annotation, a total of 37 genes from the B73_v4 annotation were lost during gene ID conversion to B73_v3. The now 42 gene IDs were compared to

previous RNA expression and proteomic data generated by the John Fowler laboratory (Oregon State University). Figure 4.6 and Figure 4.8 shows the log FPKM RNA expression data both with and without the parental B73 deletions removed, respectively. Both heatmaps are shown because some potentially important male gametophyte related genes are lost from the B73 parental haplotype that could be tested in other experiments. Heatmaps show the expression of candidate genes affected by the deletion sites within B73 seedlings, embryo sacs, ovules missing embryo sacs, tassel primordia, microspores, mature pollen, and sperm cells. Genes fall roughly into four expression categories: 1) relatively high constitutive expression regardless of tissue type, 2) expression only within the B73 seedling, embryo, and ovules lacking embryo sacs, 3) relatively low constitutive expression regardless of tissue type, 4) expression within male gametophyte related tissues. Heatmaps showing the gene descriptions instead of the gene IDs of these candidates are visualized similarly in Figure 4.7 and Figure 4.9, both with and without the parental B73 deletions, respectively.

Genes having relatively low expression levels, regardless of tissue type were removed, leaving behind 25 candidate genes that may be involved in male gametophyte transmission in PB2. Proteomic data highlighted two genes out of the total 25 candidates as being found in the mature B73 pollen proteome or both the mature pollen and germinating pollen proteome (Figure 4.8 and Figure 4.9).

4.4.3 Sequencing and Identification of Candidate Genes for PB1

PB1 samples were pooled and sequenced on the Illumina HiSeq X using the TruSeq DNA PCR Free kit. Sequencing of PB1 yielded a total of 392,162,928 paired-end reads at 27.9X with 99% of the reads mapping back to the B73 RefGen_v4 (Table 4.3).

Structural variants were called by LUMPY who detected a total 1,993 deletions within PB1.

Transmission data to *r1 C1* testers suggested that the PB1 mutation was either less tightly linked to the *r1* locus or had lower penetrance than PB2 with 23.6%±0.611% transmission of the *R1* allele. A similar linkage drag plot was made using the 'signature' of the number of new deletion mutations occurring within a sliding 500 Kb window of the PB1 mutant and the B73 reference genome. PB1 and PB2 seem to occur within the same genomic position 4.5 Mb proximal and slightly overlapping the *R1* locus (Figure 4.2).

If the shared deletions between PB1 and PB2 that start or stop within the same ten base pair intervals are flagged as originating from the B73 recurrent parent, the deletion mutations unique to PB1 or PB2 can be visualized in Figure 4.3. Although it is possible that PB1 and PB2 are caused by the same mutation and that a deletion call was made as the B73 parent incorrectly is possible, the likelihood that these deletions occur within the same ten base pair intervals is small. These minute base changes are more likely explained by differences in the alignment of the reads to the reference genome.

Within the 4.5 Mb region containing the candidate PB1 and PB2 deletions are 151 genes within the B73 RefGen_v4 genome. Most of the deletions occurring within the B73 parent, PB1, and PB2 individuals occur in intergenic regions, just skipping the start and stop positions of genes within the reference and may have existed in the initial *R-scm2* parent before plutonium-beryllium exposure (Figure 4.4).

Of the 194 deletion sites discovered for PB1, the functional consequences of the 84 predicted genes unique to PB1 were also explored using the Variant Effect Predictor on Ensembl Plants. Most of the mutations that occurred in similar locations to PB2 where deletions most often occurred upstream, downstream, in intergenic regions, or within introns (Figure 4.5). Due to time constraints, RNA expression data for PB1 was not obtained.

4.5 Discussion

The gametophyte generation of plants allows for the transmission of genetic information from one generation to the next. Mutations that arise that influence the transmission and subsequent fertilization events of this genetic information will be lost as quickly as they arise. Using plutonium-beryllium radiation as a mutagen we created two mutants that showed reduced transmission through the male gametophyte and not the female gametophyte. Male transmission of the PB1 and PB2 mutants was calculated based on linkage of the mutation(s) to the *R1* marker. PB1 had 23.6% transmission of the *R1* marker while PB1 had 1.48% transmission of the R1 marker.

Sequencing of the PB1 and PB2 mutations and visualization of the linkage-drag signatures of deletions surrounding the *R1* locus showed a 4.5 Mb area that are flanked by regions with higher rates of recombination than our PB1 and PB2 mutations (Figure 4.2). To further narrow down on the list of candidate genes, deletions shared between PB1 and PB2 were flagged as originating from either the B73 recurrent parent or initial non-mutagenized *R1* stock, the resulting deletions unique to each mutant decreased, however, many hotspots of deletion activity are present (Figure 4.3). Primarily these deletions occur in intergenic regions or positions upstream and downstream of genes in

the B73 reference genome (Figure 4.4 and Figure 4.5). RNA expression data supported 25 candidate genes affected by plutonium-beryllium induced deletions in PB2. Although it is possible that upstream and downstream deletion events could directly influence gene expression of gametophyte-related genes, these candidates were excluded for later analysis, resulting in eight genes affected in the 5'UTR, 3'UTR, introns, or by the gene feature being truncated. These genes included a calcium-dependent protein kinase, the protein MULTIPLE CHLOROPLAST DIVISION SITE 1, a BTB/POZ domain-containing protein, an E3 ubiquitin-protein ligase, syntaxin-81, SKU5 similar 5, acetyl-coA thioesterase, and one uncharacterized zinc-finger of the FCS-type domain containing gene.

All eight candidates showed RNA expression in either all the tissues surveyed or were male gametophyte-specific, expressed in the microspores or mature pollen (CHETTOOR *et al.* 2014). The BTP/POZ domain-containing protein and E3 ubiquitin protein ligase have previously been shown to work together in auxin biosynthesis for organogenesis in *Arabidopsis* (CHENG *et al.* 2008). Syntaxin-81 is localized in the endoplasmic reticulum and inhibits vesicle transport between the endoplasmic reticulum and Golgi apparatus (BUBECK *et al.* 2008), however, no studies have demonstrated its relationship with vesicle fusion near the growing pollen tube tip. *SKU5* (*similar 5*) is involved in directional root growth in *Arabidopsis* having some homology with male gametophyte related genes (SEDBROOK *et al.* 2002).

A calcium-dependent protein kinase (CPK) affected by a deletion event in PB2 is expressed only in the tassel primordia and female tissues and has been implicated in the transmission of the male gametophyte. Expressed highly in the pollen and seed tissues

(YE *et al.* 2009; VALMONTE *et al.* 2014) CPKs in Arabidopsis and petunia have been shown to localize in the plasma membrane to regulate the polarity of the pollen tube tip through Ca^{2+} homeostasis (YOON *et al.* 2006; MYERS *et al.* 2009). Recently the family of maize CPKs have been classified and have been shown to regulate pollen germination and extension. Three CPKs are present on chromosome 10, one of which is included within the deletion found in PB2 showing RNA expression in the silks (LI *et al.* 2018). Further verification work is required to determine if our CPK deletion is involved in pollen tube growth and calcium regulation.

With the lack of RNA expression data at this time it is difficult to speculate on the candidate genes for the second, plutonium beryllium induced male gametophyte mutant, PB1. Some of the affected genes are shared between PB1 and PB2 such as the CDK deletion, however, in PB1 the affecting deletion is almost 40 Kb upstream of the CDK gene. Further analysis such as sequencing of the initial, non-mutagenized *R-scm2* B73 parent along with the recurrent *r1 c1* B73 parent could help solidify which deletions were pre-existing and do not cause our phenotype. Also, sequencing of PB2 *R1* kernels that have undergone recombination events would be interesting to see if the 4.5 Mb area is broken or changes shape indicating where the recombination event took place.

Uniform Mu and Illumina Mu stocks with insertion events surrounding the top candidate genes for PB2 are being tested in 2018 in addition to visualization of PB1 and PB2 pollen phenotypes to determine where male gametophyte transmission begins to fail. Additionally, verification of the PB2 deletion in the candidate regions, as well as RNA expression studies should be performed to better understand how our candidate genes influences gametophyte transmission.

4.6 References

Andrews, S., 2010 FastQC: a quality control tool for high throughput sequence data, pp.

Bubeck, J., D. Scheuring, E. Hummel, M. Langhans, C. Viotti *et al.*, 2008 The syntaxins SYP31 and SYP81 control ER-Golgi trafficking in the plant secretory pathway. Traffic 9**:** 1629-1652.

Cheng, Y., G. Qin, X. Dai and Y. Zhao, 2008 NPY genes and AGC kinases define two key steps in auxin-mediated organogenesis in Arabidopsis. Proceedings of the National Academy of Sciences 105**:** 21017-21022.

Chettoor, A. M., S. A. Givan, R. A. Cole, C. T. Coker, E. Unger-Wallace *et al.*, 2014 Discovery of novel transcripts and gametophytic functions via RNA-seq analysis of maize gametophytic transcriptomes. Genome Biol 15**:** 414.

Danecek, P., A. Auton, G. Abecasis, C. A. Albers, E. Banks *et al.*, 2011 The variant call format and VCFtools. Bioinformatics 27**:** 2156-2158.

Dresselhaus, T., and N. Franklin-Tong, 2013 Male-female crosstalk during pollen germination, tube growth and guidance, and double fertilization. Molecular Plant 6**:** 1018-1036.

Frankel, R., S. Izhar and J. Nitsan, 1969 Timing of callase activity and cytoplasmic male sterility in Petunia. Biochemical Genetics 3**:** 451-455.

Johnson, M. A., and D. Preuss, 2002 Plotting a Course. Developmental Cell 2**:** 273-281.

Kiesselbach, T. A., 1949 *The Structure and Reproduction of Corn*. University of Nebraska, Lincoln.

Layer, R. M., C. Chiang, A. R. Quinlan and I. M. Hall, 2014 LUMPY: a probabilistic framework for structural variant discovery. Genome Biology 15**:** R84.

Li, H., 2013 Aligning sequence reads, clone sequences and assembly contigs with BWA-MEM. arXiv**:** 1-3.

Li, J., Y. Li, Y. Deng, P. Chen, F. Feng *et al.*, 2018 A calcium-dependent protein kinase, ZmCPK32, specifically expressed in maize pollen to regulate pollen tube growth. PLoS One 13**:** e0195787.

Li, X., Y. Song, K. Century, S. Straight, P. Ronald *et al.*, 2001 A fast neutron deletion mutagenesis-based reverse genetics system for plants. The Plant Journal 27**:** 235-242.

Myers, C., S. M. Romanowsky, Y. D. Barron, S. Garg, C. L. Azuse *et al.*, 2009 Calcium-dependent protein kinases regulate polarized tip growth in pollen tubes. Plant Journal 59**:** 528-539.

R Core Team, 2018 R: A language and environment for statistical computing., pp. R Foundation for Statistical Computing, Vienna, Austria.

Sedbrook, J. C., K. L. Carroll, K. F. Hung, P. H. Masson and C. R. Somerville, 2002 The Arabidopsis SKU5 Gene Encodes an Extracellular Glycosyl Phosphatidylinositol-Anchored Glycoprotein Involved in Directional Root Growth. The Plant Cell Online 14**:** 1635-1648.

Swanson, R., A. F. Edlund and D. Preuss, 2004 Species specificity in pollen-pistil interactions. Annual Review of Genetics 38**:** 793-818.

Urlaub, G., P. J. Mitchell, E. Kas, L. A. Chasin, V. L. Funanage *et al.*, 1986 Effect of gamma rays at the dihydrofolate reductase locus: Deletions and inversions. Somatic Cell and Molecular Genetics 12**:** 555-566.

Valmonte, G. R., K. Arthur, C. M. Higgins and R. M. MacDiarmid, 2014 Calcium-dependent protein kinases in plants: evolution, expression and function. Plant and Cell Physiology 55**:** 551-569.

Ye, S., L. Wang, W. Xie, B. Wan, X. Li *et al.*, 2009 Expression profile of calcium-dependent protein kinase (CDPKs) genes during the whole lifespan and under phytohormone treatment conditions in rice (Oryza sativa L. ssp. indica). Plant Molecular Biology 70**:** 311-325.

Yoon, G. M., P. E. Dowd, S. Gilroy and A. G. McCubbin, 2006 Calcium-dependent protein kinase isoforms in Petunia have distinct functions in pollen tube growth, including regulating polarity. Plant Cell 18**:** 867-878.

4.7 Figures – Plutonium-Beryllium Project

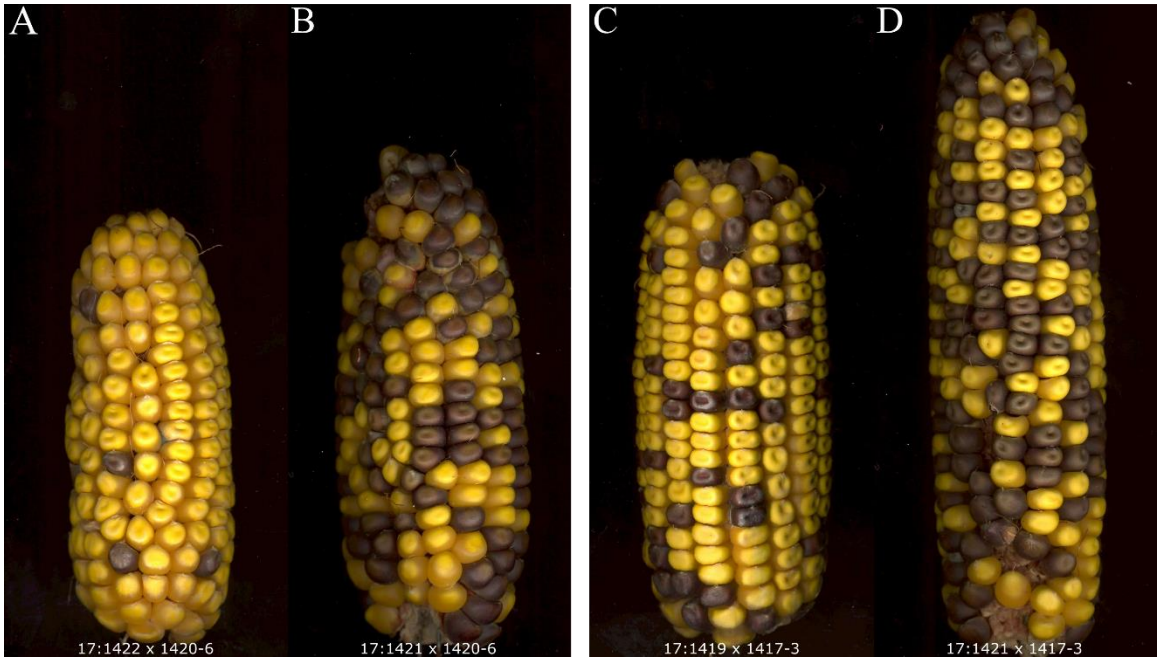

Figure 4.1. Outcrossed ears from PuBe exposed ears to r1 C1 and R1 cl testers.

A) A *r1 C1* tester resulting from a cross by PB2 with 2.56% male transmission. B) *R1 cl* tester resulting from a cross by PB2 with the expected 55.4% male transmission. C) A *r1 C1* tester resulting from a cross by PB1 with 24.8% transmission. D) *R1 cl* tester resulting from a cross by PB1 with the expected 53.7% transmission.

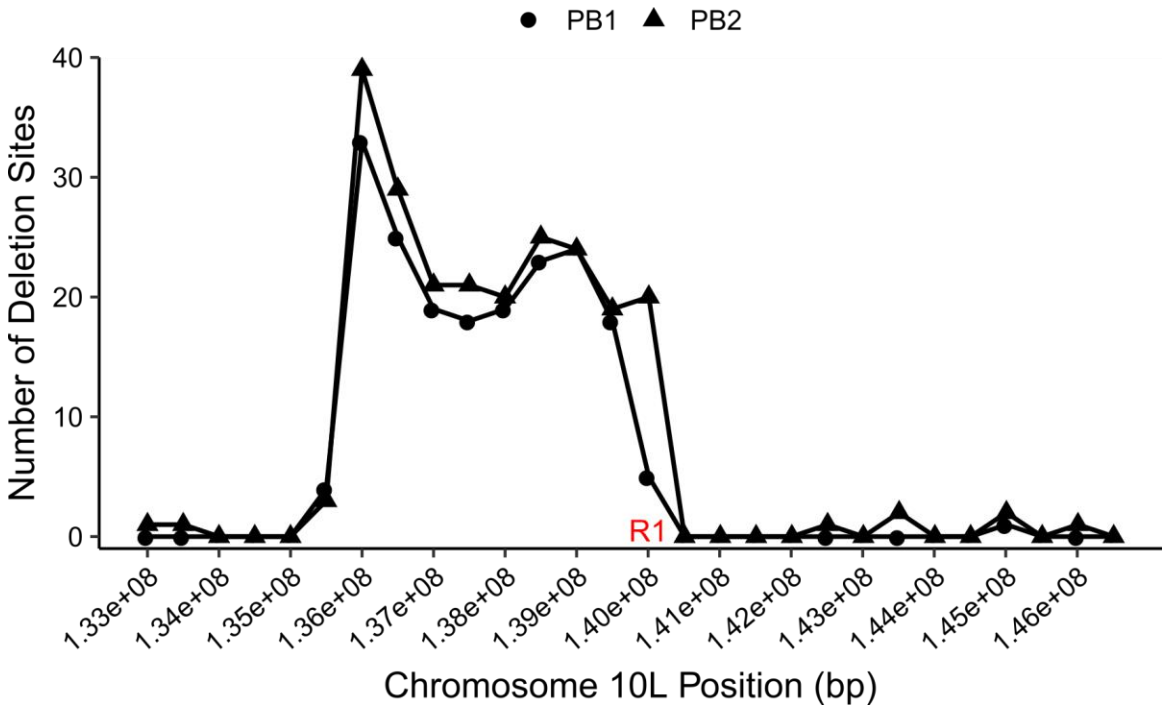

Figure 4.2. Deletion sites occurring between the B73_v4 reference and PB1 and PB2.

Deletions are counted within a sliding 500 Kb window around the *R1* locus on the long arm of chromosome 10. A 4.5 Mb 'curve' shows the genetic linkage of the putative deletion proximal to the *R1* locus. Although the recombination rate of PB1 with *R1* was larger than PB2 (2.56% and 24.8%, respectively), both mutants seem to have the putative mutation in the same genomic region.

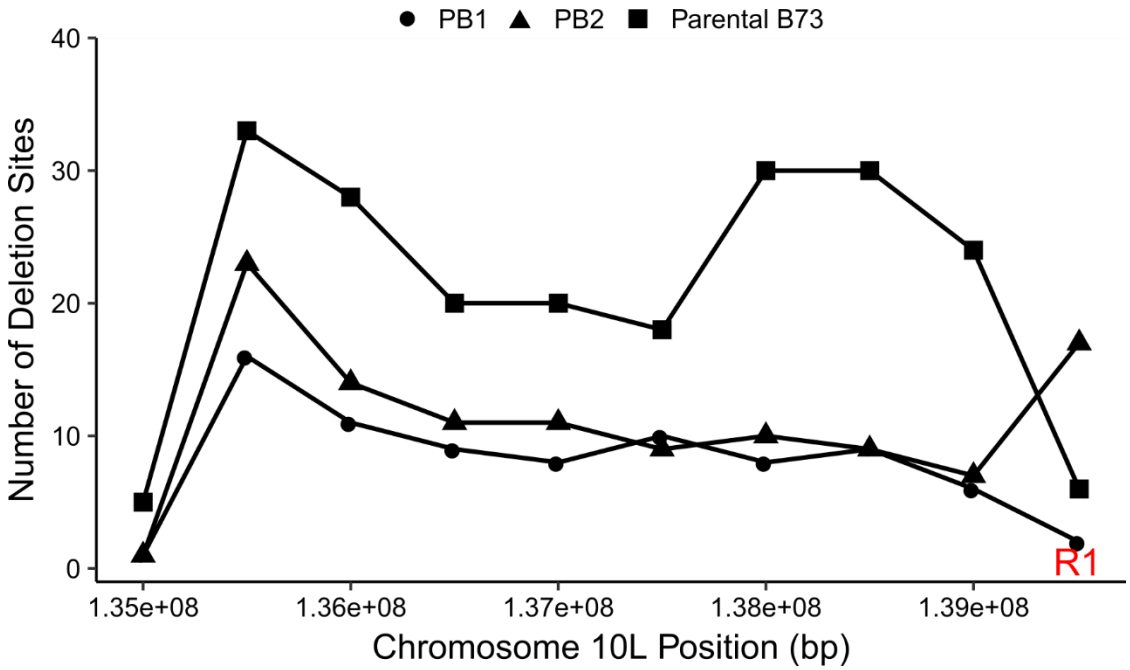

Figure 4.3. Unique deletion sites occurring between the B73_v4 reference, B73 Parent, PB1, and PB2.

Deletions are counted within a sliding 500 Kb window proximal to the *R1* locus on the long arm of chromosome 10. Only the candidate deletions within the 4.5 Mb 'curve' is shown. A peak near the left-most portion of the plot seems to be a hotspot for mutations in each haplotype.

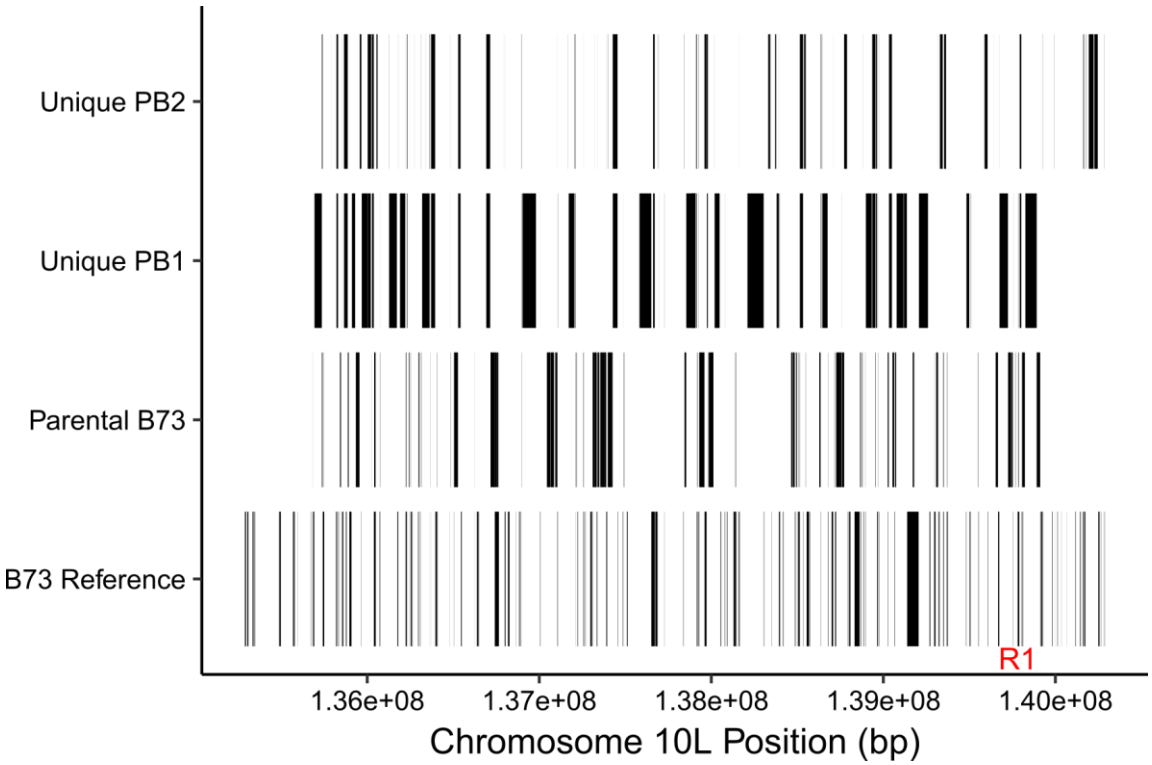

Figure 4.4. Deletion haplotypes in PB1, PB2, and the parental B73 compared to the genes present in the B73 reference.

PB1, PB2, and parental B73 show the deletions unique to each individual, the entire length of the deletion from the estimated start to stop is filled in. The B73 reference shows all 151 genes present in this interval filled-in from the start of the gene to the stop, with all exons and introns included (promoters excluded). PB1 does not include the same 'tail' of deletions distal to *R1* as PB1 due to numerous inversion calls made by LUMPY. Many of the deletions in the parental B73, PB1, and PB2 occur in intergenic regions.

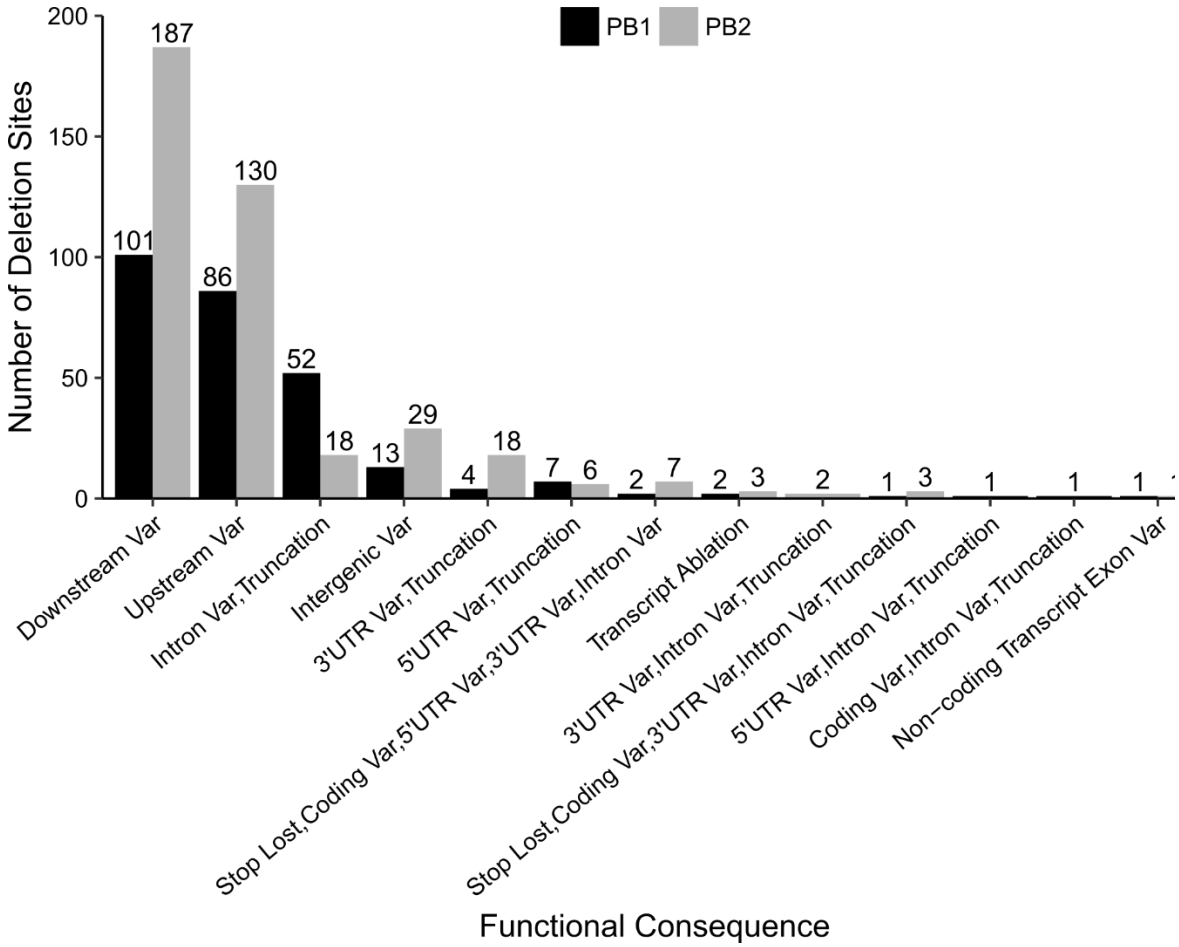

Figure 4.5. Functional consequences of the deletions for PB1 and PB2.

Consequences were generated by Ensembl Plants for the PB1 and PB2 deletions unique of the B73 parental haplotype for candidate genes falling within the 4.5 Mb region proximal to the *R1* locus. Many of the deletions are upstream or downstream of genes, possibly influencing gene expression.

Figure 4.6. Heatmap of RNA expression of PB2 candidate genes including the parental B73 deletions, showing the gene IDs.

The RNA expression (FPKM) of PB2 candidate genes over numerous developmental stages of maize. Genes shown have deletions affecting the genes listed above. The parental B73 deletions genes are included in this plot. ^^: Proteomic evidence of gene products found in the mature and germinating pollen; ^: Proteomic evidence found only in the mature pollen; *: Insertion stock not ordered and tested during the 2018 field season.

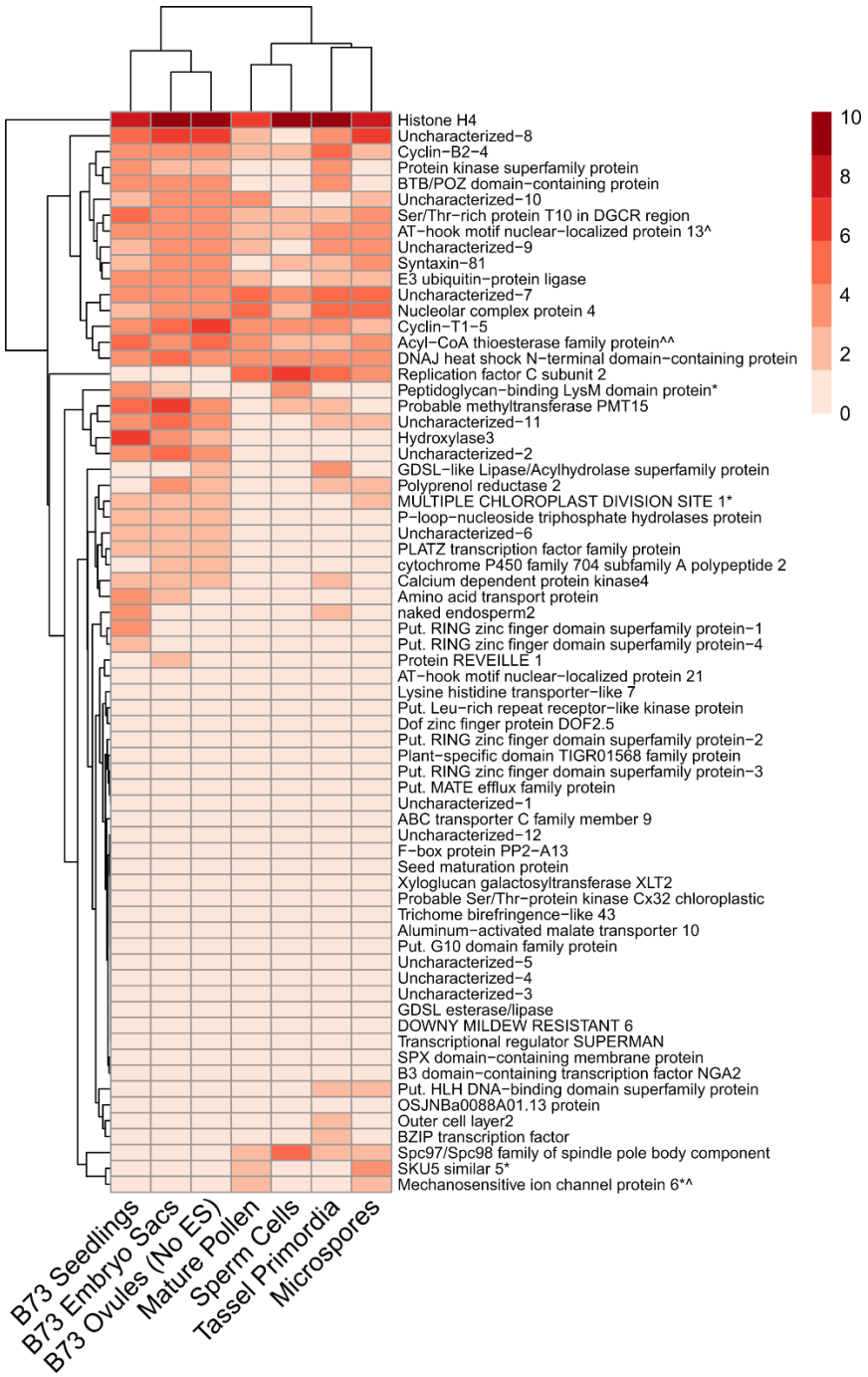

Figure 4.7. Heatmap of RNA expression of PB2 candidate genes including the parental B73 deletions, showing gene descriptions.

The RNA expression (FPKM) of PB2 candidate genes over numerous developmental stages of maize. Genes shown have deletions affecting the genes listed above. The parental B73 deletions genes are included in this plot. ^^: Proteomic evidence of gene products found in the mature and germinating pollen; ^: Proteomic evidence found only in the mature pollen; *: Insertion stock not ordered and tested during the 2018 field season.

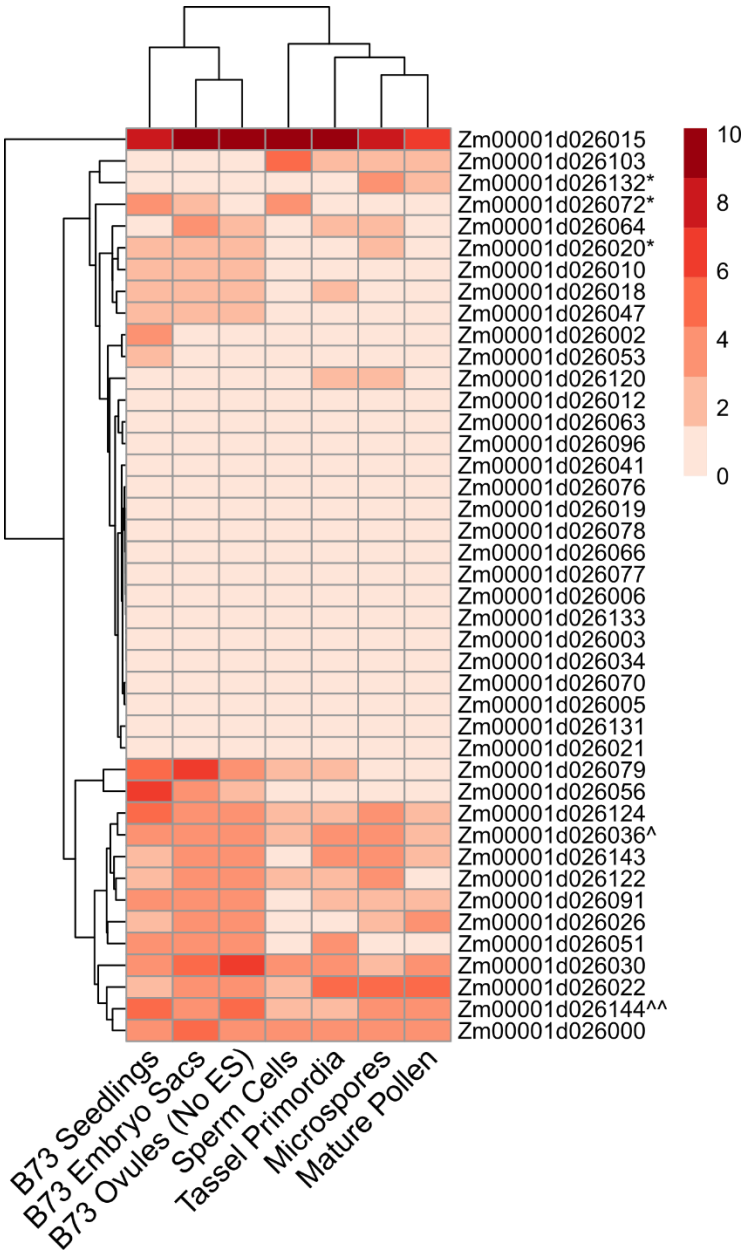

Figure 4.8. Heatmap of RNA expression of PB2 candidate genes without the parental B73 deletions, showing gene IDs.

The RNA expression (FPKM) of PB2 candidate genes over numerous developmental stages of maize. Genes shown have deletions affecting the genes listed above. The parental B73 deletions genes are removed in this plot. ^^: Proteomic evidence of gene products found in the mature and germinating pollen; ^: Proteomic evidence found only in the mature pollen; *: Insertion stock not ordered and tested during the 2018 field season.

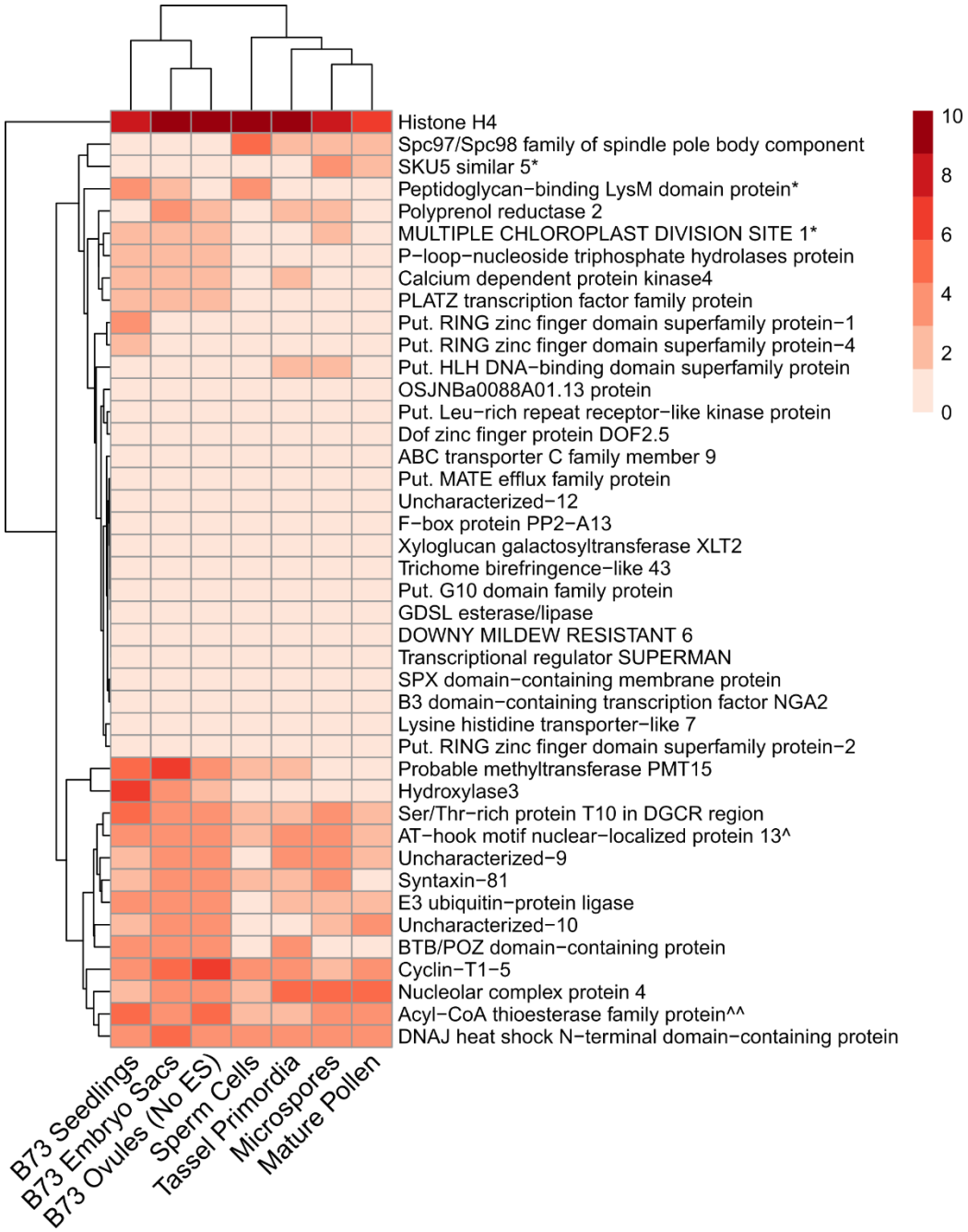

Figure 4.9. Heatmap of RNA expression of PB2 candidate genes without the parental B73 deletions, showing gene IDs.

The RNA expression (FPKM) of PB2 candidate genes over numerous developmental stages of maize. Genes shown have deletions affecting the genes listed above. The parental B73 deletions genes are removed in this plot. ^^: Proteomic evidence of gene products found in the mature and germinating pollen; ^: Proteomic evidence found only in the mature pollen; *: Insertion stock not ordered and tested during the 2018 field season.

4.8 Tables – Plutonium Beryllium Project

Table 4.1. Male gametophyte transmission linked to R1 and C1 of PB2 and PB1.

Five PB2 mutants originating from 6-months of plutonium-beryllium exposure followed a similar pattern of reduced male transmission with a mean of 1.48%±0.443% (se) (expected 50% male transmission). PB1 mutants also had reduced male transmission with a mean of 23.6%±0.611% (se). Transmission for both PB2 and PB1 was unaffected in the regions surrounding the *C1* locus. Lines listed below were propagated though the female.

	R1 Tester			*C1* Tester		
Ear	Col/Uncol	♂ Trans.	X^2	Col/Uncol	♂ Trans.	X^2
17:PB2-1	11/438	2.45%	2.59E-28	188/198	48.7%	0.61
17:PB2-6	6/228	2.56%	2.26E-15	154/124	55.4%	0.07
17:PB2-7	5/379	1.30%	7.81E-27	49/44	52.7%	0.60
17:PB2-8	1/279	0.33%	1.68E-21	94/91	50.8%	0.83
17:PB2-9	3/368	0.80%	5.27E-27	130/124	51.2%	0.71
16:PB1-3	38/107	26.2%	1.00E-08	-	-	-
16:PB1-8	42/114	26.9%	8.18E-09	-	-	-
17:PB1-2	97/328	22.8%	3.84E-29	154/156	49.6%	0.91
17:PB1-3	78/237	24.8%	3.28E-19	206/177	53.7%	0.13
17:PB1-4	101/334	23.2%	5.62E-29	163/170	48.9%	0.70

Table 4.2. Transmission of R1 linked PB1 mutation when propagated through the male.

When PB1 is propagated through the male and tested again to check for reduced male gametophyte transmission, the rate of transmission decreases from 23% to 11% as shown in the top five lines tested.

Cl	cl	% Trans	X^2
9	87	9.4%	4.07E-4
15	107	12.3%	1.19E-3
20	200	9.1%	5.05E-8
13	83	13.5%	9.15E-3
18	131	12.1%	2.70E-4
92	335	21.5%	0.09
42	123	25.5%	0.89
25	90	21.7%	0.41
21	81	20.6%	0.30
32	119	21.2%	0.27
22	101	17.9%	0.06
38	123	23.6%	0.68
27	112	19.4%	0.12
26	81	24.3%	0.86

Table 4.3. Sequencing statistics for PB-1 and PB-2.

Both mutants were sequenced on the Illumina HiSeq X with 150 bp paired end reads.

	PB2	PB1
Depth	54.1X	27.9X
Coverage	98%	-
Total Reads	882,624,074	392,162,928
Mapped (B73 RefGen4)	98.0%	99.39%
Total Deletions*	2,834	1,993

Table 4.4. Sequencing statistics for PB2 with the 10X Genomics Chromium Library.

The N50 Linked Reads per Molecule describes half of the sequence reads that came from molecules with at least this number of linked reads. The Mean DNA per GEM describes the estimated length of DNA fragments loaded into each GEM. SNPs Phased describes the percentage of heterozygous SNPs that were phased. The N50 Phase Block shows the length that half of the genome was, at least, phased into.

Parameter	Value
GEMs Detected	1,445,545
N50 Linked Reads Per Molecule	18.0
Mean Insert Size	333
Mean DNA Per GEM (bp)	367,022
SNPs Phased	94.9%
Longest Phase Block (bp)	1,347,599
N50 Phase Block (bp)	34,981
Mean Molecule Input Length (bp)	19,154
DNA Input Molecules >20kb	43.3%
DNA Input Molecules >100kb	0.616%
PCR Duplication	7.09%

Table 4.5. Summary of PB2 and PB1 predicted genes and deletions.

Both mutants seem to be in a 4.5 Mb interval mostly proximal to *R1 between* 135280968 - 140290276. The size of the potential site of the mutations linked to *R1*, the start and stop region of the predicted linked area, the number of deletion sites, the number of predicted genes (v3 and v4), and the number of genes showing support in prior RNA expression and proteomic analyses for PB2.

	PB2	PB1
Number of Deletion Sites	224	194
Unique Deletion Sites*	114	84
Number of Genes (v4)	79	74
Number of Genes (v3)	42	-
Genes with RNA or Proteomic Support	25	-

Table 4.6. Candidate genes for PB2 showing RNA expression support.

PB2 candidate genes affected by deletions caused by plutonium-beryllium mutagenesis showing RNA expression during any of the maize developmental stages. Genes affected by deletions shown here are subsetted to only include PB2 deletions and not the B73 parental deletions affecting genes.

ID	Call ID	Gene ID	Del Len	Consequence	Description	Start/Stop
PB2	1479	Zm00001d026000	-4109	Upstream Var	DNAJ heat shock N-terminal domain-containing	10:135736630 -135740739
PB2	1702	Zm00001d026002	-9225	Upstream Var	Putative RING zinc finger domain superfamily	10:135821218 -135830443
PB2	529	Zm00001d026010	-136	Upstream Var	P-loop containing nucleoside triphosphate hydrolases superfamily	10:135892344 -135892480
PB2	496	Zm00001d026010	-65	Intron Var, Truncation	P-loop containing nucleoside triphosphate hydrolases superfamily	10:135901362 -135901427
PB2	496	Zm00001d026010	-65	Upstream Var	P-loop containing nucleoside triphosphate hydrolases superfamily	10:135901362 -135901427
PB2	2110	Zm00001d026015	-6451	Upstream Var	Histone H4	10:136053826 -136060277
PB2	488	Zm00001d026018	-290	3'UTR Var, Intron Var, Truncation	calcium dependent protein kinase4	10:136178569 -136178859
PB2	488	Zm00001d026018	-290	3'UTR Var, Truncation	calcium dependent protein kinase4	10:136178569 -136178859
PB2	1707	Zm00001d026020	-2738	5'UTR Var, Truncation	Protein MULTIPLE CHLOROPLAST DIVISION SITE 1	10:136231002 -136233740
PB2	544	Zm00001d026022	-43	Downstream Var	Nucleolar complex protein 4	10:136250601 -136250644
PB2	576	Zm00001d026026	-43	Intron Var, Truncation	Uncharacterized	10:136308162 -136308205
PB2	253	Zm00001d026026	-383	Upstream Var	Uncharacterized	10:136312625 -136313008
PB2	343	Zm00001d026026	-43	Upstream Var	Uncharacterized	10:136313306 -136313349
PB2	1858	Zm00001d026030	-23570	Upstream Var	Cyclin-T1-5	10:136371208 -136394778

ID	Call ID	Gene ID	Del Len	Consequence	Description	Start/Stop
PB2	2112	Zm00001d026036	-13751	Upstream Var	AT-hook motif nuclear-localized protein 13	10:136528665 -136542416
PB2	2113	Zm00001d026047	-1264	Upstream Var	PLATZ transcription factor family protein	10:136896333 -136897597
PB2	97	Zm00001d026051	-293	3'UTR Var, Truncation	BTB/POZ domain-containing protein	10:137105174 -137105467
PB2	97	Zm00001d026051	-293	Downstream Var	BTB/POZ domain-containing protein	10:137105174 -137105467
PB2	2114	Zm00001d026053	-604	Upstream Var	Putative RING zinc finger domain superfamily	10:137211190 -137211794
PB2	254	Zm00001d026053	-41	Downstream Var	Putative RING zinc finger domain superfamily	10:137217160 -137217201
PB2	915	Zm00001d026056	-112	Downstream Var	hydroxylase3	10:137255676 -137255788
PB2	314	Zm00001d026064	-158	Downstream Var	Polyprenol reductase 2	10:137389189 -137389347
PB2	1387	Zm00001d026064	-1138	Upstream Var	Polyprenol reductase 2	10:137397656 -137398794
PB2	391	Zm00001d026072	-467	Downstream Var	peptidoglycan-binding LysM domain-containing protein	10:137687663 -137688130
PB2	2118	Zm00001d026072	-317	Downstream Var	peptidoglycan-binding LysM domain-containing	10:137691166 -137691483
PB2	275	Zm00001d026072	-151	Downstream Var	peptidoglycan-binding LysM domain-containing	10:137691713 -137691864
PB2	534	Zm00001d026072	-54	Upstream Var	peptidoglycan-binding LysM domain-containing	10:137695336 -137695390
PB2	156	Zm00001d026079	-1207	Upstream Var	Probable methyltransferase PMT15	10:137924341 -137925548
PB2	81	Zm00001d026091	-164	Intron Var, Truncation	E3 ubiquitin-protein ligase	10:138161868 -138162032
PB2	1716	Zm00001d026103	-18538	Downstream Var	Spc97/Spc98 family of spindle pole body (SBP)	10:138514745 -138533283
PB2	259	Zm00001d026120	-65	Upstream Var	Putative HLH DNA-binding domain superfamily	10:138881083 -138881148

ID	Call ID	Gene ID	Del Len	Consequence	Description	Start/Stop
PB2	211	Zm00001d026120	-84	Upstream Var	Putative HLH DNA-binding domain superfamily	10:138883127 -138883211
PB2	1579	Zm00001d026122	-6494	5'UTR Var, Truncation	Syntaxin-81	10:138957451 -138963945
PB2	1579	Zm00001d026122	-6494	Upstream Var	Syntaxin-81	10:138957451 -138963945
PB2	228	Zm00001d026122	-267	Downstream Var	Syntaxin-81	10:138972091 -138972358
PB2	228	Zm00001d026124	-267	Downstream Var	Ser/Thr-rich protein T10 in DGCR region	10:138972091 -138972358
PB2	98	Zm00001d026124	-47	Downstream Var	Ser/Thr-rich protein T10 in DGCR region	10:138973342 -138973389
PB2	539	Zm00001d026124	-59	Upstream Var	Ser/Thr-rich protein T10 in DGCR region	10:138976293 -138976352
PB2	219	Zm00001d026132	-41	Intron Var, Truncation	SKU5 similar 5	10:139325718 -139325759
PB2	1488	Zm00001d026132	-16389	Downstream Var	SKU5 similar 5	10:139328712 -139345101
PB2	1721	Zm00001d026143	-17550	Upstream Var	Uncharacterized	10:139588305 -139605855
PB2	325	Zm00001d026144	-324	Upstream Var	Acyl-CoA thioesterase family protein	10:139671784 -139672108
PB2	325	Zm00001d026144	-324	Intron Var, Truncation	Acyl-CoA thioesterase family protein	10:139671784 -139672108

Table 4.7. Candidate genes for PB1 and their functional consequences.

PB1 candidate genes affected by deletions caused by plutonium-beryllium mutagenesis. RNA expression data for these mutants is missing so genes shown here are all deletions impacting PB1 genes who may or may not be expressed at any time during maize development. Genes affected by deletions shown here are subsetted to only include PB1 deletions and not the B73 parental deletions affecting genes.

ID	Call ID	Gene ID	Del Len	Consequence	Description	Start/Stop
PB1	2358	ENSRNA049474589	-18472	Downstream Var	NA	10:138514744-138533216
PB1	2275	Zm00001d023184	-23550	Upstream Var	NA	10:136371204-136394754
PB1	2272	Zm00001d023184	-42	Downstream Var	NA	10:136367354-136367396
PB1	2274	Zm00001d023184	-90	Downstream Var	NA	10:136369074-136369164
PB1	2281	Zm00001d023185	-34	Upstream Var	NA	10:136486117-136486151
PB1	2332	Zm00001d023186	-565	Downstream Var	NA	10:137924767-137925332
PB1	2331	Zm00001d023186	-126	Downstream Var	NA	10:137925423-137925549
PB1	2344	Zm00001d023187	-431	Upstream Var	NA	10:138080731-138081162
PB1	2227	Zm00001d025998	-42536	Downstream Var	ubiquitin carboxyl-terminal hydrolase isozyme L3	10:135693519-135736055
PB1	2230	Zm00001d026003	-9196	Stop Lost, Coding Var, 3'UTR Var, Intron Var, Truncation	flavanone 3-dioxygenase 2	10:135821278-135830474
PB1	2230	Zm00001d026004	-9196	Upstream Var	ATP binding protein	10:135821278-135830474
PB1	2234	Zm00001d026005	-310	Upstream Var	B3 domain-containing protein Os02g0683500	10:135853857-135854167
PB1	2232	Zm00001d026005	-147	Downstream Var	B3 domain-containing protein Os02g0683500	10:135847348-135847495
PB1	2234	Zm00001d026006	-310	Upstream Var	NA	10:135853857-135854167
PB1	2235	Zm00001d026006	-21231	Downstream Var	NA	10:135865341-135886572
PB1	2235	Zm00001d026007	-21231	Upstream Var	NA	10:135865341-135886572
PB1	2235	Zm00001d026008	-21231	Stop Lost,	NA	10:135865341

ID	Call ID	Gene ID	Del Len	Consequence	Description	Start/Stop
PB1	2235	Zm00001d026009	-21231	Coding Var, 5'UTR Var, 3'UTR Var, Intron Var Stop Lost, Coding Var, 5'UTR Var, 3'UTR Var, Intron Var	NA	-135886572 10:135865341 -135886572
PB1	2238	Zm00001d026010	-18838	Downstream Var	helicase sen1	10:135911049 -135929887
PB1	2241	Zm00001d026012	-33515	Upstream Var	OSJNBa0088A01.13-like protein	10:135968398 -136001913
PB1	2245	Zm00001d026014	-10247	Upstream Var	Expansin-A13	10:136027924 -136038171
PB1	2251	Zm00001d026016	-43	Downstream Var	organelle RRM domain-containing protein 6, chloroplastic	10:136077034 -136077077
PB1	2251	Zm00001d026017	-43	Upstream Var	putative MYB DNA-binding domain superfamily protein	10:136077034 -136077077
PB1	2252	Zm00001d026018	-45164	Upstream Var	calcium dependent protein kinase4	10:136127260 -136172424
PB1	2256	Zm00001d026019	-2832	Downstream Var	disease resistance protein RGA2	10:136230960 -136233792
PB1	2253	Zm00001d026019	-30477	Upstream Var	disease resistance protein RGA2	10:136190716 -136221193
PB1	2254	Zm00001d026019	-281	Intron Var, Truncation	disease resistance protein RGA2	10:136224671 -136224952
PB1	2254	Zm00001d026020	-281	Downstream Var	uncharacterized LOC100277044	10:136224671 -136224952
PB1	2256	Zm00001d026020	-2832	5'UTR Var, Truncation	uncharacterized LOC100277044	10:136230960 -136233792
PB1	2263	Zm00001d026022	-69	Upstream Var	uncharacterized LOC100281607	10:136258965 -136259034
PB1	2263	Zm00001d026022	-69	Intron Var, Truncation	uncharacterized LOC100281607	10:136258965 -136259034
PB1	2262	Zm00001d026022	-36	Downstream Var	uncharacterized LOC100281607	10:136253829 -136253865
PB1	2262	Zm00001d026022	-36	3'UTR Var, Truncation	uncharacterized LOC100281607	10:136253829 -136253865
PB1	2262	Zm00001d026022	-36	Intron Var, Truncation	uncharacterized LOC100281607	10:136253829 -136253865
PB1	2263	Zm00001d026023	-69	Upstream Var	probable xyloglucan 6-	10:136258965

ID	Call ID	Gene ID	Del Len	Consequence	Description	Start/Stop
PB1	2264	Zm00001d026025	-35	Intron Var, Truncation	xylosyltransferase 1 uncharacterized LOC100382884	-136259034 10:136297969 -136298004
PB1	2264	Zm00001d026025	-35	3'UTR Var, Truncation	uncharacterized LOC100382884	10:136297969 -136298004
PB1	2272	Zm00001d026028	-42	Upstream Var	OSJNBa0013K16.16-like protein	10:136367354 -136367396
PB1	2270	Zm00001d026028	-42010	Downstream Var	OSJNBa0013K16.16-like protein	10:136319207 -136361217
PB1	2219	Zm00001d026028	-1642	Downstream Var	OSJNBa0013K16.16-like protein	10:136362565 -136364207
PB1	2274	Zm00001d026028	-90	Upstream Var	OSJNBa0013K16.16-like protein	10:136369074 -136369164
PB1	2275	Zm00001d026029	-23550	Upstream Var	uncharacterized LOC100502301	10:136371204 -136394754
PB1	2272	Zm00001d026029	-42	Downstream Var	uncharacterized LOC100502301	10:136367354 -136367396
PB1	2274	Zm00001d026029	-90	Downstream Var	uncharacterized LOC100502301	10:136369074 -136369164
PB1	2275	Zm00001d026030	-23550	Upstream Var	Cyclin-T1-5	10:136371204 -136394754
PB1	2279	Zm00001d026034	-37	Upstream Var	transcriptional regulator SUPERMAN	10:136482260 -136482297
PB1	2283	Zm00001d026036	-13855	Upstream Var	AT-hook protein 1	10:136528564 -136542419
PB1	2288	Zm00001d026047	-1225	Upstream Var	PLATZ transcription factor	10:136896371 -136897596
PB1	2291	Zm00001d026050	-127	Upstream Var	uncharacterized LOC100273177	10:137005219 -137005346
PB1	2295	Zm00001d026051	-954	Upstream Var	uncharacterized LOC100383502	10:137107863 -137108817
PB1	2299	Zm00001d026053	-1209	Upstream Var	E3 ubiquitin-protein ligase RHA1B	10:137209582 -137210791
PB1	2300	Zm00001d026053	-311	Upstream Var	E3 ubiquitin-protein ligase RHA1B	10:137211187 -137211498
PB1	2314	Zm00001d026064	-3	3'UTR Var, Truncation	polyprenol reductase 1	10:137391022 -137391025
PB1	2314	Zm00001d026064	-3	Intron Var, Truncation	polyprenol reductase 1	10:137391022 -137391025
PB1	2316	Zm00001d026066	-27841	Upstream Var	xyloglucan galactosyltransferase XLT2	10:137427271 -137455112
PB1	2317	Zm00001d026067	-138	Upstream Var	putative cytochrome P450 superfamily	10:137488757 -137488895

ID	Call ID	Gene ID	Del Len	Consequence	Description	Start/Stop
					protein	
PB1	2321	Zm00001d026070	-9411	Upstream Var	SPX domain-containing membrane protein OsI_17046	10:137661647 -137671058
PB1	2320	Zm00001d026070	-68533	Downstream Var	SPX domain-containing membrane protein OsI_17046	10:137582651 -137651184
PB1	2321	Zm00001d026070	-9411	Intron Var, Truncation	SPX domain-containing membrane protein OsI_17046	10:137661647 -137671058
PB1	2321	Zm00001d026071	-9411	Downstream Var	NA	10:137661647 -137671058
PB1	2322	Zm00001d026071	-29	Upstream Var	NA	10:137690676 -137690705
PB1	2323	Zm00001d026072	-95	Upstream Var	peptidoglycan-binding LysM domain-containing protein	10:137695294 -137695389
PB1	2322	Zm00001d026072	-29	Downstream Var	peptidoglycan-binding LysM domain-containing protein	10:137690676 -137690705
PB1	2324	Zm00001d026073	-584	Downstream Var	NA	10:137726836 -137727420
PB1	2327	Zm00001d026077	-54809	Upstream Var	NA	10:137854534 -137909343
PB1	2326	Zm00001d026077	-25227	Upstream Var	NA	10:137884021 -137909248
PB1	2328	Zm00001d026077	-2868	Transcript Ablation	NA	10:137913503 -137916371
PB1	2332	Zm00001d026078	-565	Upstream Var	F-box protein PP2-A13	10:137924767 -137925332
PB1	2331	Zm00001d026078	-126	Upstream Var	F-box protein PP2-A13	10:137925423 -137925549
PB1	2328	Zm00001d026078	-2868	Downstream Var	F-box protein PP2-A13	10:137913503 -137916371
PB1	2331	Zm00001d026079	-126	Upstream Var	probable methyltransferase PMT15	10:137925423 -137925549
PB1	2332	Zm00001d026079	-565	Upstream Var	probable methyltransferase PMT15	10:137924767 -137925332
PB1	2334	Zm00001d026080	-5295	Downstream Var	NA	10:137974172 -137979467
PB1	2334	Zm00001d026082	-5295	Non-coding Transcript	NA	10:137974172 -137979467

ID	Call ID	Gene ID	Del Len	Consequence	Description	Start/Stop
				Exon Var		
PB1	2341	Zm00001d026083	-35	Upstream Var	cytochrome P450 87A3	10:138050864 -138050899
PB1	2342	Zm00001d026083	-162	Upstream Var	cytochrome P450 87A3	10:138050831 -138050993
PB1	2344	Zm00001d026084	-431	Downstream Var	protein IQ-DOMAIN 1	10:138080731 -138081162
PB1	2348	Zm00001d026094	-94268	Downstream Var	heat shock factor protein 4	10:138210164 -138304432
PB1	2348	Zm00001d026095	-94268	Downstream Var	Sugar isomerase (SIS) family protein	10:138210164 -138304432
PB1	2349	Zm00001d026096	-204	Upstream Var	dof zinc finger protein 1	10:138348107 -138348311
PB1	2351	Zm00001d026097	-1124	Coding Var, Intron Var, Truncation	putative HLH DNA-binding domain superfamily protein	10:138397589 -138398713
PB1	2350	Zm00001d026097	-13118	Downstream Var	putative HLH DNA-binding domain superfamily protein	10:138380013 -138393131
PB1	2351	Zm00001d026097	-1124	5'UTR Var, Intron Var, Truncation	putative HLH DNA-binding domain superfamily protein	10:138397589 -138398713
PB1	2351	Zm00001d026097	-1124	Intron Var, Truncation	putative HLH DNA-binding domain superfamily protein	10:138397589 -138398713
PB1	2351	Zm00001d026097	-1124	Upstream Var	putative HLH DNA-binding domain superfamily protein	10:138397589 -138398713
PB1	2351	Zm00001d026097	-1124	5'UTR Var, Truncation	putative HLH DNA-binding domain superfamily protein	10:138397589 -138398713
PB1	2358	Zm00001d026103	-18472	Downstream Var	uncharacterized LOC103641966	10:138514744 -138533216
PB1	2358	Zm00001d026104	-18472	Upstream Var	NA	10:138514744 -138533216
PB1	2362	Zm00001d026108	-2752	Transcript Ablation	NA	10:138636998 -138639750
PB1	2363	Zm00001d026109	-2346	Downstream Var	polyphenol oxidase, chloroplastic	10:138674290 -138676636
PB1	2217	Zm00001d026109	-28806	Downstream Var	polyphenol oxidase, chloroplastic	10:138645432 -138674238
PB1	2376	Zm00001d026121	-33734	Downstream Var	amino acid transport protein	10:138898543 -138932277
PB1	2380	Zm00001d026122	-195	Downstream	Syntaxin-81	10:138969143

ID	Call ID	Gene ID	Del Len	Consequence	Description	Start/Stop
				Var		-138969338
PB1	2379	Zm00001d026122	-6431	5'UTR Var, Truncation	Syntaxin-81	10:138957515 -138963946
PB1	2379	Zm00001d026122	-6431	Upstream Var	Syntaxin-81	10:138957515 -138963946
PB1	2380	Zm00001d026123	-195	Downstream Var	NA	10:138969143 -138969338
PB1	2380	Zm00001d026124	-195	Downstream Var	Ser/Thr-rich protein T10 in DGCR region	10:138969143 -138969338
PB1	2384	Zm00001d026125	-16738	Upstream Var	NA	10:139032901 -139049639
PB1	2390	Zm00001d026126	-15	Downstream Var	uncharacterized LOC103641980	10:139066699 -139066714
PB1	2393	Zm00001d026127	-18192	Upstream Var	uncharacterized LOC103641981	10:139118725 -139136917
PB1	2395	Zm00001d026127	-52773	Downstream Var	uncharacterized LOC103641981	10:139206939 -139259712
PB1	2403	Zm00001d026134	-81	Downstream Var	GDSL esterase/lipase At4g16230	10:139371265 -139371346
PB1	2403	Zm00001d026135	-81	Downstream Var	mechanosensitive ion channel protein 5	10:139371265 -139371346
PB1	2404	Zm00001d026137	-16121	Upstream Var	OSJNBa0084K11.10-like protein	10:139483174 -139499295
PB1	2404	Zm00001d026139	-16121	Upstream Var	calcium-dependent protein kinase	10:139483174 -139499295
PB1	2406	Zm00001d026140	-1258	Upstream Var	subtilisin-like protease SBT1.8	10:139509356 -139510614
PB1	2409	Zm00001d026144	-305	Upstream Var	uncharacterized LOC100273486	10:139671802 -139672107
PB1	2409	Zm00001d026144	-305	Intron Var, Truncation	uncharacterized LOC100273486	10:139671802 -139672107
PB1	2410	Zm00001d026144	-49032	Upstream Var	uncharacterized LOC100273486	10:139675321 -139724353
PB1	2414	Zm00001d026146	-377	Downstream Var	NA	10:139755881 -139756258
PB1	2417	Zm00001d026147	-731	Intron Var, Truncation	seed color component at R1	10:139785077 -139785808
PB1	2419	Zm00001d026147	-705	Intron Var, Truncation	seed color component at R1	10:139785875 -139786580
PB1	2421	Zm00001d026147	-76	Intron Var, Truncation	seed color component at R1	10:139786890 -139786966
PB1	2423	Zm00001d026147	-9235	Downstream Var	seed color component at R1	10:139792704 -139801939
PB1	2423	Zm00001d026148	-9235	Downstream	inhibitor of striate 1	10:139792704

ID	Call ID	Gene ID	Del Len	Consequence	Description	Start/Stop
PB1	2423	Zm00001d026149	-9235	Var Downstream Var	putative S-receptor kinase	-139801939 10:139792704 -139801939
PB1	2358	zma-MIR171k	-18472	Downstream Var	NA	10:138514744 -138533216

Chapter 5: Conclusions and Future Directions – Plutonium-Beryllium Induced Gametophyte Mutants

In this study two male gametophyte mutants showing reduced transmission linked to the *R1* locus were generated using plutonium-beryllium induced mutagenesis and sequenced to determine their underlying causative genes. Although numerous candidates were detected, much work still needs to be done to understand the mode of action these mutants have during reproduction.

One of the first things that must be performed is sequencing of the recurrent B73 parent that was used to backcross the PB mutants and the initial *R1* B73 that was not-mutagenized. Though many of the deletions shared between PB1 and PB2 were flagged as originating from the B73 parent in the generated VCF files, these calls may be present in the initial non-mutagenized *R1* B73. Which parent provided the deletion, however, is not as important as distinguishing which deletions are caused by the plutonium-beryllium mutagenesis and which deletions are from the deletions in normal, *R1* B73 who does not carry the male transmission mutation. Sequencing of both B73 parents could assist in a clearer phasing of the deletion haplotypes unique to each individual.

In this study only deletion mutations were investigated as the cause of the male transmission defect. Numerous SNPs were also detected but not investigated in further detail. There is a possibility that the PB1 or PB2 phenotypes are caused by a series of SNPs in essential male transmission related genes. These SNPs should be investigated

in further detail to see if they affect any of the candidates, or new genes around the *R1* locus.

Further projects should also include verifying the top deletion affected genes to ensure that the deletions are present in the PB1 and PB2 mutants and are not sequencing artifacts. This could be done by selecting markers that amplify over samples containing the deletion compared to those who do not have the deletion, creating fragments of varying lengths. Verification of the effect these top candidate genes have is currently underway. A series of Uniform Mu, Illumina-Mu, and Ac/Ds tagged transposon induced stocks were ordered and grown in 2018. These insertion stocks contain transposable element fragments within the exons, introns, 5'UTR, 3'UTR, or estimated promoter regions of the candidate genes. Outcrossing these stocks to tester lines will help determine if the mutation linked to *R1* can be detected in an independent lineage. Additionally, visualizing pollen phenotypes could assist in narrowing the causative genes of PB1 and PB2. Determining pollen morphology, hydration capabilities on the pistil, germination capabilities of the pollen tube, and the capacity in which pollen tube growth proceeds could provide clues to candidate gene function and the mode of reduced transmission.